

Technical Report

TR 44.0015  
February 28, 1967

**IBM** Systems Development Division, Boulder Laboratory

MATERIALS FOR MA  
RECORDING

G. Bate

BY

G. BATE

LIMITED DISTRIBUTION NOTICE

This report will be published as a chapter of the forthcoming Handbook of Magnetic Materials and Their Properties, edited by P. A. Albert and G. G. Hawley, and published by Reinhold Publishing Corp.

## CONTENTS

	<u>Page</u>
I. <u>Magnetic Recording</u>	
1. Introduction	1
2. Principles	1
3. Analog Recording	4
4. Digital Recording	5
II. <u>Particles</u>	8
1. <u>Iron Oxide</u>	10
a) Preparation of Acicular Particles of $\text{Fe}_3\text{O}_4$ and $\gamma\text{-Fe}_2\text{O}_3$	10
b) $\gamma\text{-Fe}_2\text{O}_3$ Particles by Direct Precipitation	12
c) Modified Acicular Particles	12
d) Plate-like Particles of $\gamma\text{-Fe}_2\text{O}_3$ and $\text{Fe}_3\text{O}_4$	13
e) Equiaxed Plate-like Particles of $\gamma\text{-Fe}_2\text{O}_3$	14
f) Cubic Particles	15
g) Discussion	15
Precipitation Reactions	15
Oxidation-Reduction Reactions	15
h) Structure of $\text{Fe}_3\text{O}_4$ and $\gamma\text{-Fe}_2\text{O}_3$	19
i) Magnetic Properties of $\text{Fe}_3\text{O}_4$ and $\gamma\text{-Fe}_2\text{O}_3$	21
<u>Intrinsic Properties</u>	21
Saturation Intensity of Magnetization	21
Curie Temperature	23
Anisotropy Constants	23
Epitaxially - Grown Single Crystals of $\gamma\text{-Fe}_2\text{O}_3$	24
<u>Extrinsic Properties</u>	25
Coercivity	28

Effects of Particle Size on Coercivity	32
Effects of Particle Interactions	34
Remanence and Particle Alignment	34
$\gamma$ -Fe <sub>2</sub> O <sub>3</sub> versus Fe <sub>3</sub> O <sub>4</sub> Particles	39
2. <u>Iron-Cobalt Oxide Particles</u>	40
a) $\gamma$ -Co <sub>x</sub> Fe <sub>2-x</sub> O <sub>3</sub>	40
b) Cobalt-substituted Magnetite, Co <sub>x</sub> Fe <sub>3-x</sub> O <sub>4</sub>	45
3. <u>Other Ferrite Particles</u>	45
a) Cu <sub>x</sub> Fe <sub>3-x</sub> O <sub>4</sub>	46
b) Cobalt-iron Ferrites	46
4. <u>Ferrites with Hexagonal Structure</u>	47
a) Barium Ferrite, BaO.6Fe <sub>2</sub> O <sub>3</sub>	47
b) Substituted Barium Ferrites and Related Materials	50
5. <u>Oxides with Tetragonal Structure</u>	51
a) CrO <sub>2</sub>	51
6. <u>Metal Particles</u>	54
a) Reduction Process	54
b) Decomposition of Metal Carbonyls	56
c) Electrodeposition	58
d) Autocatalytic Deposition	59
e) Elongated Iron Particles by Drawing Wires	59
f) Vacuum Deposition	60
g) Pyrophoricity of Metal Particles	62
h) Metal Particles with Oxide Coating	62
i) Oxide Particles with Metal Coating	63
7. <u>Other Particles</u>	64

a) Manganese - Bismuth	64
b) Manganese - Aluminum	65
c) Iron-Cobalt-Phosphides	65
d) Ternary Alloys	65
III. <u>Thin Metal Films</u>	67
1. <u>Electrochemical Deposition</u>	67
2. <u>Autocatalytic Deposition</u>	73
3. <u>Vacuum Deposition</u>	77
4. <u>Sputtering</u>	80
5. <u>Metal Films versus Particulate Coatings</u>	81
IV. <u>Stainless Steel Recording Wire</u>	83
V. <u>Thermal Recording</u>	84
VI. <u>Cost of Recording Materials</u>	85
VII. References	86

# MAGNETIC RECORDING

## INTRODUCTION

The science of the storage of large quantities of information in a quickly-accessible form is, as yet, still in its infancy. The use of different magnetic states of a ferromagnetic material is, of course, only one of the ways in which information storage may be achieved; other methods include the photographic process, the thermoplastic process, punched tapes and cards. However, magnetic recording has proved to be simple to use, very reliable and to have additional advantages which, when added together, readily explain its popularity. These advantages are 1) the infinite reversibility of the process, 2) information is stored as a passive condition of the medium; it does not need to be regenerated continuously, i. e., it is nonvolatile, 3) the information stored is usually quite unaffected by the environment, e. g., changes in temperature or pressure, or the presence of ionizing radiations, electric and magnetic fields (smaller than the coercivity of the medium). In terms of money spent, magnetic recording surfaces account for the largest single application of permanent magnet materials.

Recording surfaces may conveniently be divided into two classes, each of which has its characteristic advantages and disadvantages. The classes are a) particulate coatings in which single domain particles are separated from each other and attached to a substrate by means of an organic binder material and b) thin, continuous, metallic films. Both types of surfaces will be treated in later sections, however, a brief review of the principles involved in magnetic recording will be given first.

## PRINCIPLES

A magnetically-soft core consisting of mu-metal laminations or ferrite blocks and having a narrow air gap ( $< 1$  mil, or  $25\mu$ ) is energized by the input signal which is applied to a coil ( $\sim 100$  turns) wound around the core. The fringing field in the vicinity of the gap is arranged to penetrate the recording surface and to change its state of magnetization in such a way that the magnetization pattern corresponds to the input signal. This is shown in Figure 1. After the surface moves away from the recording head, some demagnetization of the magnetized regions occurs. Clearly the coercivity must be such that sufficient flux remains around each region to affect the reading head. The reading process (Figure 2.) relies on the fact that the flux path around the core can have lower reluctance than the path across the air gap. Some flux then follows the preferred path around the core and through the pick-up coil. Thus when the flux changes, as a result of the relative motion of the head and the recording surface, a voltage, which is proportional to the time rate of change of the flux, is induced in the coil. As the wavelength of the recorded pattern decreases or as the separation between tape (say) and head increases, the inequality of the two reluctances (core path and air-gap path) is less likely to be true. Less

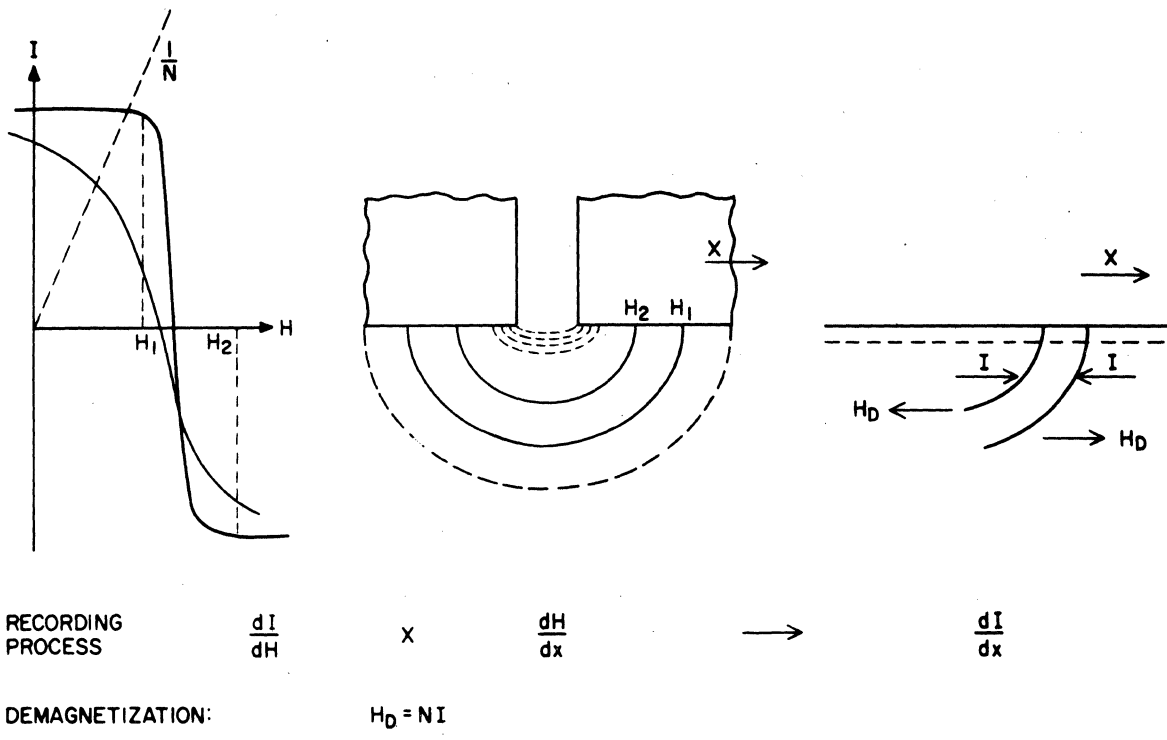


FIGURE 1

THE RECORDING PROCESS; SHOWING THE DEMAGNETIZATION CURVES FOR TWO TYPES OF RECORDING SURFACE (GIVING  $\delta I / \delta H$ ), FIELD CONTOURS FROM THE RECORDING HEAD (GIVING  $\delta H / \delta x$ ), AND A LONGITUDINAL CROSS-SECTION OF A RECORDED TRANSITION (GIVING  $\delta I / \delta x$ ). THE ESTABLISHMENT OF A PARTIALLY DEMAGNETIZED REGION IS CALLED "RECORDING DEMAGNETIZATION". THE EXPRESSION  $H_D = NI$  DESCRIBES THE SUBSEQUENT SELF DEMAGNETIZATION OF THE REGIONS IN TERMS OF A GEOMETRICAL FACTOR N AND THE MAGNETIZATION I (REPRODUCED FROM BATE, IEEE TRANS. MAG 1, 193, (1965).

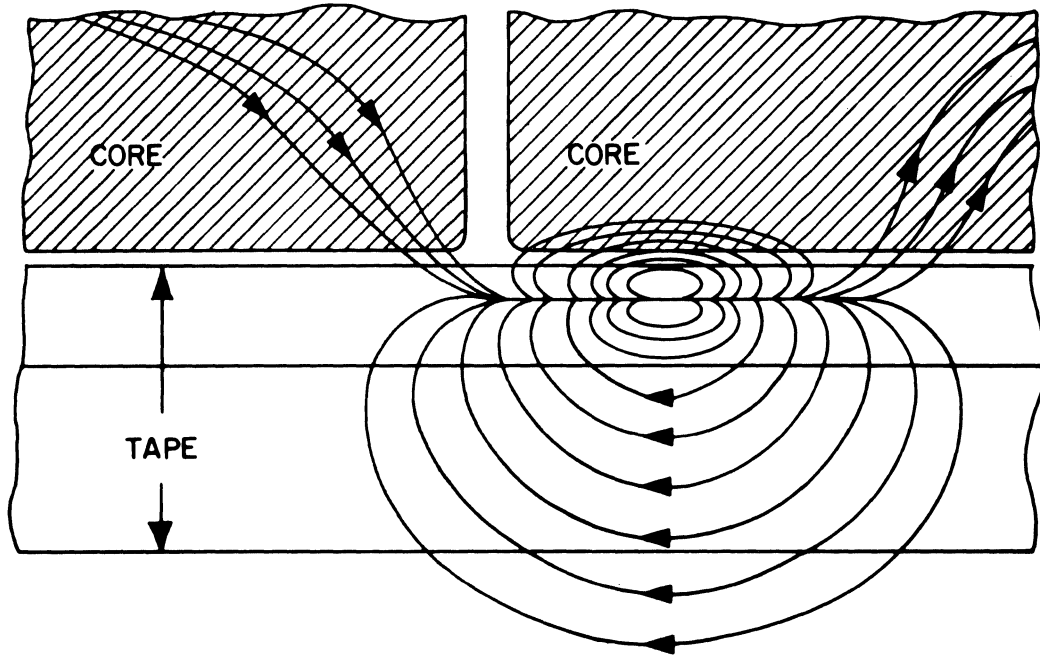


FIGURE 2

THE REPRODUCTION PROCESS; SHOWING SOME FLUX FROM THE MAGNETIZED SURFACE PREFERENTIALLY FOLLOWING THE LOW RELUCTANCE PATH AROUND THE READING-HEAD CORE.



flux follows the core path and the output signal decreases. Usually for reasons of convenience the relative motion is achieved by causing the recording medium to move past a stationary head. Occasionally the situation is reversed or, as in the case of some video recorders, both the head and the medium are in motion. Recording applications fall into two classes: analog and digital, which will now be considered.

## ANALOG RECORDING

This class of magnetic recording is used in audio, video or instrumentation applications. It is not only desired that large output signal (or, more precisely, a large signal-to-noise ratio) be obtained but also that the signal be linearly related to the input signal. This implies that, despite the obvious non-linearity of magnetization curves and hysteresis loops, the magnetization intensity in the medium must be proportional to the applied field. This linearity is usually achieved by superimposing an a. c. bias field, of frequency considerably higher than the highest frequency to be recorded, onto the signal field. Detailed knowledge of the physics of the analog recording process is lacking but the model of anhysteretic magnetization appears to be a good approximation. The model treats the case of the simultaneous application to the recording surface of a constant d. c. field and an a. c. field whose amplitude is initially large and subsequently reduced to zero. The anhysteretic remanent intensity (up to  $\sim 1/2 I_r$ , where  $I_r$  is the remanent intensity of magnetization after a saturating field  $H_s$ , has been applied and removed) is found to be proportional to the d. c. field regardless of previous magnetic history of the medium. The real situation is somewhat different since, during the recording process, the d. c. field is constant neither in magnitude nor direction. Essentially the application of the bias field alone creates a series of partly-overlapping cylinders of magnetization in which adjacent cylinders are magnetized in opposite directions. (Reference Mee). The addition of a lower frequency sinusoidal signal field results in an assymetry in the volume of adjacent cylinders so that different regions in the surface are magnetized to different depths depending on the amplitude of the signal field. As the bias field is increased, the signal output increases and its harmonic distortion decreases until the magnetization varies with depth according to the modulus of a sinusoidal function. For greater values of the bias field the distortion increases again and eventually the signal output begins to decrease when the magnetization induced by the two fields extends completely through the magnetic surface. Since the particles in the surface react to the total field (a. c. bias + signal) only a small signal field is needed to induce remanence if a substantial bias field is present. Consequently, the anhysteretic initial susceptibility can be many times greater than the normal initial susceptibility. This simplified model ignores the effect of interactions fields between the particles in the medium; these fields act in the same way as an additional d. c. bias field and their effect was discussed by Mee<sup>117</sup> and by Daniel and Levine.<sup>40</sup> The model must be further improved by taking into account the shape of the trailing edge field of the recording head and also the effect of short wavelengths. When this is done, good agreement is obtained between experimental recording results and those predicted by the anhysteretic model. At short wavelengths there can exist a marked deviation from the anhysteretic condition that the signal field

be constant during the decay of the bias field. Furthermore, as the wavelength of the recorded pattern decreases, separation losses and the demagnetizing effects became much more important. It is common in analyzing the recording process to treat only the effect of the longitudinal component of signal field and of the magnetization. Templeton and Bate<sup>169</sup>, however, showed by direct measurement that the perpendicular component of the magnetization produced by a recording head can be as large as 10% of the horizontal component.

Occasionally d. c. bias is used in applications where such high frequencies are to be recorded that the (still higher) a. c. bias frequency would be beyond the capability of the recording head and circuits. The use of d. c. bias gives higher output signal levels and better resolution but also, unfortunately, considerably higher noise levels. Recording without any bias field may be used in the case of frequency-modulated signals where amplitude linearity is irrelevant.

Noise may be present in the output signals either in the form of random, unrelated impulses (background noise), unwanted signals (e. g., print-through), or random variations of the desired signal (d. c. noise and modulation noise). Background noise is essentially the result of imperfect demagnetization of the recording surface on a scale comparable to that of the magnetic domains. The a. c. field used must not only be sufficiently large to reverse the hardest particles but also its frequency must be such that the particles are subjected to many cycles while the amplitude of the field is diminished. Background noise may be effectively reduced by using smaller particles. Modulation noise may be significantly larger than background noise and is most noticeable, in audio recording, when the signal consists of a single frequency. Eldridge<sup>50</sup> showed that modulation noise and the related d. c. noise occurred in a repeatable fashion at definite locations along a tape and that it had two primary components. These were asperities on the surface and magnetic inhomogeneities throughout the medium. The former component can be many times larger than the latter and has the same form with or without a. c. bias. This noise component is predominant with signals of long wavelength when the recording fields are below those necessary to saturate the medium. The component caused by magnetic non-uniformity is most important when a uniform, saturating field is used to record on the surface, e. g., in digital recording or, sometimes, in data recording. The method of reducing modulation noise is clearly to produce recording media which are highly uniform and have smooth surfaces.

## DIGITAL RECORDING

In this application of magnetic recording the information is first transformed into binary form. Then as each unit of information is either a binary "one" or "zero", only two states of magnetization are needed in the recording surface. Clearly, the distinction between the two states will be greatest if they correspond to the saturation of the medium in two opposite directions. Thus

a recording surface storing digital information is composed of discrete longitudinal tracks along which the magnetization changes sharply from the maximum remanent state in one direction to a maximum in the opposite direction. Erasure in digital recording usually involves the magnetization of the recording surface to saturation in one direction by means of a field from a (wide-gap) head which is energized with d. c. The most obvious information coding scheme is one in which a "one" corresponds to one direction of magnetization while a "zero" is represented by the opposite direction. Many other schemes have been proposed and used, however, and their advantages and disadvantages are discussed by Hoagland. 77, 33a,

Linearity of the magnetization as a function of applied field is quite unimportant, but it is important that the magnetization should change from  $+I_r$  to  $-I_r$  in a very small distance if good pulse resolution at high densities is to be achieved. The recording process is shown diagrammatically in Figure 1. The transition zone between oppositely magnetized areas of the surface is expected to have a curved shape (in longitudinal cross section) which reflects the head field contours and a width which depends on the slope of the hysteresis loop near the coercivity  $H_c$  and the gradient of the recording field. The creation of this partially demagnetized transition zone is often called "recording demagnetization." When the surface has moved away from the recording head, there exists a demagnetizing field which is composed of two parts; self-demagnetization and adjacent bit demagnetization. This field, which tends to broaden the transition zone, increases with the intensity of magnetization and with a geometrical factor  $N$  which increases with increasing bit density and thickness. As shown in Figure 1, the coercivity of a material is a rough measure of the material's ability to withstand demagnetizing fields (of internal or external origin). The inner of the two curves of  $I$  versus  $H$  represents the behavior of a typical oxide recording surface. This may be compared with the outer curve representing the more rectangular loop with higher coercivity which is typical of thin metallic films. Clearly, a given demagnetizing field (represented by a line of slope  $1/N$ ) results in a more serious decrease in magnetization intensity in the former case.

Since the height and shape of the output pulse from the reading head depend in part on the character of the transition zone, it is important that the zone be kept as narrow as possible so as to minimize the inference between adjacent pulses. Figure 3 shows the result of interference between adjacent "ones" in an NRZI recorded pattern. The peaks corresponding to the "ones" are displaced outwards as a result of the interference. Thus a time error can be introduced into the reproduced pattern and information would be lost if the shift were ever as great as half the natural bit period. It has been shown that the output wave form of the two "ones" (and more complex) pattern can be predicted with accuracy from the superposition of pulses obtained from single transitions. Bate et al<sup>16</sup> showed that, with thin metallic recording surfaces, superposition allowed the two "ones" peak shift to be predicted accurately to densities of at least 25,000 o. c. i. Thus to obtain good resolution at high recording densities narrow output pulses are required. This implies the need for reading heads with narrow gaps and very small core reluctances, small separation between the recording surface and the heads (particularly the

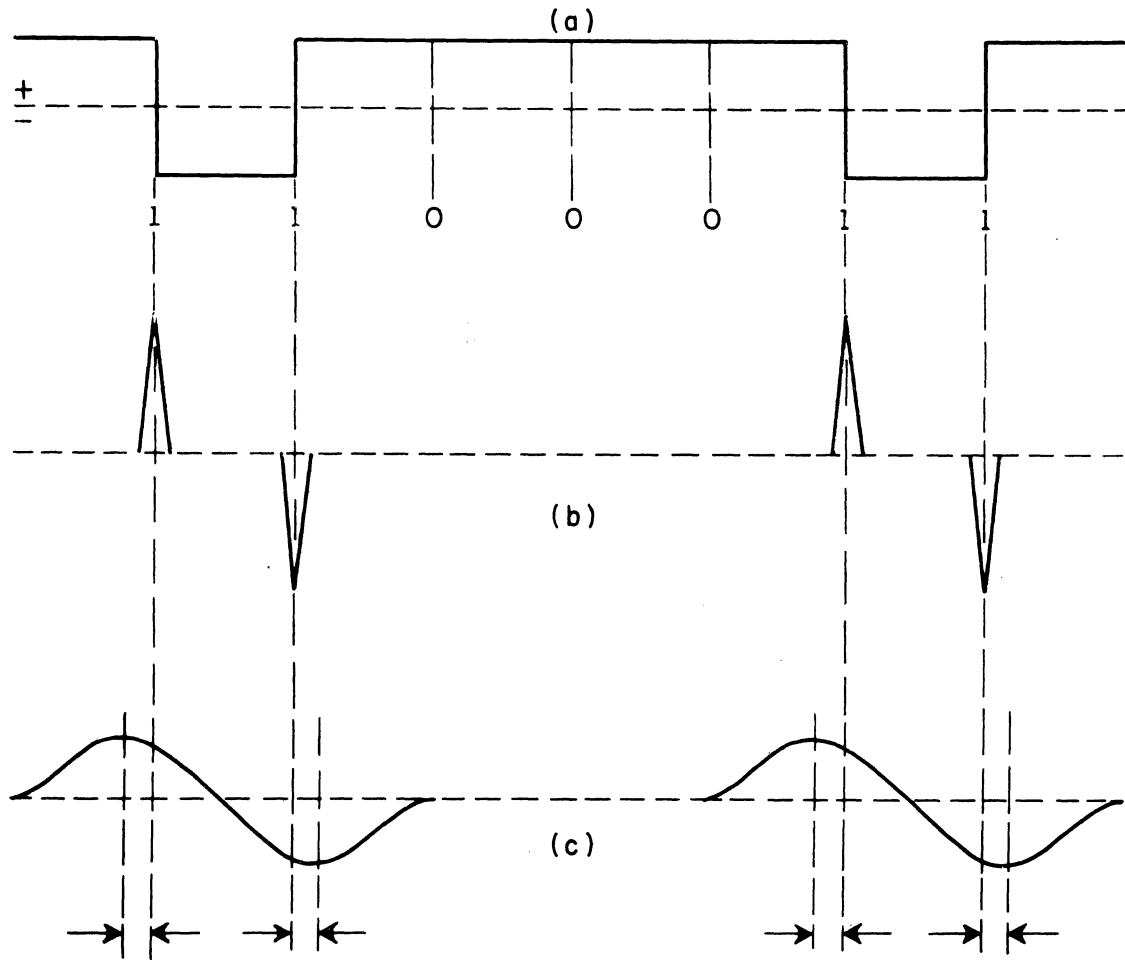


FIGURE 3

- A) THE IDEALIZED DISTRIBUTION OF MAGNETIZATION CORRESPONDING TO THE NRZI PATTERN 110011.
- B) IDEALIZED READ-HEAD OUTPUT, NON-OVERLAPPING PULSES.
- C) BECAUSE OF THE FINITE RESOLUTION INHERENT IN THE READING PROCESS, THE ACTUAL OUTPUT PULSES MAY OVERLAP AND THEIR PEAKS BE DISPLACED OUTWARDS. (REPRODUCED FROM BATE, TEMPLETON AND WENNER, IBM JOURNAL OF RESEARCH AND DEVELOPMENT, 6, 348 (1962).

reading head<sup>161</sup>), and narrow transition zones between oppositely magnetized regions of the recording surface. To obtain a narrow transition zone, we must look for materials having small thickness (to minimize the demagnetizing fields), high coercivity (to minimize the effect of a given demagnetizing field), and a rectangular hysteresis loop (to maximize  $\delta I / \delta H$  and also to reduce the effect of the demagnetizing field). Furthermore, the shape of the output pulse depends on the separation between the reading head and the recording surface. In Figure 4 it is shown diagrammatically how the layers lying closest to the head give much sharper pulses than those which are further away. This argument for thin recording surfaces is probably even more important than the question of demagnetizing factor already discussed. This is supported by experimental results<sup>161</sup> from which it is concluded that the factors which are primarily responsible for the superior high-density recording performance of thin metal films when compared with the iron oxide coatings are the thinness and the high-coercivity of the former.

## PARTICLES

By far the most common type of magnetic recording surface consists of small ( $\leq 1\mu$ ), single-domain particles of iron oxide immersed in an organic binder which serves to isolate the particles and to bond them to the substrate. The earliest proposal to use iron oxide particles for recording purposes was apparently that of Ruben<sup>143</sup> (1932). He described the coating of a flexible wire or strip with a mixture of magnetite ( $\text{Fe}_3\text{O}_4$ ) particles in a thermoplastic binder. When the strip was heated, a reorientation of the magnetic particles occurred in response to the recording head field. The earliest conventional recording tapes using iron oxide particles were probably those developed in Germany for the Magnetophone recorder prior to 1939. These particles were roughly spherical and had an average diameter of about  $1\mu$ . Their method of preparation was described in a FIAT Report (1947)<sup>55</sup> and consisted of precipitating roughly spherical particles of magnetite ( $\text{Fe}_3\text{O}_4$ ) from an aqueous solution of ferrous sulfate and potassium nitrate with an excess of ammonium hydroxide. The magnetite particles were dried and oxidized (without change of shape or size) to give reddish brown particles of  $\gamma\text{-Fe}_2\text{O}_3$ . The coercivity of the particles was usually  $\sim 90$  Oe. and never greater than 150 Oe.; these values are low when compared with a coercivity of 225-275 Oe. found in typical acicular  $\gamma\text{-Fe}_2\text{O}_3$  particles ( $\sim 1\mu$  in length and having an axial ratio of  $\sim 7:1$ ) which are used at present. The signal output obtained from tapes made of the spherical particles was low. This was presumably attributable to their low coercivity, and since about 1947-48 the magnetic constituent or recording tapes has consisted almost entirely of acicular particles of  $\gamma\text{-Fe}_2\text{O}_3$  or of particles of magnetite, with the former greatly predominating.

However, it is clear that the properties of these particles are not by any means ideal for recording, and their shortcomings are made more apparent by the continuing trend to higher recording densities in both analog and digital recording. It is to be expected that they will be replaced, in future high-performance recording systems, by smaller particles of higher moment density and higher coercivity (assuming that recording heads capable of writing on and erasing these materials are available).

In this section we shall describe in some detail the methods of preparation and the properties of various iron oxide particles and then discuss the preparation and properties of particles of other ferrites, compounds, metals and alloys which show promise of being superior recording materials.

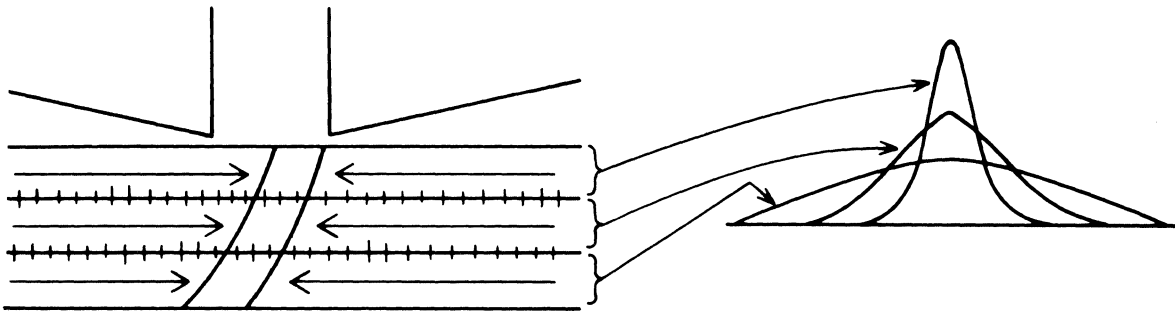


FIGURE 4

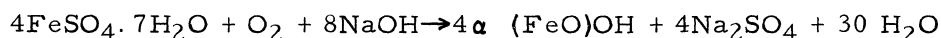
THE CONTRIBUTION TO THE OUTPUT PULSE MADE BY THREE ARBITRARY STRATA IN THE RECORDING MEDIUM SHOWING THE IMPORTANCE OF MEDIUM THINNESS. (REPRODUCED FROM BATE, IEEE TRANS. MAG1, 193 (1965))

## IRON OXIDE PARTICLES

### Preparation of Acicular Particles of $\text{Fe}_3\text{O}_4$ and $\gamma\text{-Fe}_2\text{O}_3$

Since many of the processes by which  $\gamma\text{-Fe}_2\text{O}_3$  particles are prepared involve, as an earlier step, the preparation of particles of magnetite ( $\text{Fe}_3\text{O}_4$ ) (which are then converted to  $\gamma\text{-Fe}_2\text{O}_3$  by controlled oxidation), it is convenient to discuss both oxides at the same time.

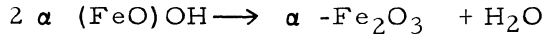
The starting material from which acicular particles of the oxides is prepared is hydrated ferric oxide ( $\alpha$  ( $\text{FeO}\cdot$ )OH = synthetic goethite), which exists in acicular crystalline form. This material is nonferromagnetic and is available commercially as a yellow pigment or it can be made by a process described originally by Penniman and Zoph<sup>137</sup> and later, in more helpful detail, by Camras<sup>35</sup>. Caustic soda solution and ferrous sulfate solution are agitated so as to allow a new surface to be continuously exposed to the atmosphere and  $\alpha$  ( $\text{FeO}\cdot$ )OH is precipitated in colloidal form according to the equation:



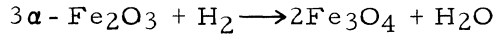
The colloidal particles are then used as nuclei in the growth of larger crystals of  $\alpha$  ( $\text{FeO}\cdot$ )OH in the next step.

More  $\text{FeSO}_4 \cdot 7\text{H}_2\text{O}$  is mixed with water and scrap iron and heated to  $60^\circ\text{C}$ . ( $140^\circ\text{F}$ .) after which the seed material produced in the previous step is added. Air is bubbled through the mixture (at  $60^\circ\text{C}$ .) for about four hours and during this time  $\alpha$  ( $\text{FeO}\cdot$ )OH grows on the colloidal nuclei to produce light-yellow acicular crystals. The sulfuric acid formed in the process then reacts with the scrap iron to replenish the ferrous sulfate. The crystals are then filtered, washed and dried and are found, by electron microscopy, to be about  $0.25 - 1.5\mu$  in length and about  $0.1 - 0.3\mu$  in width. Their composition and structure (orthorhombic) are basically that of the mineral goethite although van Oosterhout<sup>179</sup> showed recently that the synthetic material has a defective structure when compared with that of naturally occurring crystals. Goethite was until recently considered to be paramagnetic<sup>153</sup> and to obey Curie's Law, but Hryniewicz and Kulgawchuk<sup>81</sup> showed by Mössbauer experiments, and van Oosterhout<sup>179</sup> showed by the same method and by the temperature dependence of susceptibility, that the material is actually antiferromagnetic (Néel temperature  $\sim 170^\circ\text{C}$ .).

The yellow acicular crystals of  $\alpha$  (FeO)OH (prepared as described above or obtained commercially) are next dehydrated to give red acicular crystals of hematite,  $\alpha$  - Fe<sub>2</sub>O<sub>3</sub>:



The hematite crystals are then reduced, by heating in hydrogen at 300° - 400°C, to black acicular crystals of ferroso-ferric oxide (Fe<sub>3</sub>O<sub>4</sub> ≡ FeO. Fe<sub>2</sub>O<sub>3</sub> = magnetite).



--although van Oosterhout<sup>179</sup> asserts that the oxide produced at this stage contains more Fe<sub>2</sub>O<sub>3</sub> than is represented by the formula FeO. Fe<sub>2</sub>O<sub>3</sub>.

Finally, reoxidation of the magnetite at a lower temperature (~250°C.) produces reddish-brown acicular particles of  $\gamma$  - Fe<sub>2</sub>O<sub>3</sub> (maghemite). There is no appreciable change in the shape or size of the particles the series of steps: pigment → dehydrated oxide → magnetite →  $\gamma$  - Fe<sub>2</sub>O<sub>3</sub>, i. e., the transformations are isomorphic.

Since the acicular particles of magnetite have ferromagnetic properties which are often just as suitable for magnetic recording as the  $\gamma$  - Fe<sub>2</sub>O<sub>3</sub> particles derived from them, the series of processing steps can be stopped at the magnetite stage if desired. A comparison of the magnetic properties of various ferromagnetic iron oxides is given in Table III.

#### $\gamma$ - Fe<sub>2</sub>O<sub>3</sub> Particles by Direct Precipitation

A more direct method of preparing  $\gamma$  - Fe<sub>2</sub>O<sub>3</sub> particles by precipitation was described by Baudisch<sup>19, 20</sup>. It consisted of dissolving chemically pure iron in hydrochloric acid and adding an excess of pyridine and aniline (fairly strong bases) to the solution. Then air was bubbled through the solution causing the precipitation of hydrated gamma ferric oxide ( $\gamma$  -(FeO).OH = lepidocrocite). The hydrated oxide is not ferromagnetic but may be made so by gentle heating at 150-280°C; a fact known to von Kobell<sup>180</sup> in 1838. This behavior is in contrast to that of  $\alpha$  -(FeO).OH (goethite) which dehydrates to give hematite. Since the work of Baudisch was in the pre-electron microscope era, there are no details of the particle shape and size nor, unfortunately, were the magnetic properties of the particles reported.

#### Modified Acicular Particles

Fukuda<sup>65</sup> et al. described a modification of the Penniman-Zoph process in which a sheath of magnetite was grown onto the colloidal goethite particles. The colloid, which may be produced by the method described above was added to a mixture of solutions of ferric chloride (FeCl<sub>3</sub>. 5H<sub>2</sub>O) and ferrous sulphate (Fe SO<sub>4</sub>. 7H<sub>2</sub>O) whose proportions were chosen so as to give



TABLE III

OXIDE PARTICLES	$\sigma_s$ emu/gm	$\theta_c$ in °C	$H_c$ * OERSTEDS	$I_r/I_s$ *	PARTICLE SHAPE AND SIZE	REFERENCE
$\gamma\text{-Fe}_2\text{O}_3$	74	590	75 - 150		EQUIAXED; $\sim 1\mu$	55, 98
	74	590	225-275	0.5 - 0.8	ACICULAR, $\frac{l}{w} \sim 7, l \sim 0.5-1\mu$	14, 87, 116, 134, 183.
	74	590	275-300	0.5 - 0.7	PLATELIKE, $\frac{l}{w} \sim 10, \frac{w}{t} \sim 5$ $l \sim 1\mu$	10, 11
$\text{Fe}_3\text{O}_4$	82-84	575	$\sim 300$	$\sim 0.5$	EQUIAXED (NATURAL).	
	82-84	575	305-335	0.5 - 0.6	ACICULAR, $\frac{l}{w} \sim 7, l \sim 0.5-1\mu$	
	82-84	575	305-450		PLATELIKE, $\frac{l}{w} \sim 10; \frac{w}{t} \sim 5$ $l \sim 1\mu$	11.
$\gamma\text{-Co}_x\text{Fe}_{2-x}\text{O}_3$ X = 0.04 X = 0.18	$\sim 44$		380 <sup>a</sup>	$\sim 0.7^a$	EQUIAXED 0.05-0.08 $\mu$	162.
			1,100			8.
$\text{Co}_x\text{Fe}_{3-x}\text{O}_4$ X = 0.1 X = 1.0	87		100	.09	EQUIAXED $1 \sim 0.2\mu$	146
	65	520	980 4,200 $\leq 2,100$	.65 .7 .5	$1 \sim 0.1\mu$	146 116 23
			500			46.
$\text{Cu}_x\text{Fe}_{3-x}\text{O}_4$ X = 0.6 X = 1.0	25(BULK VALUE)		290			46, 157.
	68	450	5,350	.5	EQUIAXED PLATES $\frac{l}{t} = 15$ $l = 0.1\mu$	118
$\text{BaO}\cdot\text{Fe}_{11}\text{Co}_{0.5}$ $\text{Ti}_{0.5}\text{O}_{18}$	60		1,900	.5	EQUIAXED PLATES $\frac{l}{t} = 10$ $l = 1\mu$	157
$\text{PbO}\cdot 6\text{Fe}_2\text{O}_3$	50		500	.5		94
$\text{CrO}_2$ +2%(WT.) $\text{Sb}_2\text{O}_3$ (CATALYST)	99	126	57	<.5	ACICULAR, $l = 3-10\mu$ $w = 1-3\mu$	168
	92	126	349	.5	ACICULAR, $l = 0.2-1.5\mu$ $w = 0.03-0.1\mu$	168

\*DEPENDS ON DEGREE OF DISPERSION AND ALIGNMENT

the combination of  $\text{Fe}^{++}$  and  $\text{Fe}^{+++}$  of 1:2 appropriate to magnetite. The mixture was heated in a sealed vessel containing nitrogen at  $50^{\circ}\text{C}$ . and sodium hydroxide was dripped in for five hours while the mixture was vigorously agitated. The temperature was then raised to  $80^{\circ}\text{C}$ . for a period of from one to five hours. The black precipitate which was produced consisted of particles whose cores were the colloidal goethite nuclei. Around the cores had grown shells of magnetite in such a way that the particles were spindle-shaped, i. e. roughly like two cones joined together at the bases. The particles, which had average dimensions of  $0.7\mu$  in length and  $0.15\mu$  in width, could be used directly in recording surfaces or could be transformed to  $\gamma\text{-Fe}_2\text{O}_3$  by oxidizing in air at  $200 - 250^{\circ}\text{C}$ .

It is interesting to note that it is not necessary to use colloidal iron oxide as seed particles. Needle-shaped particles of zinc oxide ( $\text{Zn O}$ ) with colloidal magnetite adsorbed on the surface of the particles can also be used but lead to rather more irregular spindles than do the iron oxide particles. The magnetic properties of the spindle-shaped particles are shown in Table III the advantages claimed over conventional acicular particles are a rather higher remanence and an appreciably higher slope of the initial magnetization curve which should lead to higher output signals in surfaces used for analog recording.

#### Plate-like Particles of $\gamma\text{-Fe}_2\text{O}_3$ and $\text{Fe}_3\text{O}_4$

Ayers and Stephens<sup>10, 11</sup> described a method of preparing these particles in which the length to width ratio was about 10:1 and the width to thickness ratio 5:1. As a first step, a seeding colloid was prepared by dissolving ferrous chloride ( $\text{FeCl}_2$ ) or ferrous sulphate ( $\text{FeSO}_4$ ) in water at  $27^{\circ}\text{C}$ . in an agitating tank and adding slowly dilute sodium hydroxide. Air was bubbled continuously through the liquid for about an hour during which time the yellow-tan seed material was precipitated. Ammonium hydroxide, aniline or pyridine may also be used in the process instead of sodium hydroxide.

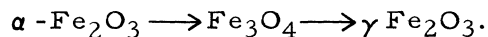
The next step involved the growth of particles around the colloidal nuclei in much the same way as was described above in the Penniman-Zoph-Camras method for growing acicular goethite particles but with two important differences. The first was the addition of zinc chloride to the mixture of ferrous chloride (or sulfate), scrap iron and seed material. As before the mixture was oxidized in a stream of air at  $60^{\circ}\text{C}$ . for 24-48 hours and the particles were filtered, washed, and dried. The second difference was that the method produced flat plate-like crystals of gamma ferric oxide monohydrate (lepidocrocite) rather than the acicular alpha ferric oxide monohydrate (goethite) produced by the Penniman-Zoph-Camras process. The crystalline particles were substantially uniform in size ( $\sim 1\mu$  in length) and were transparent when viewed in an optical microscope (under the same lighting conditions, the acicular goethite particles were opaque). Ayers and Stephens considered that the role of the zinc chloride was as a retarding agent to prevent the development of goethite particles, and they reported that zinc sulphate sodium chloride and ammonium chloride had much the same effect.

The plate-like particles were then reduced to magnetite in hydrogen as described above for acicular particles and could be used to make recording surfaces which, it was claimed, showed superior high-frequency response when compared with those made from acicular magnetite. Alternatively the plate-like magnetite particles could be re-oxidized at 200-250°C. to give particles of  $\gamma$ -Fe<sub>2</sub>O<sub>3</sub> (maghemite). As with the acicular particles, the transformations (lepidocrocite  $\rightarrow$  magnetite  $\rightarrow$  maghemite) were isomorphic. Superior high-frequency recording properties were also claimed for the plate-like  $\gamma$ -Fe<sub>2</sub>O<sub>3</sub> particles. The magnetic properties of the plate-like particles of  $\gamma$ -Fe<sub>2</sub>O<sub>3</sub> and Fe<sub>3</sub>O<sub>4</sub> are shown in Table III where it will be seen that the values of coercivity are rather higher than those of acicular particles which probably accounts for the superior high-frequency recording properties.

#### Equiaxed Plate-like Particles of $\gamma$ -Fe<sub>2</sub>O<sub>3</sub>

Goto and Akashi<sup>68</sup> described a method of making these particles in which sodium hydroxide was added to an aqueous solution of ferrous sulfate in the presence of nitrogen. The precipitated ferrous hydroxide was heated in the mother liquor at 80°C. for five hours when ferrous hydroxide particles of flattened square shape and average size  $1\mu \times 1\mu \times 0.1\mu$  were formed. The shape of the particles was ascribed to the layered structure of the Fe<sup>++</sup> and OH<sup>-</sup> ions in ferrous hydroxide (Fe(OH)<sub>2</sub>) in which the bond between the OH<sup>-</sup> layers is very weak.

Goto and Akashi described two methods by which the equiaxed platelets could be converted to  $\gamma$ -Fe<sub>2</sub>O<sub>3</sub>. In the first method the particles were slowly oxidized in a closed vessel at 300°C. In the second method the ferrous hydroxide particles were first heated to give  $\alpha$ -Fe<sub>2</sub>O<sub>3</sub> after which the usual series of processing steps was followed:



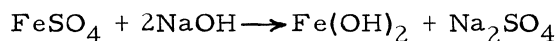
Once again the transformations from grown ferrous hydroxide to gamma ferric oxide particles are isomorphic.

Unfortunately the magnetic properties of these particles were not discussed quantitatively. Since they have the shape of square platelets, it is to be expected that on being coated onto a substrate the particles would tend to lie with their planes parallel to that of the substrate and thus show isotropic magnetic properties in that plane. Thus the recording characteristics should be equal in all directions in the plane, a property which is useful in, for example, magnetic discs or video tape in which the video information is recorded in a different direction from the audio and control information. For such applications it is clear that conventionally oriented acicular particles would not be suitable. However, it is not clear that unoriented acicular particles would be less effective than the plate-like particles described here.

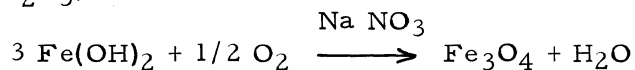
## Cubic Particles

These equiaxed particles appear in the electron microscope as cubes with rounded corners or as deformed spheres. Historically they were the earliest iron oxide particles to be made for recording purposes but, as was mentioned earlier, their coercivity (75-150 Oe.) is considered to be far too low for most present recording applications. Their method of preparation is important, however, since it can also be used to produce cubic particles in which cobalt ions replace some (2-10%) of the iron ions and, in doing so, increase the coercivity of the particles by as much as an order of magnitude. These cobalt-substituted  $\gamma$ -Fe<sub>2</sub>O<sub>3</sub> particles will be discussed later in section

Krones<sup>98</sup> described the steps by which cubic particles of  $\gamma$ -Fe<sub>2</sub>O<sub>3</sub> could be prepared. An aqueous solution of ferrous sulphate was mixed with sodium hydroxide or ammonium hydroxide and a whitish-grey precipitate of ferrous hydroxide is formed



The precipitate was then oxidized to ferroso-ferric oxide at 70° - 90°C. with sodium nitrate (chosen because its oxidizing potential was insufficient to form  $\alpha$ -Fe<sub>2</sub>O<sub>3</sub>).



The cubic magnetite particles were finally oxidized without change of shape or size to  $\gamma$ -Fe<sub>2</sub>O<sub>3</sub> as described above for the case of the acicular particles.

By varying the conditions of precipitation (concentration, pH, temperature, etc.) it is possible to exercise some control over the size of the particles in the range 0.05 to 0.3 $\mu$ . Although they appear equiaxed in the electron microscope, the length : width ratio is probably still greater than the value of 1 : 1:1 at which Osmond<sup>135</sup> deduced the contributions of magneto-crystalline anisotropy and shape anisotropy to be equal in  $\gamma$ -Fe<sub>2</sub>O<sub>3</sub>.

## Discussion

### Precipitation Reactions

In the preceding outlines of the methods by which a variety of shapes and sizes of iron oxide particles have been prepared, there is an almost bewildering similarity of methods employed. We saw, for example, that ferrous sulfate and sodium hydroxide reacted to give goethite,  $\alpha$ -(FeO)OH, in the Penniman, Zoph, Camras (PZ-C) process but gave ferrous hydroxide in the Kroner process for preparing cubic particles. The particles grown on the colloidal seeds by adding scrap iron, ferrous sulfate and air, were of  $\alpha$ -(FeO)OH in the PZ-C method but of lepidocrocite,  $\gamma$ -(FeO)OH in Ayers and Stephens process. These

examples illustrate the crucial importance of the detailed conditions of the reactions. In the first one the mixture (in the PZ-C method) was strongly agitated so as to bring the material in frequent contact with the atmosphere, thus the colloid formed was in a higher state of oxidation than the ferrous hydroxide precipitated in the Kronos method. Furthermore, the ferrous ion  $\text{Fe}^{2+}$  is very unstable in the presence of air and usually is transformed into a mixture of  $\text{Fe}^{2+}$  and  $\text{Fe}^{3+}$ . If a deliberate attempt is made to expose the ferrous ions to oxygen, the result is almost entirely ferric ion,  $\text{Fe}^{3+}$ . The tendency is made use of in one form of radiation dosimeter.

In the second example, Ayers and Stephens added zinc chloride to the reagents to inhibit the growth of acicular goethite particles and to encourage the growth of flat platelets. The mechanism of the action of the inhibitor was not specified.

These two cases are good examples of the complexity of iron oxide chemistry. Acidic conditions (pH 3.5-5) are usually used to grow the acicular particles of  $\alpha$   $(\text{FeO})\text{OH}$  since it is believed that the oxidation of  $\text{Fe}^{2+} \rightarrow \text{Fe}^{3+}$  is incomplete at higher pH values, e. g., at  $\text{pH} \sim 7$ , particles of ferrosferric oxide (magnetite) are formed which presumably would not be acicular. But Marcot<sup>113, 114</sup> et al showed that yellow acicular particles of ferric oxide monohydrate could be precipitated and grown in quite strongly alkaline solutions. They mixed aqueous solutions of ferrous sulfate with an excess of an aqueous solution of sodium hydroxide (200% of the stoichiometric amount) and aerated the mixture at 25-30°C. for about 8 hours. The yellow pigment particles were then washed, filtered and dried at 50-55°C. They claimed that the use of alkaline conditions substantially eliminated the presence of anions ( $\text{Cl}^-$  or  $\text{SO}_4^{2-}$ ) which would otherwise combine chemically the particles and result in their agglomeration during drying. Marcot et al. also recognized the importance of controlling the pH, rate of oxidation and temperature of the mixture in obtaining particles of uniform size distribution. However, they claimed that the particle size was best controlled by using compounds capable of forming complexes with the hydrated iron oxide during precipitation. Sodium silicate, tartaric and citric acids are examples of such compounds and were added in aqueous solution prior to the long oxidation process.

#### Oxidation-Reduction Reactions

The oxidation, reduction and annealing behavior of the iron oxides was treated in detail (although somewhat semi-quantitatively) by Doan<sup>45</sup> in 1941 and his work is frequently referred to in the patent literature. However, the chemistry of the reactions is quite complex and great advances in our understanding of them have taken place within the last decade as a result of more precise knowledge of the various iron oxide structures.

In the Baudisch process (1933) described above for the direct precipitation of  $\gamma$   $(\text{FeO})\text{OH}$ , the particles were transformed directly into ferromagnetic  $\gamma$   $\text{Fe}_2\text{O}_3$  by gentle heating. In contrast, in the Ayers and Stephens process (1962), the  $\gamma$   $(\text{FeO})\text{OH}$  particles were first reduced to magnetite and then

reoxidized to  $\gamma$ -Fe<sub>2</sub>O<sub>3</sub>. The reasons for the apparently unnecessary extra steps in the latter process is that the efficiency of direct conversion of gamma ferric oxide monohydrate to ferromagnetic  $\gamma$ -Fe<sub>2</sub>O<sub>3</sub> is quite low. Some of the material is transformed on heating to  $\alpha$ -Fe<sub>2</sub>O<sub>3</sub> and in consequence, the magnetic properties suffer (lowered coercivity and remanence).

The process of reoxidation of the magnetite particles to  $\gamma$ -Fe<sub>2</sub>O<sub>3</sub> must be performed carefully since too high a temperature results in the formation of hematite ( $\alpha$ -Fe<sub>2</sub>O<sub>3</sub>) which is so weakly ferromagnetic as to be useless for recording purposes. Camras<sup>35</sup> advised that the process be carried out at the lowest temperatures consistent with economical processing time; these temperatures are usually in the range 200-250°C. He showed that at about 380°C. the remanence was reduced to about half that of particles oxidized at 200°C., while at 665°C. the remanence had virtually disappeared.

David and Welch<sup>42</sup> later showed that the presence of water is essential for the oxidation of magnetite to  $\gamma$ -Fe<sub>2</sub>O<sub>3</sub>; if the oxidation proceeds in the dry state only  $\alpha$ -Fe<sub>2</sub>O<sub>3</sub> is formed. Furthermore, they showed that the gamma oxide itself contained a small amount of water which could not be removed without changing the characteristic structure of the material.

In magnetite powders which have been prepared according to the methods described in the previous sections it is more than likely that the particles contain water either from the solutions in which they were originally formed or as adsorbed water. However, natural magnetite in the form of bulk samples does not contain water. Recently Elder<sup>49</sup> showed that, while natural magnetite crystals ground in water to a particle size of  $< 1 \mu$  were converted to  $\gamma$ -Fe<sub>2</sub>O<sub>3</sub> at 250°C. (75% conversion), larger particles  $\geq 25 \mu$  were converted only to  $\alpha$ -Fe<sub>2</sub>O<sub>3</sub> under the same conditions. He further showed that the smaller particles ground in dry acetone and heat in dry oxygen produced only  $\gamma$ -Fe<sub>2</sub>O<sub>3</sub>, thus indicating the importance of both particle size and water in the oxidation of magnetite. Elder's results are shown in Figure 5 in which the saturation intensities of magnetization of the oxidized powders are plotted as a function of the divalent ion content  $[\text{Fe}^{2+}]$  expressed as FeO. On this scale magnetite (FeO·Fe<sub>2</sub>O<sub>3</sub>) is represented by an FeO content of 31.3 per cent. The simple conversions to the metastable  $\gamma$ -Fe<sub>2</sub>O<sub>3</sub> and the stable  $\alpha$ -Fe<sub>2</sub>O<sub>3</sub> are shown by the dotted lines. The experimental points marked with circles refer to small ( $< 1 \mu$ ) particles ground in water; the numbers beside the points indicate the temperatures at which oxidation (in flowing air for one hour) was carried out. It will be seen that, at temperatures below about 250°C., incomplete oxidation occurs while at high temperatures ( $> 450^\circ\text{C}.$ ) oxidation was complete but  $\alpha$ -ferric oxide was formed. At a temperature of about 250°C., oxidation was also substantially complete, but magnetic measurements show that  $\gamma$ -Fe<sub>2</sub>O<sub>3</sub> was formed. The experimental points marked "x" correspond to the larger particles ( $\geq 25 \mu$ ) which, on oxidation, formed only  $\alpha$ -Fe<sub>2</sub>O<sub>3</sub>.

Kojima<sup>93</sup> in 1954 investigated the changes in coercivity of Fe<sub>3</sub>O<sub>4</sub> powders on being oxidized at different temperatures, e. g., oxidation at 450°C. he found produced  $\gamma$ -Fe<sub>2</sub>O<sub>3</sub> particles with a coercivity  $> 200$  Oe. higher temperatures

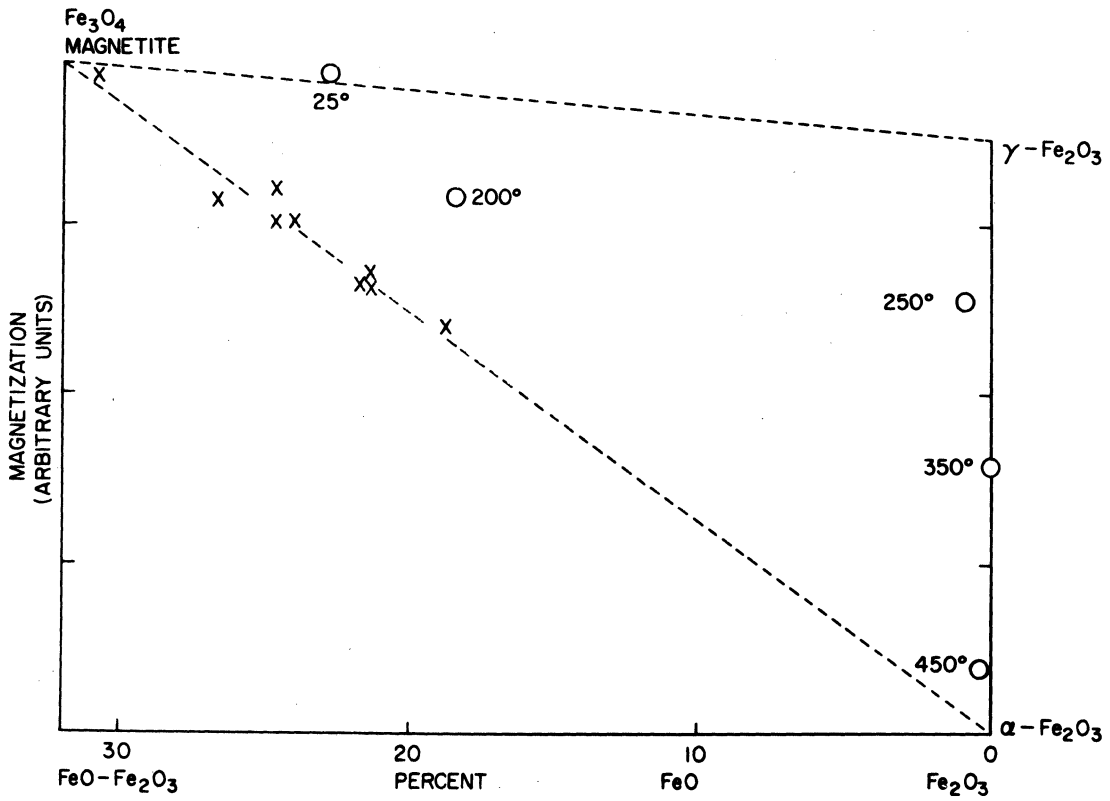


FIGURE 5

OXIDATION OF  $\text{Fe}_3\text{O}_4$  TO  $\text{Fe}_2\text{O}_3$ . THE INTENSITIES OF OXIDIZED POWDERS PLOTTED AS A FUNCTION OF DIVALENT ION  $[\text{Fe}^{2+}]$  CONTENT. THE TEMPERATURES MARKED ARE THOSE AT WHICH THE OXIDATION WAS CARRIED OUT. (AFTER ELDER, JOURNAL OF APPLIED PHYSICS, 36, 1012 (1965)).

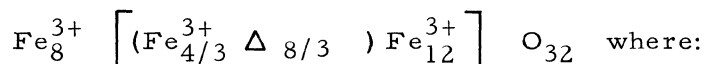
resulted in a progressive decrease in the coercivity until at 700°C. the coercivity was zero, i. e., only hematite was formed. However, it must be remembered that  $H_c$  is an extrinsic property which depends strongly on particle size and not just on the temperature at which oxidation was carried out.

Colombo et al <sup>37, 38</sup> interpreted their results on the oxidation of natural and synthetic magnetites in terms of a mechanism in which oxygen is adsorbed and ionized with the electrons supplied by the oxidation of  $Fe^{2+}$  to  $Fe^{3+}$ . This is followed by a diffusion of ferrous ions from the inside of the crystals to the surface leading to the formation of a solid solution of  $\gamma$ - $Fe_2O_3$  in  $Fe_3O_4$ . Since the precipitated particles have imperfect structures (cf. natural magnetite), the diffusion rate of iron ions is high, and oxidation proceeds rapidly until  $\gamma$ - $Fe_2O_3$  is formed. However, these authors do not consider the important part played by water in the oxidation reactions of magnetite. The iron oxide reactions are summarized in Figure 6.

### Structure of $Fe_3O_4$ and $\gamma$ - $Fe_2O_3$

Magnetite has the typical inverse spinel structure  $Fe^{3+} [Fe^{2+} Fe^{3+}] O_4$  where the square brackets include the ions situated on octahedral (B) sites. The lattice constant of the face-centered cubic unit cell is 8.39Å <sup>42</sup>, and there are eight molecules of  $Fe_3O_4$  per unit cell.

On oxidation to  $Fe_2O_3$ , the oxygen lattice decreases slightly ( $a=8.33\text{Å}$ ). The cubic unit cell of  $\gamma$ - $Fe_2O_3$  then contains 8/9 of the number of iron ions in magnetite and a defect spinel structure is obtained with the formula  $Fe_8^{3+} [Fe_{40/3}^{3+}] O_{32}$ . Van Oosterhout and Rooijmans (1958), <sup>182</sup> after indexing a number of weak x-ray reflections, concluded that the lattice vacancies were arranged on a superlattice on such a way that the unit cell is actually tetragonal with  $c/a=3$ . Thus one third of a complete unit cell has the formula



$\Delta$  indicates cation vacancies and the square brackets denote cations on octahedral sites. The ordinary brackets ( ) indicate cations situated on the lithium sites in ordered lithium ferrite  $Fe_8 (Li_4 Fe_{12})O_{32}$  which, as Braun <sup>29</sup> suggested, possesses the same superlattice structure as  $\gamma$ - $Fe_2O_3$ . Confirmation of this structure was provided by the neutron diffraction results of Ferguson and Hass <sup>54</sup>. They compared the ratios of the intensities of (400) and (440) reflections and obtained a value 0.443 for the ratio. The calculated values assuming a random distribution of vacancies, and preferential distributions over tetrahedral and octahedral sites were respectively 0.482, 0.580, and 0.433.

In 1962, Aharoni, Frei and Schieber <sup>3</sup> verified a suggestion by Kojima <sup>93</sup> that  $\gamma$ - $Fe_2O_3$  was produced, as an intermediate phase, during the reduction in hydrogen of  $\alpha$ - $Fe_2O_3$  to  $Fe_3O_4$ . This was done first by measuring the Curie points of the reduced samples. The Curie point of  $\gamma$ - $Fe_2O_3$  is 590°C. which is sufficiently different from that of  $Fe_3O_4$  (575°C.) to enable the presence of  $\gamma$ - $Fe_2O_3$  phase to be detected. In addition the Mössbauer spectra are quite



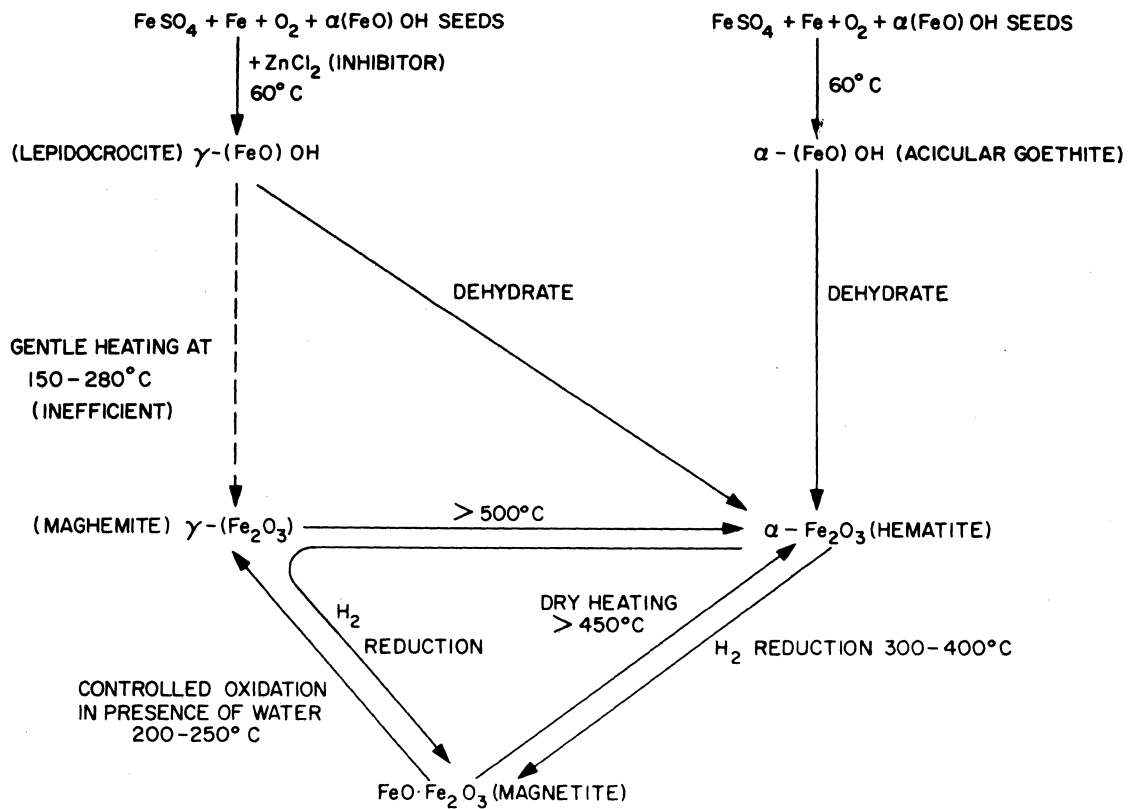


FIGURE 6

REACTIONS INVOLVING IRON OXIDES RELEVANT TO THE PREPARATION OF PARTICLES FOR RECORDING SURFACES.

different for the two oxides and the application of this technique to the reduced samples again showed that  $\gamma$ -Fe<sub>2</sub>O<sub>3</sub> was formed during the reduction of  $\alpha$ -Fe<sub>2</sub>O<sub>3</sub>. This is a difficult result to accept since it involves the conversion of the more stable alpha ferric oxide to the less stable gamma oxide. To explain it Aharoni, et al. support Braun's suggestion that  $\gamma$ -Fe<sub>2</sub>O<sub>3</sub> consists of a solid solution of two materials. The first is the defect spinel discussed above, and the other is a hydrogen iron spinel, H Fe<sub>5</sub>O<sub>8</sub> which is isomorphous with the lithium ferrite. They showed that when  $\gamma$ -Fe<sub>2</sub>O<sub>3</sub> was heated, hydrogen was evolved in amounts of about 70% of that required to give the formula, H Fe<sub>5</sub>O<sub>8</sub>.

However, in 1963 Schrader and Büttner<sup>147</sup> studied the x-ray diffraction lines of samples of  $\gamma$ -Fe<sub>2</sub>O<sub>3</sub> prepared by a number of different methods. They found that the whole system of x-ray lines, including the very weak ones, correspond to the tetragonal structure (a=8.33Å, c/a=3) described above. Thus they concluded that  $\gamma$ -Fe<sub>2</sub>O<sub>3</sub> exists in only one uniform phase and that it is unnecessary to invoke a stabilizing phase of, for example, hydrogen iron spinel.

Despite the disagreement over the presence or absence of stabilizing ions and phases, the basic structure of  $\gamma$ -Fe<sub>2</sub>O<sub>3</sub>, i. e., a defect spinel with the cation vacancies arranged on a tetragonal superlattice, is generally accepted.

### Magnetic Properties of Fe<sub>3</sub>O<sub>4</sub> and $\gamma$ -Fe<sub>2</sub>O<sub>3</sub>

It is appropriate to divide the magnetic properties into intrinsic properties, i. e., those fundamental properties which belong to the material itself and extrinsic properties which depend on the state of preparation of the material. The saturation intensity of magnetization I<sub>s</sub>, and the Curie temperature  $\theta_c$  are examples of intrinsic magnetic properties. The coercivity H<sub>c</sub> and remanent intensity of magnetization I<sub>r</sub>, are extrinsic properties since they depend on, among other things, the shape and size of the oxide particles.

#### Intrinsic Properties

##### Saturation Intensity of Magnetization

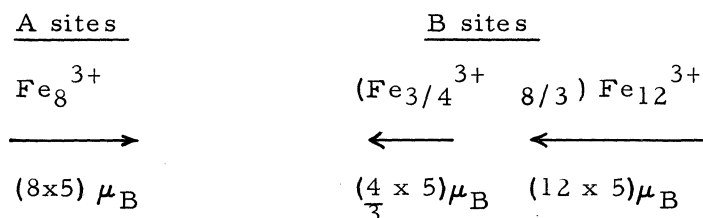
Magnetite has the simple inverted spinel structure which can be represented magnetically as follows:



Since the moments on the tetrahedral (A) and octahedral (B) sites are opposed, the resultant magnetic moment of the molecule is just that of the  $\text{Fe}^{2+}$  ion, i. e.,  $4\mu_B$ . Smit and Wijn<sup>157</sup> give  $4.1\mu_B$ /molecule as the experimental value. Using the molecular weight of magnetite ( $M=231.6$ ), the saturation moment per unit mass at  $0^\circ\text{K}$ ,  ${}_0\sigma_s$ , can be calculated from  ${}_0\sigma_s = \frac{5585 n_B}{M}$ ; where  $n_B$  is the number of Bohr magnetons per molecule. This gives  ${}_0\sigma_s = 97$  emu/gm. Smit and Wijn<sup>157</sup> give  $\sigma_s = 92$  emu/gm as the value at room temperature. The average value for  $\sigma_s$  of a number of powder samples measured in this laboratory on a susceptibility balance was 84 emu/gm. Aharoni et al<sup>3</sup> found experimentally  $\sigma_s = 82$  emu/gm at  $20^\circ\text{C}$ .

Using a value of 5.22 gm/cc for the density of magnetite and Smit and Wijn's value of  $\sigma_s$ , the saturation intensity of magnetization per unit volume is found to be 480 emu/cc.

One unit cell of the defect spinel structure of  $\gamma\text{-Fe}_2\text{O}_3$  is represented magnetically as:



Thus the resultant moment per unit cell is  $(16/3 \times 5) \mu_B$  and so the moment per molecule of  $\gamma\text{-Fe}_2\text{O}_3$  is  $\frac{3}{32} \times \frac{16}{3} \times 5 \mu_B = 2.5 \mu_B$ . Note that if the limiting hydrogen spinel formula,  $\text{FeO}(\text{H}_{0.5}\text{Fe}_{1.5})\text{O}_3$ , is used, we get the same result, and so this question does not affect the value of  $\sigma_s$ .



The resultant moment is again  $2.5 \mu_B$  per molecule or  $1.25 \mu_B$  per iron atom. Henry and Boehm<sup>75</sup> found experimentally a value of  $1.18 \mu_B$ /atom at  $4.2^\circ\text{K}$  and from this  ${}_0\sigma_s$  can be calculated as 82.3 emu/gm. If the theoretical value of  $1.25 \mu_B$ /atom is used, then  ${}_0\sigma_s = 87.4$  emu/gm. Brown and Johnson<sup>33</sup> showed both experimentally and theoretically that  $\frac{\sigma_{290^\circ\text{K}}}{\sigma_{0^\circ\text{K}}} = 0.900$ , thus the

values of  $\sigma_s$  at room temperature became 74.1 emu/gm and 78.7 emu/gm. (using  $1.18 \mu_B$  iron atom and  $1.25 \mu_B$ /iron atom respectively). The average value of  $\sigma_s$  for a large number of powder samples obtained from different

sources and measured in this laboratory was 74 emu/gm. This agrees well with the result of 73 emu/gm found experimentally by Aharoni et al.<sup>3</sup>

Taking the density of  $\gamma$ -Fe<sub>2</sub>O<sub>3</sub> as 5.24 gms/cc. the theoretical value of I<sub>s</sub>, the saturation intensity of magnetization per unit volume, is 413 emu/cc. at 20° C. when the value of 1.25 μ<sub>B</sub>/iron atom is used. If the experimental value of 1.18 μ<sub>B</sub>/iron atom is used, then I<sub>s</sub> = 389 emu/cc.

Since the magnetic powders to be used in recording surfaces are almost invariably weighed, the values of σ<sub>s</sub> are more useful than those of I<sub>s</sub> in specifying the magnetic properties of the surfaces and have the additional advantage of being independent of the presence of cavities.

### Curie Temperature

Aharoni et al.<sup>3</sup> measured σ vs. T for magnetite samples in an atmosphere of pure helium and found θ<sub>c</sub> = 575° C. They repeated the experiment in an atmosphere of oxygen and obtained the value θ<sub>c</sub> = 585° C. which is commonly found in the literature.<sup>3</sup> However, on examining the samples after heating, the x-ray diffraction pattern showed that this material had been partially oxidized to α-Fe<sub>2</sub>O<sub>3</sub>, whereas the samples heated in helium remained Fe<sub>3</sub>O<sub>4</sub>. Smith<sup>158</sup> also measured the Curie point of single crystals of magnetite in a protective atmosphere of CO<sub>2</sub> CO and found θ<sub>c</sub> = 575° C.

The obvious difficulty in determining the Curie temperature of  $\gamma$ -Fe<sub>2</sub>O<sub>3</sub> is that the material is rapidly converted to alpha form when heated above 500° C.

One approach to the problem was to prepare a series of compounds in which  $\gamma$ -Fe<sub>2</sub>O<sub>3</sub> was combined with small amounts of a material which is structurally similar to the iron oxide. It has been known for some time (Selwood<sup>153</sup> p. 307) that  $\gamma$ -Fe<sub>2</sub>O<sub>3</sub> could be stabilized in this way, against structural changes on heating. The method was then to determine the Curie temperature from the σ - T curves as a function of the amount of the added compound and then to extrapolate to zero additive. Michel<sup>121</sup> et al. used up to 7% Al<sub>2</sub>O<sub>3</sub> and deduced the Curie temperature of  $\gamma$ -Fe<sub>2</sub>O<sub>3</sub> to be 591° C. Aharoni et al more recently measures σ<sub>s</sub> as a function of temperature in an atmosphere of pure helium and concluded that θ<sub>c</sub> = 590° C.

A higher value was obtained by Brown and Johnson<sup>33</sup> who fitted a Néel molecular field model, neglecting A-A and B-B interactions, to experimental results of σ - T. They found that the best fit between theory and experimental occurred when θ<sub>c</sub> = 647° C.

### Anisotropy Constants

Bickford<sup>24</sup> (1950) used a ferromagnetic resonance adsorption method to determine the magnetocrystalline anisotropy constant K<sub>1</sub> of natural and synthetic single crystals of magnetite. He obtained the result that, at room temperature,

$$K_1 = -1.10 \times 10^5 \text{ erg/cm}^3.$$

Later Bickford et al.<sup>25</sup> used the torque method on synthetic single crystals and again found  $K_1 = 1.10 \times 10^5 \text{ erg/cm}^3$ . It was also possible from their measurements to make an upper-limit estimate of the second order anisotropy constant which they gave as  $K_2 = -2.8 \times 10^5 \text{ ergs/cm}^3$ . Smith (1956) measured the magnetization curves in a vibrating-sample magnetometer of a single crystal of magnetite along the principal cubic directions and deduced that the room temperature value of  $K_1$  was  $-1.2 \times 10^5 \text{ erg/cm}^3$ .

The determination of the anisotropy constants for  $\gamma\text{-Fe}_2\text{O}_3$  presents a problem. The usual method of cutting samples from a single crystal and measuring the magnetic properties at different angles to the crystal axes cannot be used since it has not yet been found possible to grow single crystals which are large enough. However, it is possible to determine the first-order anisotropy constant of powdered  $\gamma\text{-Fe}_2\text{O}_3$  by indirect methods.

Birks<sup>26</sup> (1950) measured the complex permeability of powders as a function of wavelength in the microwave region. From these measurements he deduced that  $|K_1| = 4.7 \times 10^4 \text{ ergs/cm}^3$  for  $\gamma\text{-Fe}_2\text{O}_3$  and  $|K_1| = 1.3 \times 10^5 \text{ ergs/cm}^3$  for magnetite. The latter value is quite close to those determined from single crystals of magnetite. This suggests that the method may also have given a reasonably accurate value of  $|K_1|$  for  $\gamma\text{-Fe}_2\text{O}_3$ .

More recently Valstyn<sup>176</sup> et al (1962) studied the ferromagnetic resonance spectra of three powder samples of different particle shapes and sizes. To get agreement between theory and experiment, they found it necessary to take a value of  $|K_1| \approx 2.5 \times 10^5 \text{ ergs/cm}^3$  which is larger by a factor of five than Birk's result.

### Epitaxially-Grown Single Crystals of $\gamma\text{-Fe}_2\text{O}_3$

After the above section was written (mid 1965) H. Takei and S. Chiba (Jour. Phys. Soc. Japan 21, 1255 (1966) reported the results of a successful attempt at growing single crystals of  $\gamma\text{-Fe}_2\text{O}_3$ . They used a method which involved the decomposition of ferrous bromide (by water vapor and oxygen) onto freshly cleaved {100} surfaces of a magnesium oxide crystal. The optimum growth conditions were found to be

- a) an atmosphere consisting of a mixture of 2 parts oxygen and 1 part water vapor;
- b) temperature during growth in the range  $650^\circ - 700^\circ \text{C}$ ;
- c) a reaction time of 3 hours is needed to obtain a film of about  $1 \mu$  thickness (the maximum thickness at which a film possessing a pure-spinel structure is possible by this method).

It is remarkable that these conditions should include a deposition temperature which is considerably in excess of that normally required to convert  $\gamma\text{-Fe}_2\text{O}_3$  to  $\alpha\text{-Fe}_2\text{O}_3$ .

Colorimetric analysis showed that the films did not contain ferrous ions. The lattice constant was found to be  $8.35 \text{ \AA}$  (cf.  $8.33 \text{ \AA}$  found by Van Oosterhout and Rooijmans<sup>181</sup>). In contrast to the structure found in polycrystalline  $\gamma\text{-Fe}_2\text{O}_3$ <sup>181</sup> no ordered arrangement of vacancies was found in the epitaxial single crystal films.

The Curie temperature was measured as  $470^\circ \text{C}$  which is considerably below the values of  $590^\circ \text{C}$  found by Aharoni<sup>3</sup> and of  $647^\circ \text{C}$  determined by Brown and Johnson<sup>33</sup> on polycrystalline samples. The saturation magnetic moment per ferric ion was found to be  $1.45 \mu_{\text{B}}$  (cf.  $1.18 \mu_{\text{B}}$  found experimentally by Henry and Boehm<sup>75</sup>). The excess magnetic moment was tentatively explained in terms of vacancies occupying sites (in the epitaxially grown films) which do not contain vacancies in the polycrystalline material. The room-temperature value of  $I_{\text{S}}$  was measured as  $369.5 \text{ emu/cc}$ . by ferromagnetic resonance at X-band. This value is smaller than  $413 \text{ emu/cc}$  obtained from the theoretical value of  $1.25 \mu_{\text{B}}/\text{atom}$ , a density of  $5.24 \text{ gm/cc}$ . and  $\frac{\sigma_{290^\circ\text{K}}}{\sigma_{0^\circ\text{K}}} = 0.900$ <sup>33</sup>.

It is also smaller than the value of  $I_{\text{S}} = 389 \text{ emu/cc}$  obtained by using the experimental value of  $1.18 \mu_{\text{B}}/\text{ion atom}$ .<sup>75</sup> The  $g$ -value was also determined in these measurements as  $2.09$  which should be compared with the expected value of  $2.00$  for ferric ions.

The resonance measurements were used to determine the magnetocrystalline anisotropy in the crystals. The easy axes were the  $\langle 110 \rangle$  and the hard directions were  $\langle 100 \rangle$ . Thus the magnetocrystalline easy axis coincides with the magneto-static easy axis of  $\gamma\text{-Fe}_2\text{O}_3$  particles which was determined by Van Oosterhout<sup>178</sup>. The anisotropy constant  $K_1$ , was found to be  $-4.64 \times 10^4 \text{ ergs/cc}$  which is in excellent agreement with the value  $K_1 = -4.7 \times 10^4 \text{ ergs/cc}$  found by Birks<sup>26</sup> by R. F. measurements on powders.

### Extrinsic Properties

The theory of the magnetic properties of fine particles in general has been reviewed comprehensively by Wohlfarth.<sup>189, 189a</sup> Consequently we need only consider here how these theories apply to the particles of iron oxide. Since the extrinsic properties of the particles depend markedly on the particle shape and size, it is appropriate to consider this question first.

Particles large enough to support domain walls may reverse their magnetization direction by wall motion which usually occurs at much smaller fields than are required to rotate the magnetic moments of single-domain particles. Thus the coercivity of multidomain particles should be smaller than that of single-domain particles as was found experimentally by, for example, Morrish and Watt<sup>124</sup> and Amar<sup>5</sup> discussed the difficulties involved in a theoretical treatment of multidomain particles, but we shall not consider this question here since the particles used in recording surfaces are almost always single domains.

The size at which the behavioral change single domain  $\longleftrightarrow$  multi-domain occurs

is not at all well defined. It was calculated for particles of  $\text{Fe}_3\text{O}_4$  and  $\gamma\text{-Fe}_2\text{O}_3$  by Morrish and Yu<sup>125</sup> by comparing the energy of the single domain configuration with the energy of multi-domain configurations which reduced the external flux. Only exchange energy and magnetostatic energy were considered for the former, i. e., magnetocrystalline energy was neglected. They found that particle-shape also was important; the critical size for single domain behavior was larger for acicular particles than for spherical particles and the greater the acicularity the greater the critical particle size. Morrish and Yu predicted that the critical size for particles of  $\gamma\text{-Fe}_2\text{O}_3$  should be larger than that for  $\text{Fe}_3\text{O}_4$  particles. Watt and Morrish<sup>183</sup> checked this prediction by reducing some large, but still single domain particles of  $\gamma\text{-Fe}_2\text{O}_3$  to  $\text{Fe}_3\text{O}_4$ . The resulting particles tended to show multidomain behavior.

Kondorskii<sup>96</sup> showed theoretically that multidomain particles near the critical size might rotate their magnetization direction, like single domain particles, when compacted. Some experimental evidence that this happens was produced by Morrish and Watt.<sup>124</sup>

At the other end of the range of single domain behavior, i. e., in particles smaller than a certain critical size, random thermal forces are large enough to cause the magnetization direction to rotate spontaneously. Néel calculated the average time between reversals and found it to be an exponential function of the ratio of particle volume to the absolute temperature. These particles are described as being "superparamagnetic" since they show paramagnetic behavior but possess a magnetic moment which is very many times that of the atomic dipoles originally treated by Langevin<sup>100</sup>. A recent review of superparamagnetism was given by Bean and Livingston<sup>21</sup>.

The colloidal particles of iron oxide which are used to develop the recorded patterns on tape and so make them visible, are examples of superparamagnetic particles. Their size ranges from 20-200 Å, i. e., below the limiting size of approximately 300 Å for iron oxide. Since the magnetization direction in superparamagnetic particles is constantly changing, the particles are useless for magnetic recording.

The range over which  $\gamma\text{-Fe}_2\text{O}_3$  and  $\text{Fe}_3\text{O}_4$  acicular particles show single-domain behavior, i. e., the useful range for recording purposes, is then roughly from  $0.03\mu$  to  $2\mu$  (particle length). In practice, of course, the particles show a distribution in size and shape. The aim in preparing the particles should be to make the range as narrow as possible since a wide distribution range leads to a sheared hysteresis loop which is not appropriate in recording surfaces. In Figure 7 are given Morrish and Watt's<sup>124</sup> results for the axial ratio of  $\gamma\text{-Fe}_2\text{O}_3$  particles prepared in the usual way from  $\alpha\text{-(FeO)OH}$ . The lengths of the particles in each sample ranged from  $0.1 - 1.5\mu$  with a mean length of  $0.5 - 0.6\mu$ . These results were obtained by measuring the dimensions of about fifty particles in each sample in an electron microscope. The particles used

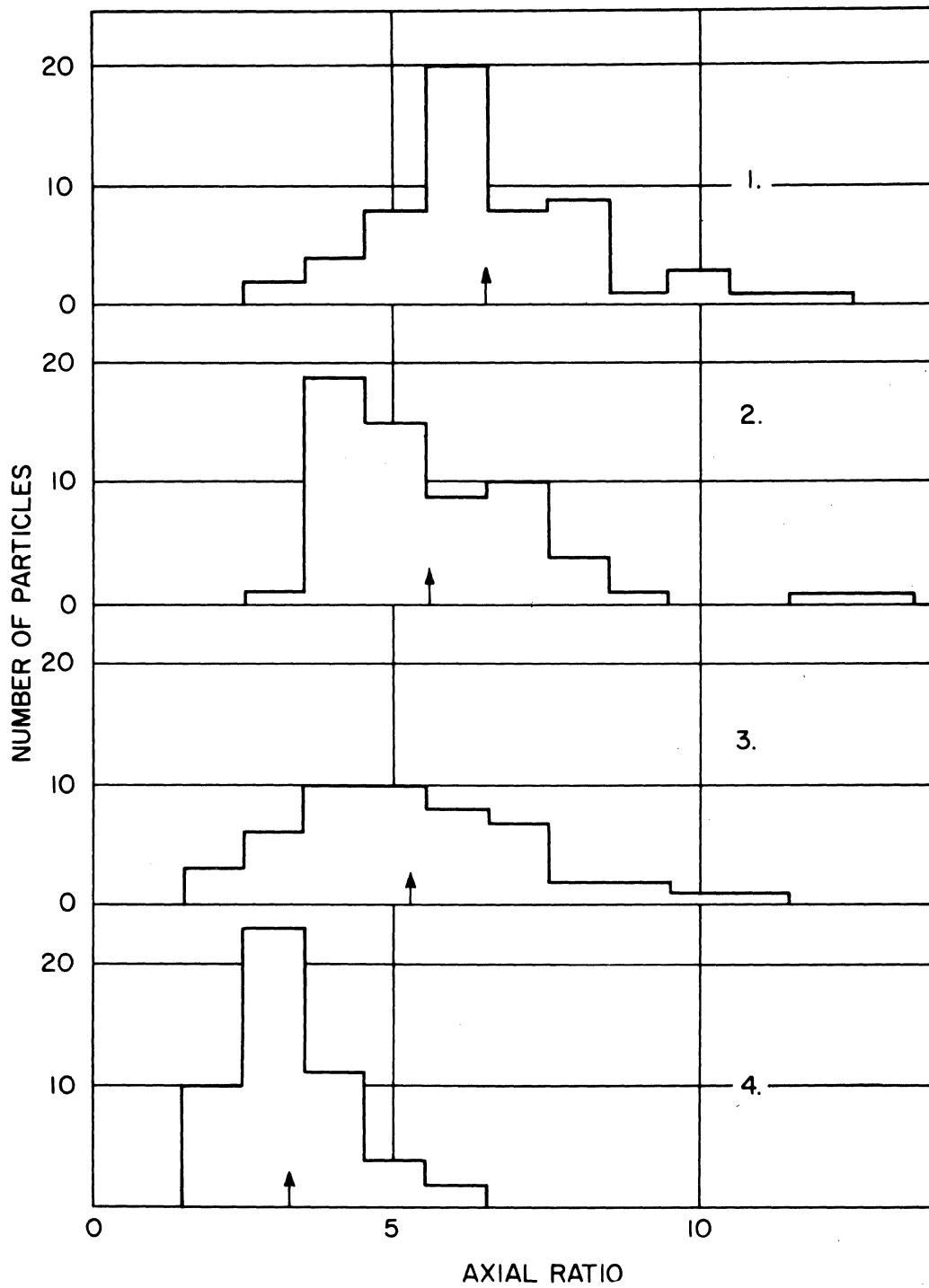


FIGURE 7

AXIAL RATIO DISTRIBUTIONS, DETERMINED BY ELECTRON MICROSCOPY, FOR PARTICLES OF  $\gamma\text{-Fe}_2\text{O}_3$ , (FROM MORRISH AND WATT, PHYSICAL REVIEW, 105, 1476 (1957)).



in typical recording surfaces have lengths of roughly  $0.5 - 1.0 \mu$  axial ratios of about 7:1; Figure 8 is an electromicrograph of such particles.

Van Oosterhout<sup>178</sup> concluded from selected-area electron diffraction photographs supported by other crystallographic and mineralogical arguments that the long dimension of the  $\gamma$ - $\text{Fe}_2\text{O}_3$  particles is  $[110]$ . This direction arises from the "c" axis  $[001]$  of the orthorhombic  $\alpha$ -(FeO)OH particles and is the direction of the long chains<sup>179</sup> of "FeO<sub>2</sub>" in the acicular goethite crystals. This result is in disagreement with the earlier work of Campbell<sup>34</sup> who concluded that the long axes of the particles had low order directions  $\langle 111 \rangle$ ,  $\langle 211 \rangle$ ,  $\langle 221 \rangle$  etc., but that no one set of directions was preferred in any sample.

### Coercivity

The magnetization reversal behavior of isolated single domain particles possessing shape anisotropy was calculated by Néel<sup>128</sup> and later (and in more detail) by Stoner and Wohlfarth<sup>165</sup>. They found that the coercivity  $H_c$  may be written:  $H_c = (N_b - N_a)I_s$  where  $N_b$  and  $N_a$  are, respectively, the demagnetizing factors along the semi-minor and semi-major axes of the (ellipsoidal) particle. The maximum value which  $(N_b - N_a)$  can take is  $2\pi$ , and so we can calculate the maximum coercivity of an acicular particle of  $\gamma$ - $\text{Fe}_2\text{O}_3$  by assuming ellipsoidal geometry and by substituting the value  $I_s \approx 400 \text{ emu/cm}^3$  discussed above. This leads to a value of about 2500 Oe. which is greater by almost an order of magnitude than the experimental values. Even allowing for a random assembly of similar ellipsoids only reduces the coercivity to  $H_c = 0.48 (N_b - N_a)I_s$ . In practice, however, one more often encounters the case of a random assembly of rather dissimilar particles.

Johnson and Brown<sup>87</sup> observed that while the axial ratio ( $m$ ) of  $\gamma$ - $\text{Fe}_2\text{O}_3$  particles is found by electron microscopy to be at least 5, the value of "m" determined from magnetic measurements and an "unaveraging" process was at most 1.6. They concluded that interactions between particles were insufficient to account for the lack of agreement between the experimental results and those of the Stoner, Wohlfarth theory, and that an incoherent magnetization reversal process occurred. The incoherent reversal processes were postulated (1955-60) primarily to account for the fact that the coherent process used in the Stoner, Wohlfarth theory almost invariably overestimated  $H_c$ . In the coherent process it is assumed that the magnetic moments throughout the single-domain particle remain parallel during the reversal, i. e., they all rotate together. On the other hand, Jacobs and Bean<sup>85</sup> showed that magnetization reversal could be accomplished with less expenditure of energy if the moments did not remain parallel during the reversal. They postulated a chain of spheres model in which the magnetization "fanned" in opposite directions for adjacent spheres along the chain. Wohlfarth<sup>192</sup>, using this model, calculated that the maximum effective value of the axial ration,  $m$ , was 1.4. This was less than



FIGURE 8

ELECTRON MICROGRAPH OF PARTICLES OF  $\gamma\text{-Fe}_2\text{O}_3$  WITH LENGTHS  $0.1 - 0.5\mu$  (REPRODUCED BY PERMISSION OF MINERALS, PIGMENTS AND METALS DIVISION, CHAS. PFIZER & CO. LIMITED).

Johnson and Brown's value of 1.6 obtained from magnetic measurements but much closer to it than to the value of 5 given by the electron microscope. The theory of incoherent reversal processes in single domain particles is discussed by Wohlfarth<sup>189, 189a</sup>.

Additional support for the incoherent mode of reversal in  $\gamma\text{-Fe}_2\text{O}_3$  particles was provided by the measurements of Bate<sup>14</sup> on tapes composed of oriented acicular particles. In Figure 9 is plotted the coercivity as a function of the angle between the direction of orientation and the applied field direction. A coherent reversal model leads to a monotonically decreasing coercivity with increasing angle while the incoherent models predict a peak in the angular dependence as was found experimentally.

When an assembly of single domain particles is rotated with respect to a steady magnetic field, the magnetization direction of the particles reverses discontinuously, absorbing energy which is not returned if the direction of specimen rotation is reversed. This is called "rotational hysteresis"  $W$ , and may be measured conveniently on a torque balance as a function of applied field. The rotational hysteresis integral  $\int_0^\infty (W/I_s) d(I/H)$  can then be calculated and compared with the predictions of the coherent and incoherent models:

<u>Theory</u>	{	Coherent rotation (Stoner, Wohlfarth <sup>165</sup> )	$\int_0^\infty (W/I_s) d(I/H)$	0.4
		Incoherent rotation (e.g., Jacobs, Luborsky <sup>86</sup> )		4.0
<u>Experiment:</u>	-	$\gamma\text{-Fe}_2\text{O}_3$ , (Bate <sup>14</sup> )		1.6

This provides further indication that the mechanism of magnetization reversal in single domain particles of  $\gamma\text{-Fe}_2\text{O}_3$  is one of incoherent rotation.

Flanders and Shtrikman<sup>59</sup> measured the distribution of particle switching fields involving only those particles lying at  $\sim 90^\circ$  to the applied field where only coherent processes should apply. They found that, when the particles studied were forced to switch coherently in this way, a close agreement was obtained between the "magnetic" axial ratio and that determined in the electron microscope.

Thus far only the contribution of shape anisotropy to the coercivity of the particles has been considered. In spherical single domain particles in which only magnetocrystalline anisotropy is effective the expression for

the coercivity is  $H_c = \frac{a |K_1|}{I_s}$  where "a" lies in the range 0.64 - 2.00.

The lowest value of a corresponds to a random assembly of particles.

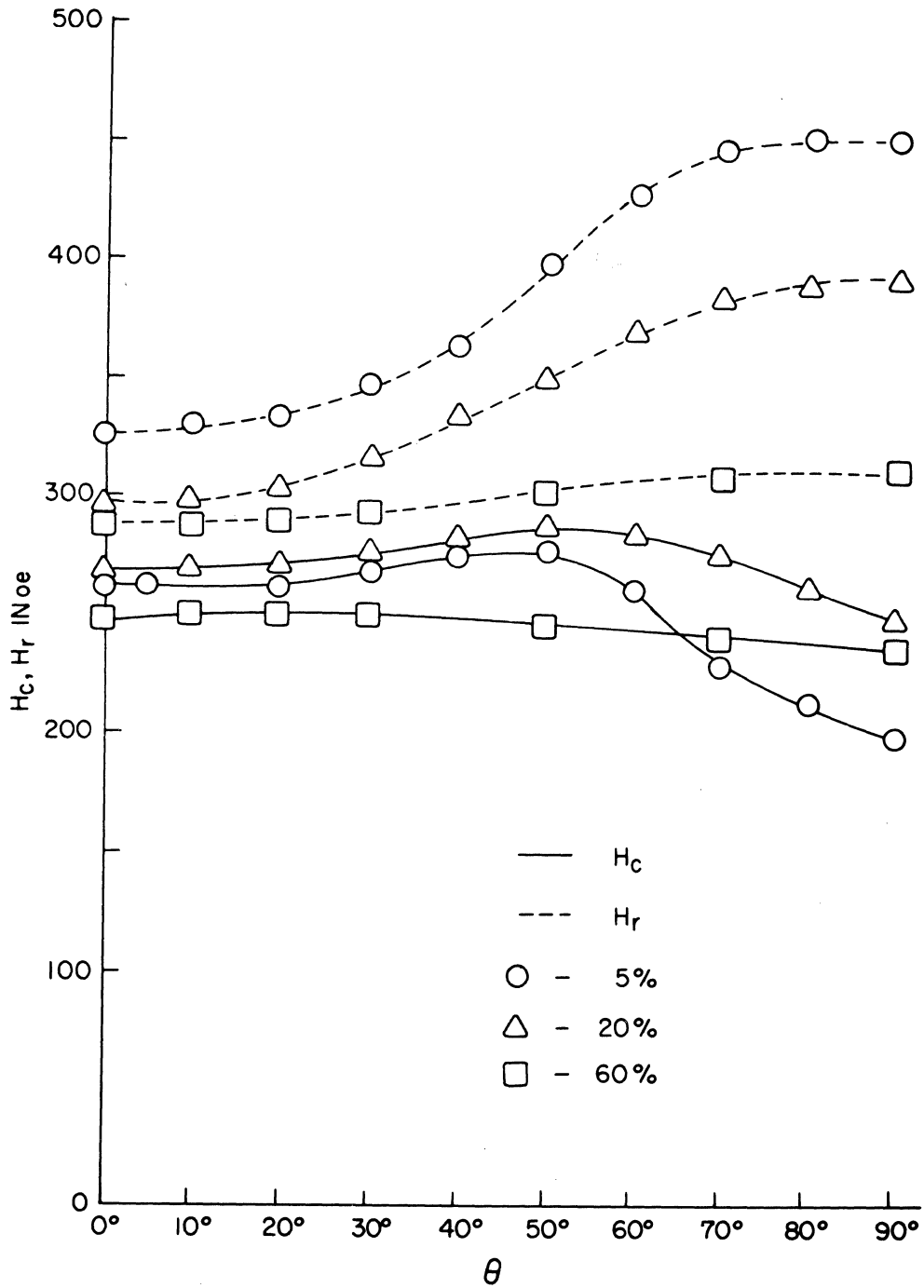


FIGURE 9

COERCIVITY  $H_c$ , AND REMANENCE COERCIVITY  $H_r$ , OF PARTIALLY ALIGNED ASSEMBLIES OF  $\gamma$ - $Fe_2O_3$  PARTICLES AS A FUNCTION OF THE ANGLE BETWEEN THE ALIGNMENT DIRECTION AND THE MEASUREMENT DIRECTION. (FROM BATE, JOURNAL OF APPLIED PHYSICS, 32, 239S, (1961).

On substituting  $|K_1| = 4.7 \times 10^4$  ergs/cm<sup>3</sup> and  $I_s = 390$  cmu/cm<sup>3</sup> one obtains  $H_c = 77$  Oe. which is considerably lower than the experimental values of 225 - 275 Oe. found for acicular particles but agrees with coercivity<sup>186</sup> of the spherical "Magnetophon" particles.

Further evidence that shape anisotropy predominates in the magnetization reversal process of acicular  $\gamma$ -Fe<sub>2</sub>O<sub>3</sub> particles is provided by the relatively temperature-independent coercivity of these particles. This is shown in Figure 10, over the temperature range 70-430°K. From the formula  $H_c = (N_b - N_a) I_s$  it will be seen that, since the shape (i. e.,  $N_b - N_a$ ) does not change and  $I_s$  decreases only slightly with increasing temperature, the independence of  $H_c$  and temperature is expected in this range. On the other hand, the anisotropy constants,  $K$ , usually are highly temperature dependent<sup>25</sup>. Johnson and Brown<sup>87</sup> also found that the particle shape distribution which they calculated was independent of temperature in the range 77-293°K. They concluded that the observed coercivity of their assemblies of  $\gamma$ -Fe<sub>2</sub>O<sub>3</sub> particles was controlled by the shapes of the particles and was not affected to any great extent by magnetocrystalline anisotropy nor by superparamagnetic effects.

Smith<sup>158</sup> found that the  $\langle 111 \rangle$  directions of magnetite crystals were the easy directions of magnetization. If this were also true for  $\gamma$ -Fe<sub>2</sub>O<sub>3</sub>, since the long particle axis is apparently  $[110]$  (van Oosterhout<sup>178</sup>), the two anisotropies (shape and magnetocrystalline) would cooperate to some extent to determine the magnetization direction with respect to the long axis of the particle.

#### Effect of Particle Size on Coercivity

Both the coherent model and the chain-of-spheres (fanning) model predict the independence of coercivity and particle size in the single domain region. However, the later and more sophisticated models of incoherent reversal which are based on the "micromagnetics" approach of Brown<sup>32</sup>, Strikman and Treves<sup>165</sup> consider other reversal processes (buckling and curling) and conclude that the coercivity decreases as the particle diameter increases. This behavior is found experimentally for both fine metal particles and particles of iron oxide (see Tables III and IV) and suggests that the magnetization reversal mode is one of buckling or curling.

In the electron micrographs of Figure 8 can be seen "cavities" in the acicular particles of  $\gamma$ -Fe<sub>2</sub>O<sub>3</sub>. However, there still exists a considerable difference of opinion concerning the exact nature of these features. Osmond<sup>134</sup> considered that the presence of voids was very likely in view of the evolution of oxygen during the preparation of the particles. He assumed that their effect on the (shape anisotropy dependent) coercivity was to replace  $I_s$  by  $VI_s$  in the formula ( $H_c = N_b - N_a$ ) $I_s$ ; where  $V$  is the volume fraction of cavities. Thus, the coercivity of a particle containing

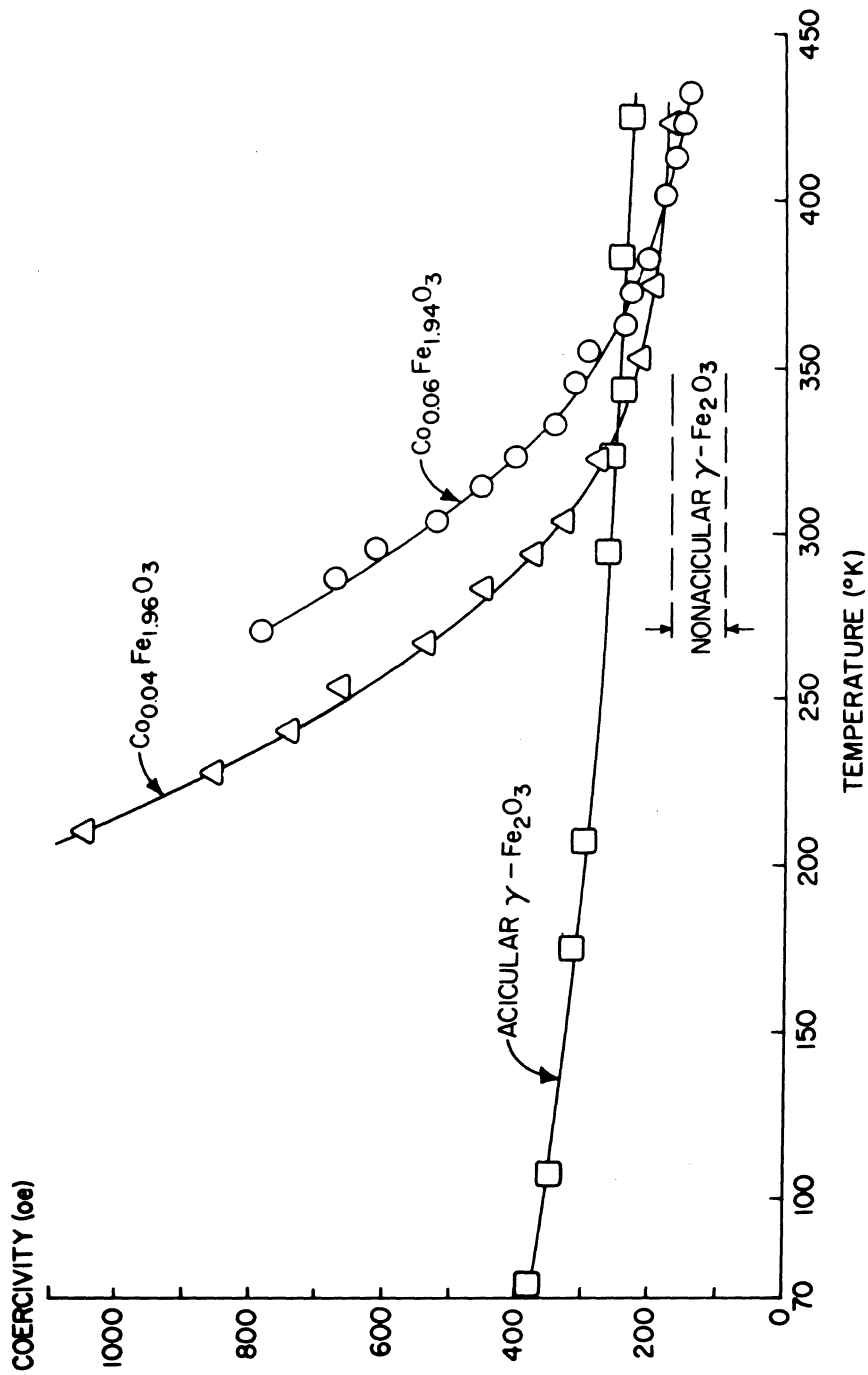


FIGURE 10

COERCIVITY AS A FUNCTION OF TEMPERATURE FOR PARTICLES OF  $\gamma$ -Fe<sub>2</sub>O<sub>3</sub> AND PARTICLES OF COBALT-SUBSTITUTED  $\gamma$ -Fe<sub>2</sub>O<sub>3</sub>. (FROM SPELIOTIS, MORRISON, BATE, PROC. INT. CONFERENCE, MAGNETISM, NOTTINGHAM, ENGLAND, p. 623, (1965).

voids should be less than that of a solid particle of the same dimensions. Consequently better agreement was obtained between the theoretical values of  $H_c$  (for coherent reversal) and the experimental results.

#### Effects of Particle Interactions

The theories of single domain behavior discussed above treated the particles as being so far apart that they were non-interacting. In practice, of course, this is far from being the case. Figure 11 is a photomicrograph of a partially-oriented assembly of  $\gamma$ - $Fe_2O_3$  particles coated on tape at very low loading, (5% of 40% for practical tapes). Even when great care is taken to prepare samples of dry powders for electron microscopy, it is a relatively rare event to observe a single isolated particle. Figure 12 is an electron micrograph of a particle of  $\gamma$ - $Fe_2O_3$  which is either lying across a smaller particle or has dendritic growths. The particle has been treated with colloidal iron oxide (Craik and Griffiths<sup>39</sup>) which is preferentially attracted to the magnetic poles. The distribution of colloid around the particles was found to be the same whether the powder had been a.c. demagnetized or not. This result suggested very strongly that the particles were single domains.

Néel<sup>128</sup> in 1947 discussed the effect of interactions on the coercivity of an assembly of particles by calculating the magnetostatic interaction energy. He obtained the formula  $H_c = H_{co}(1-p)$ ; where  $H_{co}$  is the coercivity of isolated particles and  $p$  is the packing factor. Only moderate agreement has been obtained between experimental results on powder and Néel's equation; the reasons for this were reviewed by Wohlfarth<sup>189</sup>.

Several attempts have been made recently to take account of particle interactions. These approaches were usually based on Preisach's<sup>139</sup> formal model in which a particle was assumed to have a symmetrical hysteresis loop when isolated but an asymmetrical loop of the same size when subjected to the fields of neighboring particles. This difficult and as yet largely unrewarding subject was recently reviewed critically by Wohlfarth<sup>190</sup>.

#### Remanence and Particle Alignment

The ratio of the remanent intensity to the saturation intensity of magnetization for a random assembly of uniaxial single domain particles was shown theoretically<sup>165</sup> and is found experimentally to be 0.5. We saw earlier that the output of a recording surface, at least at low frequencies, can be enhanced by increasing the remanent intensity of the surface and thus driving more flux through the reading head. Consequently the acicular  $\gamma$ - $Fe_2O_3$  particles in tapes are usually partially aligned during manufacture by passing them through a strong magnetic field ( $\geq 1000$  Oe.) while the coating is still fluid. In this way the ratio  $I_r/I_s$  measured along the alignment direction can be increased to 0.7 to 0.8; the value

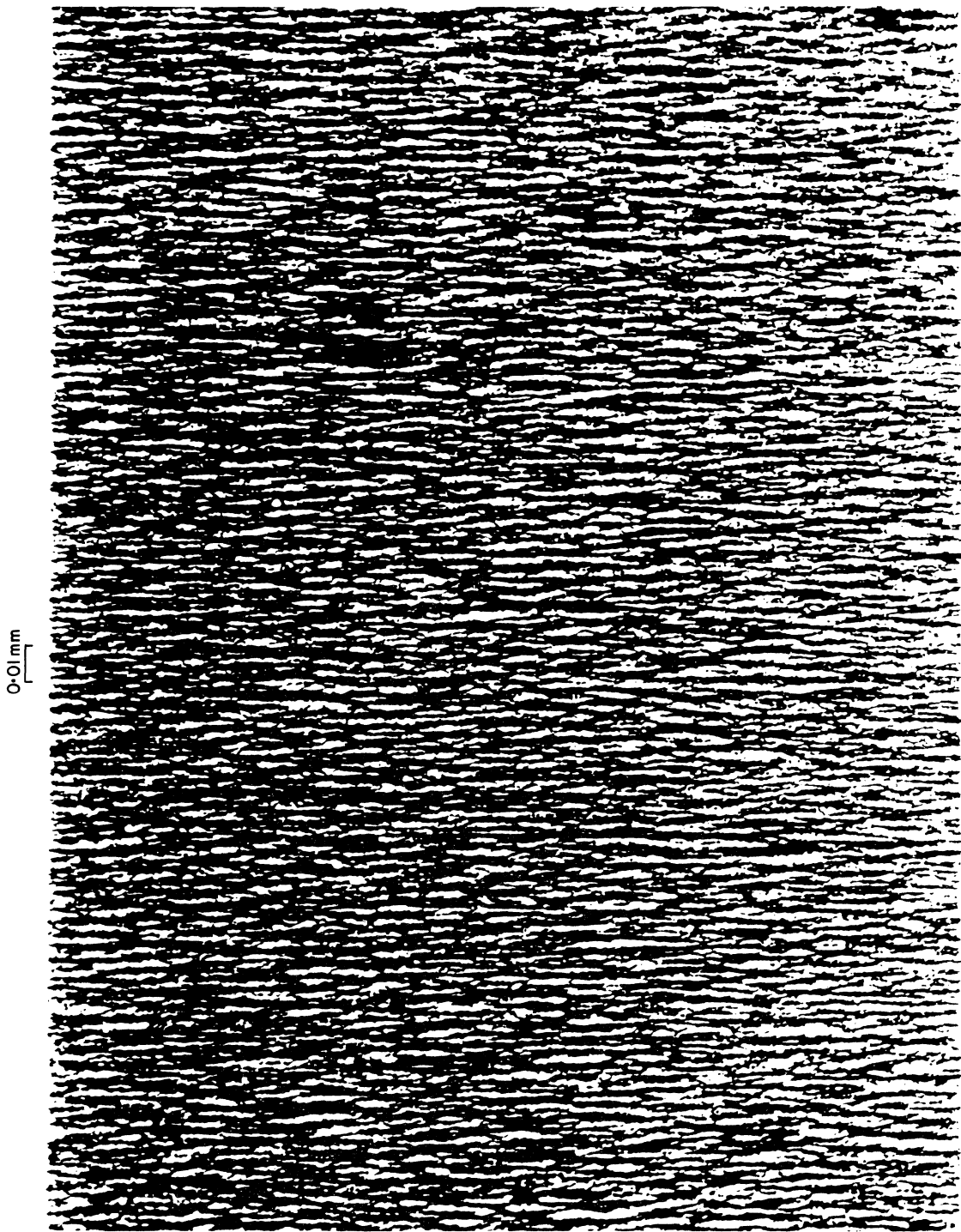


FIGURE 11

PHOTOMICROGRAPH OF AN ORIENTED TAPE CONTAINING 5% (BY VOLUME) OF  $\gamma$ - $\text{Fe}_2\text{O}_3$ . THE ORIENTATION WAS PRODUCED BY A FIELD OF 800 oe.





FIGURE 12

ELECTRON MICROGRAPHIC OF AN ACICULAR PARTICLE OF  $\gamma\text{-Fe}_2\text{O}_3$  TO WHICH BITTER PATTERN COLLOID HAS BEEN APPLIED. (BATE AND CAMERON, PREVIOUSLY UNPUBLISHED).

attained with a particular coating depending on the size, shape, packing fraction and degree of dispersion of the particles. The remanence is increased by orientation since, on average, the angle through which the magnetization must relax from the saturated to the remanent direction in each particle is reduced. Even without an orienting field the remanent magnetization curve for a tape sample is higher than that for a powder since, in the drying process, the particles are, in general, pulled into the plane of the coating. That is, instead of the spherically-random array of particles in the powder the particles in the tape coating form a planar array. However, this array is not quite random since some directionality is usually introduced by the coating process. The anhysteretic magnetization curve for  $\gamma$ -Fe<sub>2</sub>O<sub>3</sub> particle is also improved by aligning the particles.

Perfectly aligned and isolated single domain particles would have  $I_r/I_s = 1$  when measured along the alignment direction and  $I_r/I_s = 0$  at 90° to this direction. In practice, for a tape sample containing 40% by volume of  $\gamma$ -Fe<sub>2</sub>O<sub>3</sub>, these values would be 0.7 - 0.8 and  $\sim 0.4$  respectively. This discrepancy may be partially explained by the presence of multi-domain particles and by interactions between the particles but the principal cause is undoubtedly the imperfect particle alignment. Even the optical microscope reveals, as in Figure 11, a considerable amount of "cross-hatching" while in the electron microscope we find that, on a particle scale, there is gross misalignment.

Clearly then, since particle alignment leads to higher remanence and thus to higher output (at least, at densities below about 3,000  $\phi$ . c. i.) and probably to a smoother signal envelope, it is important to be able to produce well-aligned coatings. Unfortunately it is not simply a matter of applying a sufficiently large magnetic field to the particles during the drying process of the coating. Such a field would be quite ineffective unless the particle agglomerates had been broken down. Consequently the problem of obtaining a good dispersion of the particles must be tackled first. This is commonly achieved by adding dispersing agents to the particle-binder mixture but the precise details of the additives and the manner of their addition are usually shrouded in commercial secrecy. Iron oxide particles exhibit a strong attraction for water molecules<sup>71</sup> which, if not removed, hinder the proper wetting of the particles by the organic binder. Healey<sup>71</sup> et al. investigated the surface of a ferric oxide powder by water adsorption and calorimetric measurements and found that two thirds of the surface adsorbed water in the region of relative pressure where monolayer coverage is normally encountered.

The remainder of the surface chemisorbed water which could be released only by activation at temperatures up to 450° C. Thus the dispersing agents must not only assist in breaking down the particle agglomerates but also in wetting the particles so that they are firmly held in the coating.

Since the method of producing  $\gamma$ -Fe<sub>2</sub>O<sub>3</sub> particles was initially developed in many instances for the manufacture of paint pigments and since deflocculation is also important in these materials, we find references in this

literature to the use of dispersing agents. For example, the Marcot<sup>113</sup> patent already discussed described the coating of the iron oxide pigment particles with a lyophilic organic coating which serve, among other things, to improve the dispersibility of the particles. More specifically water-insoluble carboxylic acids, e.g., aleic, ricinoleic, naphthenic, etc, etc, were recommended. As these organic acids are soluble in aqueous alkaline solutions but insoluble in acids, they may conveniently be applied to the particles as an alkaline solution. The organic coating of the iron oxide particles are then treated with acid to render the coatings insoluble and dried at about 140° C. In this way a substantially monomolecular layer of the coating agent is obtained.

Another way of increasing the remanence of the tape coating would be to increase the proportion of magnetic particles in the coating. The requirement that the particles be sufficiently coated with binder so that they adhere firmly to each other and to the substrate places a practical limit on the packing fraction which is usually 38-40% of the total coating volume. Adams and Knees<sup>2</sup> proposed that this fraction could be increased by adding fatty diamine salts to the particle-binder mixture after milling. The role of the added salts was apparently to displace adsorbed gases on the surface of the particles and thus allow them to be wetted more effectively by the binder.

Two principal methods of mixing the particles and binder materials are used. In the first the ingredients are tumbled in a rotating mill which also contains steel or ceramic balls. In the second method the vessel remains stationary while the coating materials and the balls are stirred by means of a rotating axle with hardened steel arms attached radially to it. In either method the effect is to produce relative motion within the mixed ingredients which tends to break up agglomerates by shearing and to coat the individual particles with binder. The choice of ball size is important, and since the larger balls are more effective in breaking up large agglomerates and the smaller ones in producing a homogeneous final product, the ball size is often sequentially reduced during the milling process. The time of milling must also be controlled empirically since although the magnetic and physical characteristics of the mixture improve at first as a function of time, prolonged milling leads eventually to a deterioration of these properties. This is caused partly by a breaking up of the particles and partly by re-agglomeration as the coating of dispersant on the particles is removed. Finally the coating of the particle-binder mixture onto the substrate must be performed as soon as possible after the milling is completed if settling is to be avoided.

The point in the drying process at which the orienting field is applied is also important. If this is done too late, the viscosity of the coating does not permit alignment, while if it is done too early, disalignment may occur after the coating has left the region of the magnetic field. In practice the correct point must be established by experiment in each case. The magnetic fields used are usually in the range 1000-5000 Oe. and may

be conveniently obtained from one or more permanent magnets or by passing the coated substrate through a solenoid. In the latter case both d.c. and a.c. fields (or combinations of the two) have been found to be effective. Considerable particle agitation is produced by the use of a.c. fields, and this is apparently helpful in maintaining a good dispersion of the particles. The behavior of magnetic particles in d.c. fields and a.c. fields of differing frequencies was discussed by Dean and Davis<sup>45</sup> and by Stoller<sup>164</sup>.

Arrington<sup>7</sup> observed that while the orientation ratio (remanence parallel to alignment direction: remanence perpendicular to this direction) is often as high as 2:1 in tapes containing oriented acicular particles, there is little evidence of crystallographic orientation in x-ray diffraction experiments. He showed that if the usual orientation procedures involving d.c. and/or a.c. fields is followed by a mechanical stretching of the coating, very much greater orientation ratios as high as 8:1 could be achieved. Furthermore, in these coatings at least 50% of the total normalized azimuthal x-ray diffraction intensity was within an angle of  $14^\circ$  of the direction of orientation. The values of  $I_r/I_s$  (parallel) were  $\sim 0.90$  and  $I_r/I_s$  (perpendicular)  $\sim 0.10$  compared with the ratios of 0.75 and 0.35 found in oriented commercial tapes. However, since the elongation of the coating should be at least 100% of the original dimension, the application of the technique to tape production would not be without problems.

If only the level of the output signal obtainable from the recording surface is considered then the most appropriate direction of particle alignment is clearly along the direction of travel. However, in high-density digital recording, resolution of adjacent pulses is equally important. Bate et al.<sup>18</sup> showed that the resolution could be improved appreciably by orienting the particles at a large angle to the direction of tape travel. The outward shift of the peaks of two adjacent pulses was steadily reduced as the alignment angle  $\theta$  was increased from  $0^\circ$  (along the direction of travel) to about  $70^\circ$ . The output signal also decreased with increasing angle, and so a compromise between signal level and pulse resolution must be made. However, the rate of decrease of output with angle is lower, and it was found that at  $\theta \approx 45^\circ$  the peak shift had decreased by more than 50% while output was rather less than 20% below its value at  $\theta = 0^\circ$ .

#### $\gamma$ -Fe<sub>2</sub>O<sub>3</sub> versus Fe<sub>3</sub>O<sub>4</sub> Particles

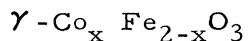
The use of  $\gamma$ -Fe<sub>2</sub>O<sub>3</sub> particles for magnetic recording purposes is much more common than that of Fe<sub>3</sub>O<sub>4</sub> particle and yet the reasons for this preference are at first difficult to see since the magnetic properties of the two oxides are so similar. Actually the saturation intensity of Fe<sub>3</sub>O<sub>4</sub> particles (Table III) is 20% higher than that of  $\gamma$ -Fe<sub>2</sub>O<sub>3</sub> particles which should lead to a higher signal output at least at low recording densities. Furthermore, the coercivity of Fe<sub>3</sub>O<sub>4</sub> particles is usually higher by about 15% than the coercivity of  $\gamma$ -Fe<sub>2</sub>O<sub>3</sub> particles of the same size and shape,

and this would tend to balance the adverse effect of the higher magnetization intensity at high recording densities. Finally, as acicular  $\text{Fe}_3\text{O}_4$  particles are usually produced in the preceding step to the formation of  $\gamma\text{-Fe}_2\text{O}_3$ , the manufacturing process (and cost) should be somewhat lower.

Nevertheless there is considerable reluctance in the industry to use  $\text{Fe}_3\text{O}_4$  particles for several reasons not all of which, by any means, appear to be well documented in the literature. The first reason concerns the thermal properties of the particles. The magnetocrystalline anisotropy constant of  $\text{Fe}_3\text{O}_4$  is higher and consequently the coercivity decreases more rapidly with increasing temperature than is the case with  $\gamma\text{-Fe}_2\text{O}_3$  particles. Furthermore, since  $\text{Fe}_2\text{O}_3$  represents a higher oxidation state, there will be a tendency for the  $\text{Fe}_3\text{O}_4$  particles, particularly the smaller ones, to oxidize. Thus the long term stability of information stored on  $\text{Fe}_3\text{O}_4$  surfaces may be suspect, but this is not at all well-established. Secondly, magnetic accommodation effects appear to be more pronounced in  $\text{Fe}_3\text{O}_4$  particles which means that it is difficult to demagnetize the recording surfaces by simply using a diminishing a. c. field. This disadvantage would, of course, be more serious for analog than for digital recording.

The last disadvantage of  $\text{Fe}_3\text{O}_4$  particles concerns the phenomenon of "print-through" in recording tapes. This occurs when the tape is wound on a reel. The recorded messages on adjacent layers are separated only by the thickness of the substrate (1-1.5 mils, 25-38 $\mu$ ). Consequently each recorded pattern experiences a magnetic field from neighboring layers which may be sufficient to change the state of magnetization of the pattern. This can be particularly noticeable and objectionable in the case, for example, of audio tapes where a low-level signal is sometimes heard from what should be a silent (i. e., demagnetized) part of the tape. As the fields involved are small compared with those used in writing, a recording surface will be resistant to print-through if its remanence is not susceptible to small fields. Thus the curve of remanence as a function of applied field should show negligible remanence until a critical field of about 150 Oe. is reached after which it should rise steeply (and linearly for analog recording) to its maximum value. Recording surfaces made of  $\text{Fe}_3\text{O}_4$  particles are traditionally regarded as being more subject to print-through than are those of  $\gamma\text{-Fe}_2\text{O}_3$  particles.

## IRON-COBALT OXIDE PARTICLES



Smaller particles than those of the conventional  $\gamma\text{-Fe}_2\text{O}_3$  are desirable for some recording applications since, possessing higher coercivities, they are better able to withstand the effects of internal and external demagnetizing

fields. Thus for this reason and because their background noise level is lower and the recording surfaces are potentially smoother, they should be particularly useful for recording at high frequencies, i. e., at high bit densities. To avoid dangers of thermal instability, the average particle size should not be close to the lower end of the single domain range since there is always a finite width to the size distribution function.

Bickford et al.<sup>25</sup> showed that the substitution of a small amount of cobalt for iron in magnetite single crystals (i. e.,  $\text{Co}_x\text{Fe}_{3-x}\text{O}_4$ ) caused a large increase in the magnetocrystalline anisotropy. Kroner<sup>99</sup> added from 2 to 10 at % cobalt to cubic-shaped iron oxide particles of about  $0.1\mu$  in size and observed an increase in coercivity from 100 Oe. to about 800 Oe. Nobuoka et al.<sup>131</sup> described a method of preparing similar particles. They co-precipitated cobalt and iron hydroxides from an alkaline solution of ferric chloride ( $\text{FeCl}_3 \cdot 6\text{H}_2\text{O}$ ) and cobaltous nitrate ( $\text{Co}(\text{NO}_3)_2 \cdot 6\text{H}_2\text{O}$ ) and heated the mixture at 130-170° C. under pressure in an autoclave to obtain a fine grained crystalline precipitate. This precipitate was then rinsed, dried and heated in a reducing atmosphere at 350-400° C. after which the composition presumably was that of cobalt-substituted magnetite. Finally the particles were re-oxidized at 200-550° C. to form cobalt-substituted  $\gamma$ - $\text{Fe}_2\text{O}_3$  in which the cobalt content was in the range 0.2-30%.

An alternative method of preparing cobalt-substituted  $\gamma$ - $\text{Fe}_2\text{O}_3$  was given by Arshinkov et al.<sup>8</sup>. They precipitated a mixed iron-cobalt oxalate from an aqueous solution of ferrous sulphate and cobalt nitrate by the addition of oxalic acid. The precipitate was rinsed, dried at 105° C. and finally decomposed to the oxide at 385° C. Powders containing from 2 to 30% cobalt were made in this way and found to have the following magnetic properties:

Cobalt Content	$H_c$	$B_r$	$(BH)_{\max}$
2%	275 Oe.	1193 gauss	$0.14 \times 10^6$ gauss Oe.
9%	1100	1680	$0.60 \times 10^6$
30%	830	1070	$0.22 \times 10^6$

The thermomagnetic properties of particles of cobalt-substituted  $\gamma$ - $\text{Fe}_2\text{O}_3$  were studied by Speliotis et al.<sup>162</sup>. These particles were found by electron microscopy to be cubic and to be of quite uniform size ( $0.05 - 0.08\mu$ ). The saturation intensity of magnetization for the powder which contained 2% cobalt was found to be about 12% lower than that of  $\gamma$ - $\text{Fe}_2\text{O}_3$  and to be independent of temperature in the range studied (200-450°K). The remanent intensity however, decreased with increasing temperature much more rapidly than occurred with  $\gamma$ - $\text{Fe}_2\text{O}_3$ .

Most ferrites including  $\text{Fe}_3\text{O}_4$  have a negative first-order anisotropy constant  $K_1$ , i. e., the easy axes of magnetization are  $\langle 111 \rangle$ . However, Bickford et al.<sup>25</sup> found that for cobalt-substituted magnetite crystals  $K_1$  was positive at least up to a temperature of 450° C. Thus the easy axes

became  $\langle 100 \rangle$  and there are then six equivalent easy directions of magnetization. Wohlfarth and Tonge<sup>193</sup> calculated for a completely random spatial distribution of identical particles the dependence of  $I_r/I_s$  on the number ( $n$ ) of equivalent easy axes possessed by each particle. For  $n = 6$  they found that  $I_r/I_s = 0.825$  and this value is very close to that found experimentally at low temperatures for the cobalt-substituted  $\gamma$ - $\text{Fe}_2\text{O}_3$  powders.

The particles used in these experiments were relatively small ( $\sim 0.1$  x length of typical acicular  $\gamma$ - $\text{Fe}_2\text{O}_3$  particles) and consequently at high temperatures it is possible that some crossed the threshold into the superparamagnetic region. This led to the low values of  $I_r/I_s$  observed at the higher temperatures.

In their temperature dependence of coercivity the acicular ( $\gamma$ - $\text{Fe}_2\text{O}_3$ ) and the non-acicular (cobalt-substituted  $\gamma$ - $\text{Fe}_2\text{O}_3$ ) showed a difference in behavior which is even more pronounced. This is shown in Figure 10. Bickford et al.<sup>25</sup> reported that first-order anisotropy constant in cobalt-substituted magnetite increased linearly with cobalt content for small amounts of cobalt. Since the saturation magnetization intensity of cobalt-substituted

$\gamma$ - $\text{Fe}_2\text{O}_3$  was found to be independent of temperature, the temperature dependence of  $H_c$  shown in Figure 10 can be interpreted as arising from changes in a resultant anisotropy coefficient  $K$  (where  $H_c \sim \frac{K}{I_s}$ ). It was found that, over the temperature range studied, the increase in coercivity on substituting 3 at. % Co in  $\gamma$ - $\text{Fe}_2\text{O}_3$  was roughly a factor of 1.5 times the effect of substituting 2 at. % cobalt. Thus the anisotropy additivity effect observed by Bickford in cobalt-substituted magnetite appears also to be present for small amount of cobalt substituted in  $\gamma$ - $\text{Fe}_2\text{O}_3$ . Since these particles are non-acicular and have a markedly temperature dependent coercivity which at room temperature is higher than that of an assembly of

$\gamma$ - $\text{Fe}_2\text{O}_3$  particles, it is concluded that the dominant anisotropy is magnetocrystalline and that it is attributable to the substitution of  $\text{Co}^{2+}$  ions. Slonczewski<sup>156</sup> showed theoretically how the increased anisotropy could arise in cobalt-substituted magnetite by assuming that the  $\text{Co}^{2+}$  ions replace some of the  $\text{Fe}^{2+}$  ions on the octahedral sites of the spinel. It appears likely that a modification of this theory can be used to explain the effects of substituting cobalt for iron in  $\gamma$ - $\text{Fe}_2\text{O}_3$ .

Particles which derive their magnetic hardness from magnetocrystalline anisotropy are expected to show less dependence on particles interactions than those possessing shape anisotropy. In the latter case the presence of neighboring particles may completely change the flux distribution around a given particle and thus change its effective demagnetizing factors. For systems of isolated particles Wohlfarth<sup>191</sup> showed that the following relation between remanence values should hold:

$I_D(H) = I_R(\infty) - 2I_R(H)$  where  $I_R(\infty)$  is the remanent intensity which exists after a saturating field has been applied in one direction (say positive); if this is

followed by a field  $H$  in the negative direction then  $I_D(H)$  is the remanent intensity.  $I_R(H)$  is the remanent intensity after a field ( $+H$ ) has been applied to a sample in an a.c. demagnetized state. The relation is based on the assumption of no particle interactions and Bate<sup>15</sup> used the discrepancy between the experimental values of  $I_R(H)$  and those predicted by the relation as a measure of the importance of particle interactions in the sample. The results of this test are shown in Figure 13 in which the circles mark the experimental points and triangles mark the points calculated from the formula after measuring  $I_D(H)$  and  $I_R(\infty)$ . Figure 13 shows the results obtained for a 20% (by volume) non-oriented assembly of  $\gamma$ - $\text{Fe}_2\text{O}_3$  particles and the results for a 40% sample of cobalt-substituted  $\gamma$ - $\text{Fe}_2\text{O}_3$ . It is clear that, even though the  $\gamma$ - $\text{Fe}_2\text{O}_3$  sample is more dilute, the deviation between the curves is much more pronounced and thus, interactions are more important in this case than in the cobalt-substituted material.

In materials with many easy directions of magnetization these directions are obviously separated from each other by relatively small angles. Thus as Wohlfarth and Tonge<sup>193</sup> showed, the ratio  $I_r/I_s$  will always be higher than for, say, a random spatial array of uniaxial particles. Hence there is not so much improvement in  $I_r/I_s$  to be made by orienting the particles in a magnetic field, and this step is usually omitted.

The small, non-acicular particles of cobalt substituted  $\gamma$ - $\text{Fe}_2\text{O}_3$  show superior recording properties (higher output and lower peak-shift) when compared with the performance of the usual acicular  $\gamma$ - $\text{Fe}_2\text{O}_3$  material. This is presumably attributable to their higher coercivity at room temperature. However, the sharply temperature-dependent coercivity could be distinctly disadvantageous for some recording applications. It has been found in this laboratory<sup>126</sup> that storage for short periods at elevated temperatures results in a permanent decrease in the signal output. For example tapes stored at  $160^\circ\text{C}$ . for 20 minutes lost roughly 50% of their output at densities up to 100 b.p.i.; the percentage decrease at higher densities was less, however.

It was also observed that the action of running a tape-loop sample repeatedly over a recording head generated enough heat by friction to cause a considerable reduction in signal output. In contrast, tapes of  $\gamma$ - $\text{Fe}_2\text{O}_3$  showed virtually no decrease in signal under the same conditions. On re-recording onto the iron-cobalt oxide tapes the full signal level returned at first and then the output again diminished with running time. This phenomenon was apparently a thermal effect rather than a stress effect since the application of very large stresses to the recorded tape had no effect on the signal level. The conditions of these experiments were admittedly severe but the effects observed were large and suggest a potentially serious disadvantage in the use of cobalt-substituted iron oxide particles in applications where high temperatures are encountered during storage or generated in use.



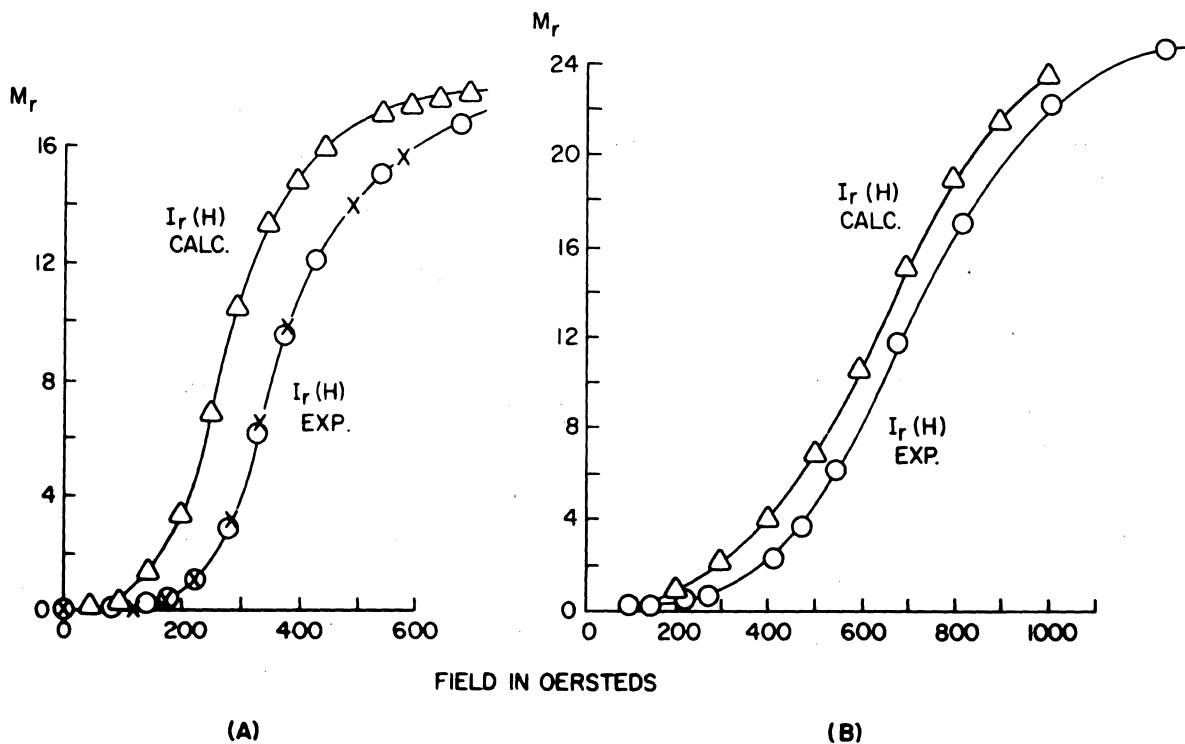


FIGURE 13

GROWTH - OF - REMANENCE CURVES FOR A)  $\gamma$ - $\text{Fe}_2\text{O}_3$  PARTICLES, B) COBALT-SUBSTITUTED  $\gamma$ - $\text{Fe}_2\text{O}_3$  PARTICLES. THE CURVES LABELLED " $I_r(H)$  calc." WERE CALCULATED ON THE ASSUMPTION OF NO PARTICLE INTERACTIONS. THE EXPERIMENTAL CURVE ( $I_r(H)$  exp) FOR THE NON-ACICULAR, COBALT-SUBSTITUTE PARTICLES IS CLOSER TO THE CALCULATED CURVE THAN IS THE CASE WITH ACICULAR  $\gamma$ - $\text{Fe}_2\text{O}_3$  PARTICLES, SHOWING THE GREATER IMPORTANCE OF PARTICLE INTERACTIONS IN THE LATTER CASE. (AFTER SPELIOTIS, MORRISON, BATE, PROC. INT. CONFERENCE, MAGNETISM, NOTTINGHAM, ENGLAND, p. 623 (1965).

## Cobalt-substituted Magnetite, $\text{Co}_x\text{Fe}_{3-x}\text{O}_4$

Sato et al.<sup>146</sup> prepared particles of cobalt-substituted magnetite and studied the effect of cobalt content (x) on the magnetic properties. They obtained particles which were roughly cubic and whose average size decreased with increasing cobalt content from  $0.2\mu$  at  $x = 0.1$  to  $0.1\mu$  at  $x = 1.0$ . The magnetic properties changed with cobalt content in the following way: as x increased from 0 to 1.0, the saturation magnetization intensity decreased from  $\sigma_s = 87$  emu/gm to 65 emu/gm, the remanent intensity increased from 8 emu/gm to 42 emu/gm and the coercivity increased from 100 to 980 Oe.

Sigiura<sup>167</sup> showed that uniaxial anisotropy could be induced by magnetic annealing single crystals of  $\text{Co}_{0.8}\text{Fe}_{2.2}\text{O}_4$ . This suggests a possible method by which the undesirable thermal effects in the cobalt-substituted iron oxide powders might be overcome.

The composition  $\text{CoFe}_2\text{O}_4$  corresponds to the substitution of  $\text{Co}^{2+}$  for all the divalent iron ions in magnetite. A method of preparing fine powders of this material was given by Schuele and Deetscreek<sup>151</sup>. Aqueous solutions of cobalt chloride and ferric chloride (in molar proportions of 1:2) were added to boiling sodium hydroxide solution and the mixture was vigorously stirred. The resulting precipitate was shown by x-ray diffraction to contain only the inverted spinel  $\text{CoFe}_2\text{O}_3$ . The particles produced in this way were extremely small and were encouraged to grow by being heated for many hours ( $\sim 8-400$ ) in the solution in which they were precipitated. This had the effect of dissolving the smaller particles and of increasing the size of the larger ones. The magnetic properties could then be studied as a function of particle size (i. e., growing time) but unfortunately no quantitative estimates of the particles sizes were given. Earlier results by Berkowitz and Schuele<sup>23</sup> on  $\text{CoFe}_2\text{O}_3$  micro-powders have coercivities in the range 100-2100 Oe. (at room temperature and  $I_r/I_s \leq 0.5$  for particles of crystallite size from 70-2000  $\text{\AA}$ ). The highest coercivities were obtained with powders having particle size (determined by x-ray line broadening and electron micrographs) in the range 300-700  $\text{\AA}$ .

## OTHER FERRITE PARTICLES

A wide variety of ferromagnetic particles may be made by substituting divalent metallic ions ( $\text{Me}^{2+}$ ) for the  $\text{Fe}^{2+}$  ions in magnetite (ferrous ferrite,  $\text{FeO} \cdot \text{Fe}_2\text{O}_3$ ). In general the coercivities of these particles are found to be considerably higher than that of magnetite particles; coercivities  $\geq 1000$  are not uncommon. However, the saturation magnetization is decreased as can be seen from the following table of Smit and Wijn<sup>157</sup> from some simple ferrites with the spinel structure:

Table I

<u>Ferrite</u>	$\sigma_s$ emu/gm	$I_s$ emu/cc	$4\pi I_s$ gauss	$\theta_c$ °C
$Fe_3O_4$	92	480	6000	585
$MnFe_2O_4$	80	400	5000	300
$CoFe_2O_4$	80	425	5300	520
$NiFe_2O_4$	50	270	3400	585
$CuFe_2O_4$	25	135	1700	455
$MgFe_2O_4$	27	120	1500	440
$Li_{0.5}Fe_{2.5}O_4$	65	310	3900	670

The values given for the saturation magnetization are those measured at 20° C.

The variety of materials available is very large since  $Fe_3O_4$  and  $Me^{2+}Fe_2O_4$  are the limiting compositions and there exist other ferrites of intermediate composition given by  $Me^{2+}_xFe_{3-x}O_4$ . The intrinsic magnetic properties ( $\sigma_s$ ,  $\theta_c$ ) are found to vary smoothly with composition throughout the range. Furthermore mixed ferrites of general composition  $A_xB_yFe_{3-(x+y)}O_4$  etc., etc. are frequently encountered. The preparation and properties of a few representative ferrites which have either been used or proposed for recording surface will now be considered.

#### $Cu_xFe_{3-x}O_4$

Downs<sup>46</sup> described a method of preparing fine particles of copper-iron ferrite in which either synthetic magnetite ( $Fe_3O_4$ ) or synthetic goethite  $\alpha-(FeO)OH$  powder was heated with a suitable preparation of cupric oxide or carbonate at 730-1040° C. The ferrite powders produced in this way ranged in composition from  $Cu_{0.6}Fe_{2.4}O_4$  to  $CuFe_2O_4$ . The coercivity of particles having these compositions were respectively 500 Oe. and 290 Oe. No values of the saturation magnetization nor  $I_r/I_s$  were given, however, it can be seen from Table I that the value of  $\sigma_s$  for  $CuFe_2O_4$  is 25 emu/gm cf. 92 emu/gm for magnetite.

#### Cobalt-iron Ferrites

Fukuda et al.<sup>65</sup> discussed the improvements in magnetic properties of

various cobalt-iron ferrites which were brought about by magnetic annealing prior to coating. The method was to heat the powder, which was in a closed tube filled with nitrogen, to a temperature of 200° C. - 500° C. for about 30 minutes in a d.c. magnetic field ( ~ 1000 Oe. ). The particles were then slowly cooled also in the presence of the field. In some cases the particles were agitated by means of an ultrasonic wave (at 80 kc.) during the magnetic annealing. During the coating process the particles were aligned in a d.c. field of 500 Oe. and an a.c. field of 200 Oe. at 10 kc.

The magnetic annealing was carried out at temperatures below those at which sintering of the ferrites would occur ( ~ 600° C. ) and resulted in an increase of both coercivity and remanence. The results are given in the following table:

Table II

Ferrite	Coercivity		Remanence of coated tapes, $4\pi I_r$		Ir/Is	
	anneal	no anneal	anneal	no anneal	anneal	no anneal
$\text{Co}_{0.06} \text{Ni}_{0.15} \text{Fe}_{2.79} \text{O}_4$	300 Oe.	240	1150 gauss	670	0.84	0.65
$\text{Mg}_{0.06} \text{Ni}_{0.15} \text{Co}_{0.42} \text{Fe}_{2.37} \text{O}_4$	1030	850	980	550	0.85	0.61
$\text{Co}_{0.09} \text{Mn}_{0.29} \text{Fe}_{2.67} \text{O}_4$	305	200	980	630	0.81	0.60
$\text{Co}_{0.33} \text{Fe}_{2.67} \text{O}_4$	1100	870	1200	700	0.80	0.66

Assuming a particle fraction of ~ 0.40, the remanence of these ferrite tapes is close to but somewhat below that of oriented  $\gamma$ -Fe<sub>2</sub>O<sub>3</sub> tapes of the same loading.

#### FERRITES WITH HEXAGONAL STRUCTURE

The ferrite materials which have been considered thus far have had the cubic spinel structure. There also exist ferrites, of which the most common example is barium ferrite Ba Fe<sub>12</sub>O<sub>19</sub> (= BaO.6 Fe<sub>2</sub>O<sub>3</sub>), which have the complex hexagonal close packed structure of the mineral magnetoplumbite (Smit and Wijn<sup>157</sup> p. 180). The characteristic feature of these materials is their extremely high coercivity; this is often > 1000 Oe. at room temperature.

#### Barium Ferrite, BaO.6Fe<sub>2</sub>O<sub>3</sub>

The usual method of preparation of the hexagonal ferrites is to heat to-

gether appropriate mixtures of oxides at temperatures sufficiently high to produce sintering of the particles. Then, since high coercivities are found only in the powdered material, it is necessary to grind the sintered ferrite and so produce particles whose size is  $\sim 1\mu$ . The effect of grinding on the magnetic properties will be discussed later.

Other methods of preparation which have been used are electrolytic coprecipitation<sup>22</sup> and chemical precipitation techniques<sup>118</sup> in which such satisfactory initial mixing of the oxides is obtained that only relatively low firing temperatures are needed. This has the advantage that the ferrites are formed without sintering and consequently grinding is unnecessary. Mee and Jeschke<sup>118</sup> used the chemical method to produce particles in the form of small platelets with diameters in the range 800-1500 Å and with diameter to thickness ratios of about 15 to 1.

The magnetic moment per formula unit  $\text{BaO} \cdot 6\text{Fe}_2\text{O}_3$  is obtained as follows: The moments of the seven octahedral  $\text{Fe}^{3+}$  ion and the ion in the close-packed oxygen layer containing the barium ion are opposed by the moments of the two octahedral and two tetrahedral  $\text{Fe}^{3+}$  ions. Since all the magnetic ions are  $\text{Fe}^{3+}$  having a magnetic moment of  $5\mu_B$ , the magnetization per formula unit is  $(1 + 7 - 2 - 2) \times 5\mu_B$ . Smit and Wijn<sup>157</sup> reported that this agreed with the experimental measurements on polycrystalline barium ferrite at liquid hydrogen temperature and corresponds to a value of  $\sigma_s$  of 100 emu/gm. At room temperature this decreases to 72 emu/gm or 380 emu/cc. Torkar and Fredriksen<sup>173</sup> found that the saturation magnetization of small single domain particles of barium ferrite gave values of saturation magnetization which were slightly smaller than this; Mee and Jeschke<sup>118</sup> found  $\sigma_s = 68$  emu/gm for their  $0.1\mu$  particles. The Curie temperature of barium ferrite is  $450^\circ\text{C}$ .

Smit and Wijn<sup>157</sup> observed that, while grinding the sintered ferrite was necessary to produce the desirable single domain behavior, prolonged grinding resulted in a subsequent decrease in coercivity. They attributed this decrease to a plastic deformation of the particles and supported their arguments with experimental results on annealing the particles at a temperature of  $\sim 1000^\circ\text{C}$ . (below the sintering temperature). On annealing for an hour in air the coercivity of a powder sample increased from 1600 Oe. to 3400 Oe. However, Tenzer<sup>170</sup> ascribed this change to a sintering of the superparamagnetic particles to single domain size.

He interpreted the effects of grinding on coercivity in terms of changes in particle size through the range multidomain--single domain--superparamagnetic. That is, after sintering the particles are multidomains and, as the particle size is reduced on grinding, they become first single domains and ultimately superparamagnetic particles. The peak in the curve of the  $H_c$  vs. grinding time shifts to longer times (i.e., smaller particles) as the temperature at which  $H_c$  was measured is lowered. This behavior is consistent with the postulated transition from single domain to superparamagnetic particles since this transition is expected to be strongly

temperature sensitive. The critical (upper) size for single domain behavior was given by Smit and Wijn<sup>157</sup> (p. 321) as  $0.5 \mu$ . In comparison the calculated value of the thickness of a domain wall in barium ferrite was  $\frac{2}{10^{-6}}$  cm. They give the critical (upper) diameter as proportional to  $\sqrt{\frac{K_1}{I_s}}$  where the first-order anisotropy constant  $K_1 = +3.3 \times 10^6$  erg/cc. This quantity increases with increasing temperature until it begins to fall rapidly to zero in the vicinity of  $\theta_c$ .

Heimke<sup>72</sup> considered that the two principal factors in the coercivity of barium ferrite particles were a) particle size and b) the presence of dislocations induced by the process of grinding. Van Oosterhout and Klomp<sup>18</sup> after investigating the effect of grinding time on the magnetic properties of magnetite and zinc ferrite, concluded that the main effect of grinding was the accumulation of dislocations in the particles up to a maximum concentration determined by the temperature during grinding process. Their view of the role of dislocations is not as a hindrance to the movement of Bloch walls but rather as finite islands of highly (and non-uniformly) stressed material in which  $H_c = \frac{\lambda \sigma_s}{I_s}$  where  $\lambda$  is the saturation magnetostriction. However, Tenzer<sup>170</sup> found that on subjecting the barium ferrite particles to high pressures ( $\sim 10^5$  psi) the coercivity increased by about 15%. Since this treatment should result in a reduction in the number of dislocations in the particles, it appears that the effect of dislocations on coercivity is not important in the high-coercivity barium ferrite particles. The action of applied pressure is probably somewhat similar to that of sintering in that the smaller particles which are more subject to thermal fluctuations, are joined to become stable single domain particles. Pressures  $> 8000$  psi, however, result in further sintering to give multidomain particles and reduced coercivities<sup>171</sup>.

Shtol'ts<sup>154</sup> studied the effect of sintering temperature on coercivity. He found that while material prepared at  $1400^\circ$  C. was coarse-grained and of low coercivity ( $\sim 20$  Oe.) the ferrite prepared at  $1200^\circ$  C. was fine grained and of high coercivity ( $\sim 2000$  Oe.). On grinding the two materials to the same average particle size ( $\sim 2 \mu$ ) the coercivity of the former increased to  $\sim 550$  Oe. and that of the latter decreased to  $\sim 1500$  Oe. The saturation magnetization  $\sigma_s$  decreased from 70-65 emu/gm and 67-49.5 emu/gm respectively. Shtol'ts concluded from these observations that not only was the crystal structures of the two materials different but also that the structure changed on grinding.

Mee and Jeschke<sup>118</sup> found their  $0.1 \mu$  plate-like particles to have the extremely high coercivity of 5350 Oe. at room temperature. They assumed that the magnetocrystalline easy direction was normal to the plates and that this was opposed by the shape anisotropy of the particles. Thus for a random array of particles  $H_c = 0.48 \left[ \frac{2K}{I_s} - 4\pi I_s \right]$ . Good agreement was found between the theoretical curve and the measured values of the precipitated barium ferrite. Furthermore, since the contribution of the crystalline term to the expression for  $H_c$  is a factor of 3-4 times larger

than that of the shape factor, it is to be expected that particle interaction effects would not be important in these particles. This suggests strongly that the Stoner-Wohlfarth theory of isolated single domain particles in which the magnetization reversal process is one of coherent rotation applies to the small particles of barium ferrite.

The anisotropy constants of higher order than  $K_1$  are apparently negligible in barium ferrite. Furthermore, the magnetization  $I_s$  and  $K_1$  change with temperature at almost the same rate (Smit and Wijn, p. 205) thus the anisotropy field,  $H_a = \frac{2K_1}{I_s}$  is practically independent of temperature in the range 100 - 500°K. Consequently single domain particles of barium ferrite, unlike those of cobalt-substituted iron oxide, are quite stable with respect to changes in temperature.

### Substituted Barium Ferrites and Related Materials

The principal objection to the use of barium ferrite as a material for magnetic recording purposes is that the coercivity is usually so high that it is beyond the writing and erasing capabilities of present heads. The high coercivity is caused by the high magnetocrystalline anisotropy with a single easy direction of magnetization along the "c" -axis, i. e., perpendicular to the basal plane of the hexagonal structure. However, there exists a group of substituted barium ferrites in which the basal plane is the easy plane and the c-axis is an unpreferred direction of magnetization. These materials were discussed by Jonker et al.<sup>88</sup> and by Stuijts and Wijn<sup>166</sup>. The anisotropy constant in these materials is usually lower than that of ordinary barium ferrite and also there are six equivalent easy directions in the basal plane. Thus we should expect the coercivity to be reduced but the value of  $I_r/I_s$  to be increased when compared with the values found for  $BaO \cdot 6Fe_2O_3$ . Furthermore, the plate-like particles may be oriented in a tape coating<sup>47</sup>, and since they are difficult to magnetize normal to the particle plane, the resolution of adjacent pulses should be good.

These materials have the general compositions  $Ba_2Me_2Fe_{12}O_{22}$  or  $Ba_3Me_2Fe_{24}O_{41}$  where Me represents divalent metal ions, e. g., Co, Ni, Mn, Fe, Mn or Zn, or mixtures of these ions as in the case of  $Co_{0.8}Fe_{1.92}Ba_3Fe_{24}O_{41}$  discussed by Duinker et al.<sup>47</sup>.

Materials of composition  $MO \cdot 6Fe_2O_3$ , where M = Pb or Sr, also show hard magnetic properties and the range of available oxides with the magnetoplumbite structure may be increased still further by the substitution of  $Bi_2O_3$ ,  $TiO_2$ ,  $Al_2O_3$ ,  $SiO_2$  etc., for part of MO or  $Fe_2O_3$ . These substitutions are made during the initial mixing and heating of the iron oxide and, say, the barium oxide. The effect of the additional on the magnetic properties of the ferrites is quite complex (see for example Kojima<sup>95</sup>,

Mones and Banks<sup>122</sup>). Some slight increase in  $\sigma_s$  and  $H_c$  is often found over a narrow range of composition, but otherwise the effect is to reduce the saturation magnetization and coercivity. Kojima considered that the primary role of the additionals was to change the apparent density of the ferrite and to control its grain growth. However, they are also believed to promote sintering.

Kojima<sup>94</sup> investigated the properties of lead ferrite of magneto plumbite structure, which appears to show promise for recording applications. The coercivity of this material decreased with increasing sintering temperature from  $> 1000$  Oe. at  $900^\circ$  to  $< 500$  Oe. when sintered at  $1150^\circ$  C. In the same sintering temperature range  $I_s$  increased from 190 emu/cc to 270 emu/cc with  $I_r$  remaining at roughly 135 emu/cc. Work of the complex ferrites of the barium ferrite type which was done before 1959 was reviewed by Wohlfarth<sup>189</sup>.

The substitutions in  $BaO \cdot 6Fe_2O_3$  which have been discussed so far all involved metal ions. Frei et al.<sup>62</sup> suggested the replacement of two of the nineteen oxygen atoms by fluorine to give  $BaF_2 \cdot 5(Fe_2O_3) \cdot 2(FeO)$ . The effect of this substitution should be to increase the magnetic moment per formula unit from  $20 \mu_B$  to  $22 \mu_B$ . The material was prepared by mixing barium fluoride and ferric oxide in a ball mill for 24 hours; alcohol was added as a wetting agent. The mixture was then dried and pre-fired at  $1100^\circ$  C. for 12 hours, reground with alcohol, dried and finally fired at  $1280^\circ$  C. in dry oxygen. A similar compound was made in which the divalent iron was replaced by divalent cobalt giving the formula  $BaF_2 \cdot 5(Fe_2O_3) \cdot 2(CoO)$ . This material showed a preferred direction of magnetization in the basal plane. Unfortunately no measurements of coercivity or  $I_r/I_s$  were reported.

#### Oxides with Tetragonal Structure

In 1859 Wohler<sup>188</sup> found that an oxide of chromium was ferromagnetic, and since then there have been many conflicting reports on the magnetic properties and structure of compounds with compositions between  $CrO_3$  and  $Cr_2O_3$ <sup>142</sup>. Since the chemistry of the system is quite complex, this uncertainty was not at all surprising. However, in 1943 Michel and Bernard showed that  $CrO_2$ , which was one of the decomposition products of chromyl chloride  $CrO_2Cl_2$ , was ferromagnetic and possessed the tetragonal rutile structure.

Swoboda<sup>168</sup> et al reported that very pure  $CrO_2$  could be obtained from the thermal decomposition of  $CrO_3$  in the presence of water at high pressure. Equimolar amounts of  $CrO_3$  and water were enclosed in a thin-walled platinum vessel which in turn was enclosed in a thick-wall pressure vessel. The mixture was heated at  $400-525^\circ$  C. and 500-3000 atmospheres pressure; the reaction time was 5 to 10 minutes. Oxygen was needed to stabilize the  $CrO_2$  and was produced by the decomposition reaction  $CrO_3 \rightarrow CrO_2 +$



$1/2 \text{O}_2$ . It was found that, in general, the higher the reaction temperature, the higher the pressure needed to produce  $\text{CrO}_2$  and that high temperatures, high pressures and long reaction times tended to result in larger particles being formed. Darnell<sup>41</sup> reported that  $\text{CrO}_2$  particles could also be formed by vapor deposition from chromyl chloride.

The thermal decomposition method gives particles which are dark gray and somewhat acicular with average lengths 3-10  $\mu$  and widths 1-3  $\mu$ . More highly acicular particles of smaller size were made by adding metal oxides as catalysts to the reaction vessel. The most effective catalysts were found to be  $\text{RuO}_2$ <sup>132</sup> and  $\text{Sb}_2\text{O}_3$ <sup>82</sup>. An additional advantage of the use of  $\text{Sb}_2\text{O}_3$  was that the reaction temperature and pressure could be reduced as low as 300° C. and 50 atm. X-ray diffraction patterns of the  $\text{CrO}_2$  particles showed only the presence of a tetragonal, rutile crystal structure with  $a = 4.41 \text{ \AA}$  and  $c = 2.91 \text{ \AA}$ .

The room temperature value of  $\sigma_s$  was 98 to 100 emu/gm. The  $\sigma$ -T curve showed a pronounced foot and so the Curie temperature was determined by the intercept of the tangent of greatest slope and found to be 126  $\pm$  2° C. Some changes in the intrinsic and extrinsic magnetic properties of the material were observed whenever the catalyst concentration was  $\geq 0.1\%$  by weight of  $\text{CrO}_3$ . For the largest catalyst concentration used (2%) the saturation magnetization decreased from 98-100 emu/gm. to 90-94 emu/gm. The Curie temperature was not noticeably changed, however, the modified  $\text{CrO}_2$  particles were somewhat less thermally stable than those made without a catalyst<sup>168</sup>.

Selected area electron diffraction photographs showed that the smaller particles were single crystals and X-ray studies showed that the tetragonal axis lay along the particle axis. The magnetocrystalline anisotropy was found (in larger single crystals) to be uniaxial with  $K_1 = +3 \times 10^5$  erg/cc, but the easy axis was apparently at  $\sim 40^\circ$  to the tetragonal axis.

The influence of the catalysts was most noticeable on the particle size and, therefore, on the coercivity. As the amount of catalyst was increased, the particle size decreased until particles of 0.2 - 1.5  $\mu$  in length and 0.03-0.1  $\mu$  in width were formed at a concentration of 2%. The coercivity of the  $\text{CrO}_2$  particles (length 3-10  $\mu$ , width 1-3  $\mu$ ) which were prepared without the use of catalysts was 57 Oe., whereas the addition of 2%  $\text{Sb}_2\text{O}_3$  resulted in smaller, more acicular particles with a coercivity of 349 Oe. at room temperature. Under identical reaction conditions the catalyst  $\text{RuO}_2$  produced particles which were rather more acicular but which had lower coercivity (= 312 Oe.). Darnell<sup>41</sup> calculated the critical (upper) size for single domain behavior by the method used by Morrish and Yu<sup>125</sup> for iron oxides. That is, the size is found at which the magnetostatic energy of a single domain particle is equal to the wall energy in a two-domain particle. Using  $I_s = 490$  emu/cc,  $K = 3.0 \times 10^5$ , and an axial ratio of 5:1 he found that the largest minor axis for single domain behavior was 0.46  $\mu$ . This value is reasonable since it is larger than that measured

for the Sb-modified particles ( $H_c \sim 350$ ) but smaller than that observed for the particles prepared without a catalyst ( $1-3 \mu$ ,  $H_c \sim 60$  Oe.).

The average theoretical value of coercivity for a spatially-random assembly of single domain particles of axial ratio 5:1 would be 585 Oe. for crystalline anisotropy 1230 Oe. for shape anisotropy with coherent rotation and 590 Oe. with the chain-of-spheres incoherent model. Darnell<sup>41</sup> found, by fitting the experimental curve for the temperature dependence of coercivity with the theoretical curves for crystalline and shape anisotropy, that the best fit was obtained on the assumption of shape anisotropy.  $H_c$  ascribed the difference between the measured values of  $H_c$  and the theoretical ones for single domain particles to the presence of multidomain particles. The dominance of shape anisotropy was further suggested by measurements of the anisotropy field from torque curves. This field (2150-2500 Oe.) was much too large to be explained by magnetocrystalline anisotropy ( $\frac{2K}{I_s} = 1200$  Oe.). The values of the rotational hysteresis integral  $\int_0^\infty \frac{W_s}{I_s} d\left(\frac{1}{H}\right)$  were found to lie between 1.10 and 1.36 which suggests that the mechanism of magnetization reversal is one of incoherent rotation.

Ingraham and Swoboda<sup>83</sup> discussed the effect of replacing some of the oxygen in  $CrO_2$  with fluorine to the extent of 0.1 to 5% by weight. Because of the valency difference between the two ions, it is necessary that some of the chromium ions have a valency  $< 4$  or be absent in order to preserve charge neutrality in the lattice. Alternatively the fluorine could be added in the form of metal fluorides in which the metal had lower valency than 4. These fluorine-modified chromium oxides were produced in the form of irregularly shaped particles of a few tenths of a micron in diameter. The saturation magnetization  $\sigma_s \leq 85$  emu/gm and the coercivity was in the range 20-100 Oe. An interesting property of these materials was that their Curie temperature could be as low as  $80^\circ$  C. (cf  $126^\circ$  C. for  $CrO_2$ ). Thus although their coercivity is too low for conventional recording purposes, the possibility exists of using these materials in some form of Curie point recording scheme.

A process for the preparation of  $CrO_2$  of more uniform particle size was claimed by Arthur and Ingraham<sup>9</sup>. It consisted of the hydrothermal decomposition of chromium oxides with compositions between  $Cr_3O_8$  and  $Cr_2O_5$ . The improvement in the particle uniformity was ascribed to the relative insolubility of the oxides;  $\leq 1\%$  in water at  $25^\circ$  C. The chromium oxide  $Cr_3O_8$  was prepared by heating  $CrO_3$  in oxygen at  $250^\circ$  C. for 2-5 days; if  $CrO_3$  was heated at  $360^\circ$  C. for 8-24 hours, then  $Cr_2O_5$  was formed. Alternatively the starting oxides may be obtained from the thermal decomposition of chromic nitrates  $Cr(NO_3)_3 \cdot 9H_2O$  at  $150-380^\circ$  C. and atmospheric pressure.

The chromium oxides were then broken down to particles  $< 2 \mu$  in diameter in a ball mill and converted to  $CrO_2$  by hydrothermal decomposition at

temperatures between 330° C. and 400° C. and pressures  $\leq 800$  atmos. for times in the range 1-10 hours. The decomposition was carried out in the presence of water or an aqueous solution of nitric acid in amounts to 50% by weight of the starting oxide. As before the use of additives  $\text{Sb}_2\text{O}_3$ ,  $\text{RuO}_2$ , etc. enabled particles to be made whose properties covered a wider range  $H_c$ ,  $\text{Ir/Is}$  and  $\theta_c$ . However, the use of additives was not essential to the attainment of usable magnetic properties. The final product consisted of acicular particles of  $\text{CrO}_2$  of length  $\sim 0.5-1.0 \mu\text{s}$ , width  $0.02 - 1.0 \mu$  and axial ratio 3-10; the coercivities ranged from 220-420 Oe. and the value of  $\text{Ir/Is}$  was about 0.5.

## METAL PARTICLES

The oxides discussed above were all ferrimagnetic materials. They have a lower saturation intensity of magnetization than that of the ferromagnetic metals (and their alloys) since some of the magnetic moment of the ions is lost as a result of the antiferromagnetic (i. e., antiparallel) coupling. Thus metal particles can be used advantageously in recording surfaces since their higher saturation magnetization leads to higher output signals at low recording densities when compared with oxide particles having the same volume packing fraction. Conversely, similar output levels can be obtained by using a lower packing fraction with possibly better mechanical properties or by making thinner surfaces and thereby improving the pulse resolution at high recording densities. The high density performance is further helped by the high coercivities which are obtainable with metallic single domain particles.

Four methods of preparation of fine metallic powders will be discussed. These are 1) Reduction of oxides hydroxides, oxalates, formates, etc.; 2) Decomposition of metallo-organic compounds; 3) Electrodeposition and autocatalytic deposition and 4) Vacuum deposition.

### Reduction Process

In principle any of the methods described in the earlier sections of producing fine particles of iron oxide or iron-cobalt, etc. may be used as an initial step in the preparation of metallic particles. Carman<sup>36</sup> described the reduction of iron oxide in shallow nickel boats over which dry hydrogen flowed at about 600  $\ell/\text{h}$ . at a temperature of  $\sim 350^\circ \text{C}$ . Below  $350^\circ \text{C}$ . a hydrogen recirculating apparatus was used. At higher temperature sintering of the particles is likely to occur with consequent reduction in  $H_c$  and  $\text{Ir/Is}$ . Forming gas (a mixture of hydrogen and nitrogen) may also be used to provide the reducing atmosphere and has the advantage that it can be allowed to pass into the atmosphere without burning. In this way metal particles of Fe, Co, Ni and their alloys may be made in which the particle shape of the starting (oxide) material is preserved with some reduction of acicularity. Typically particles of iron of 250  $\text{\AA}$  diameter

and axial ratio 2:1 have a coercivity  $\sim 600$  Oe. A similar method using a solution of iron formate and cobalt formate has been used<sup>159</sup> to produce alloy particles (  $\sim 73\%$  Fe and  $27\%$  Co) of very high coercivity. When compacted to densities comparable to that of bulk material, these alloys had magnetic properties ranging from  $H_c = 560$  Oe,  $I_r = 750$  emu/cc to  $H_c = 1400$  Oe. with  $I_r = 100$  emu/cc.

A method of preparation of fine metal particles from the metal oxalates was described by Schuele<sup>148,152</sup>. Since the oxalates are practically insoluble in water, it is possible to precipitate the metal oxalates quantitatively from a solution of the metal chloride by adding a soluble oxalate. Moreover, as the oxalates of iron, cobalt and nickel are isomorphous, precipitation from a solution containing two ions results in oxalate crystals with both metal ions in the same lattice. The ratio of metal ions in the precipitate will be the same as that in the original metal chloride solution, and thus the composition of the final product may be controlled.

Metal sulfates or chlorides in the required proportions were dissolved in distilled water at  $60^\circ$  C. A stoichiometric amount of ammonium oxalate was also dissolved in water at the same temperature and added rapidly to the metal salt solution and the mixture was vigorously stirred. The resulting precipitate was then washed, filtered and dried and found to be crystalline with particle sizes  $\sim$  a few microns. Then the oxalates were heated in air at  $400^\circ$  C., decomposition to the oxide occurs with the evolution of CO and  $CO_2$ . The average particle size of the resulting oxides was  $300-700 \text{ \AA}$  and was found to depend on the temperature required for decomposition; lower temperatures giving smaller particles. Reduction to the metal may then be effected by heating in hydrogen at  $390^\circ$  C. for one hour.

When iron and nickel were used, alloys were obtained which had a maximum saturation magnetization when the nickel content was  $\sim 20\%$  in agreement with results on bulk samples. Similarly iron and cobalt formed a range of powders whose structure was the same as that of the bulk material at each composition.

Iwasaki and Nagai<sup>84</sup> prepared an alloy powder of Fe, Co, Ni (in proportions 55:40:5) by adding oxalic acid to an aqueous solution of the metal salts. The resulting precipitate of iron-cobalt-nickel oxalate was in the form of acicular particles of length  $\sim 1 \mu$  and axial ratio  $\sim 7:1$ . On reduction to the alloy in hydrogen, agglomerates of much smaller particles ( $0.1 \mu$ ) were produced. After being coated onto tapes and aligned in a magnetic field, the particles had a very high coercivity (760-830 Oe.) measured along the direction of particle alignment. The ratios of  $I_r/I_s$  measured in the alignment direction and perpendicular to it were very similar to those found for oriented  $\gamma$ - $Fe_2O_3$  particles, i.e., 0.76 and 0.45 respectively. However, the remanent intensity was very much higher in the metal particle tapes; 222-238 emu/cc compared with 120 emu/cc for  $\gamma$ - $Fe_2O_3$  at the same particle packing fraction of 0.40.

The use of oxalic acid esters in place of oxalic acid or ammonium oxalate has also been reported<sup>6</sup>. In particular, dimethyl oxalate was added to a mixture of  $\text{FeCl}_2 \cdot 4\text{H}_2\text{O}$ ,  $\text{CoCl}_2 \cdot 6\text{H}_2\text{O}$  and  $\text{NiCl}_2 \cdot 6\text{H}_2\text{O}$  in solution. The proportions of the metal chlorides (by weight) was 40:55:5. The resulting precipitate was filtered, dried at  $100^\circ\text{C}$ , for four hours and finally reduced to metal particles in hydrogen at  $390^\circ\text{C}$ . The process was claimed to produce particles whose magnetization intensity was 60-70% greater than that reported by Iwasaki and Nagai.

Oppegard et al.<sup>133</sup> prepared single domain particles of iron and iron-cobalt by reduction of  $\text{Fe}^{2+}$  and  $\text{Co}^{2+}$  to the metals by means of potassium borohydride. A 1 M solution of  $\text{KBH}_4$  was slowly added to an equal volume of 1M.  $\text{FeSO}_4$  (or  $\text{FeSO}_4$  and  $\text{CoCl}_2$ ). The mixture was stirred and placed in the magnetic field ( $\sim 1000$  Oe.) of a permanent magnet. Metallic iron or iron-cobalt was deposited as fine particles which formed chains several microns in length. Iron deposited in this way had the following magnetic properties;  $H_c = 645$  Oe.  $\sigma_s = 159$  emu/gm,  $I_r/I_s = 0.57$ . Particles prepared in the absence of a magnetic field were  $0.1 - 1.0 \mu$  in length and had a coercivity of 515 Oe. The authors concluded that the particles acted as single domains in which the magnetization reversed incoherently. The coercivity was also reduced by particle agglomeration and the presence of some superparamagnetic particles.

#### Decomposition of Metal Carbonyls

This process is commonly used to prepare metals in a chemically pure form; however, as the particles are usually spherical and from  $1-10 \mu$  in diameter, the coercivity and  $I_r/I_s$  are normally extremely low.

A method has been described<sup>159</sup> in which the fine particles are removed from the region of decomposition as soon as they are formed thereby encouraging the production of small particles with high coercivity. A mixture of hydrogen and iron carbonyl was bubbled into an oil bath which was heated to  $300^\circ\text{C}$ . The carbonyl  $[\text{Fe}(\text{Co})_5]$ <sup>51</sup> then decomposed and the iron precipitates in the oil. Ether may be added to accelerate precipitation after cooling. Iron particles produced in this way and compacted to a density of 5 gm/cc had a coercivity of 450 Oe. and a remanent intensity of 333 emu/cc.

More recently Harte and Thomas<sup>70</sup> described a method whereby single domain particles were obtained from the decomposition of a cobalt carbonyl and immediately enveloped in a polymer coating. The latter was made from a copolymer of methyl methacrylate, ethyl methacrylate, and vinyl pyrrolidene which was stirred and refluxed under nitrogen. The single domain cobalt particles formed long chains, and the coercivity was found to be typically 540 Oe. Figure 14 is an electron micrograph of these particles.



FIGURE 14

ELECTRON MICROGRAPHS OF COBALT PARTICLES PREPARED BY DECOMPOSITION OF THE CARBONYLS. (REPRODUCED BY PERMISSION OF DR. J. R. THOMAS, CHEVRON RESEARCH COMPANY, RICHMOND, CALIFORNIA).

## Electrodeposition

Luborsky<sup>105</sup> has described the basic steps whereby elongated single domain (E. S. D) particles of iron or iron-cobalt alloy may be produced by electrodeposition. The steps are 1) electrodeposition of iron or iron-cobalt from an aqueous electrolyte into a mercury cathode. The current density, time of deposition, temperature, pH, electrolyte concentration and uniformity of current are chosen so as to lead to the formation of elongated fibers 100-200 Å in diameter; 2) thermal growth of the particles in the mercury to remove the dendrites and form the trunk of the particles to a shape having optimum magnetic properties; 3) addition of a reactive metal to the iron-mercury dispersion which forms an intermetallic compound or adsorbed layer and increases the coercivity force; 4) removal of the magnetic particles from the bath with a permanent magnet; 5) removal of the remaining mercury by vacuum distillation.

The current density during electrodeposition is one of the principal factors controlling the structure of the initial fibers; values between 5 and 90 ma/cm<sup>2</sup> were reported. During the process of thermal growth in which the fibers lose their dendrites and become thicker, temperatures from 100-200° C. for 15 minutes were used depending on the composition and current density used. Particles having average diameters of about 125-325 Å and axial ratios greater than 10:1 were prepared by this method. In the electron microscope the particles were seen to have a "peanut-shaped" structure, i. e., they resembled a chain of spheres in which the spheres were firmly attached to each other. Consequently it is not surprising that the dependence of coercivity on packing fraction and on orientation angle agrees well with the chain-of-spheres fanning model of incoherent magnetization reversal. This mechanism is further supported by the value of the rotational hysteresis integral (1.2 - 1.3) and by the lack of size dependence of the extrinsic properties. The coercivity and remanent magnetization of aligned ESD particles varied within the range 700 Oe. and 700 emu/cc to 1000 Oe. and 760 emu/cc. Increasing measurement temperatures resulted, increasing coercivities, and this was ascribed by Luborsky<sup>108</sup> et al. to a negative crystal anisotropy contribution since the long axis of the particles corresponds to a magnetically hard direction [111].

Elongated particles of diameter ~200 Å can also be made of alloys of iron with up to 90% cobalt<sup>106</sup>. From measurements of coercivity as a function of composition the magnetocrystalline energy of the particles is inferred to be negligible at about 20% and 80% cobalt. This results in maxima in  $H_c$  of about 910 Oe. and 1000 Oe. at these compositions. No composition dependence of  $I_r/I_s$  was found for the oriented and compacted particles. The saturation magnetization changed with composition in a similar way to that found in bulk materials, i. e., a peak in  $I_s$  at about 40% Co.

Luborsky and Opie<sup>111</sup> reported that the addition of materials capable of forming intermetallic compounds with iron to electrodeposited and therm-

ally-grown particles resulted in an increase in coercivity. Since there was no change in the magnetic moment of the particles (at least, with Mn, Zn, Sn and Sb), the authors conclude that the additive was adsorbed as a monomolecular layer on the iron. Thus, no compound formation occurred. The increase of coercivity (as much as 15% with Sn and Zn) was ascribed to the decreased magnetostatic interaction of the coated particles. Another advantage of the coating<sup>194</sup> is that it stabilized the particles with respect to the temperatures  $\sim 250^{\circ}$  C. encountered during the removal of the mercury by vacuum distillation.

## AUTOCATALYTIC DEPOSITION

Autocatalytic plating of thin Co-P and CoNi-P films having high coercivity is discussed on page 73. The principle<sup>104</sup> of the method is that spontaneous plating of the metal occurs when a catalytic substrate is immersed in an aqueous plating solution. The deposited metal then itself catalyzes the reaction and causes it to continue autocatalytically. However, if any of the three rate-controlling parameters, temperature, pH, and reactant concentration are increased excessively, the homogeneous reaction occurs. This consists of a reaction between metal ions in the solution and the adjacent reductant ions to form metal atoms distributed throughout the solution. These atoms then catalyze the deposition of additional metal, and this results in the rapid formation of a metallic slurry which collects on the bottom of the vessel. On filtering and drying, the particles are found to have a crystallite size which is usually 200-700 Å and to have coercivities in the range 100-1000 Oe. depending on the deposition parameters.

### Elongated Iron Particles by Drawing Wires

Levi<sup>102, 103</sup> reported a method of preparing elongated iron particles by a method which is completely different from any described thus far. This consisted of taking a bundle of iron and copper wires, enclosing the bundle in a copper sheath and drawing it down to a wire of diameter between 0.002" and 0.030". Repeated bundling and drawing with anneals in between results in the formation of extremely fine and elongated particles of iron with diameters as small as 300 Å. The coercivities reported were between 100 and 410 Oe., depending on the final diameter of the iron and the particle packing fraction. Luborsky<sup>105</sup> concluded from measurements of the coercivity of these particles as a function of orientation with respect to the measuring field that the magnetization reversal process was an incoherent one. Since nearly perfect particle alignment is expected in view of the method of preparation, it is not surprising that the value of  $I_r/I_s = 1.0$ .



## Vacuum Deposition

Morelock<sup>123</sup> described a technique for growing whiskers of iron, whose diameters were  $<1.0\ \mu$  and whose lengths  $\leq 300\ \mu$  by deposition from the vapor phase. Iron sheets on molybdenum screens were used as substrates. The metal to be evaporated was formed into a cylinder and placed with the substrates in an evacuated and outgassed fused-silica tube. The whole assembly was heated by means of a platinum wire-wound furnace to a temperature which was about  $50^\circ\text{C}$ . below the filament temperature; typical temperatures being  $1100^\circ\text{C}$ . and  $1150^\circ\text{C}$ . respectively. In this way the whisker growth occurred in a supersaturated metal vapor. Pressures of  $\sim 10^{-6}$  mm Hg were maintained during the deposition. It was found possible to grow whiskers whose diameter was  $\leq 200\ \mu$  under evaporation temperatures and times which ranged from  $1060^\circ\text{C}$ . and 16 hours to  $1150^\circ\text{C}$ . and one hour.

Luborsky et al.<sup>108,109</sup> examined the whiskers in an electron microscope and used selected area diffraction to establish the crystallographic orientation. They found that the smaller diameter whiskers of iron or iron-cobalt were b.c.c. with  $\langle 111 \rangle$  orientation. The cobalt whiskers were h.c.p. with  $\langle 11.0 \rangle$  along the whisker axis.

Most of the larger whiskers (i.e., diameter  $>700\ \text{\AA}$ ) showed a second diffraction pattern of  $\text{Fe}_3\text{O}_4$  (or possibly  $\gamma\text{-Fe}_2\text{O}_3$ ) oriented such that the  $\langle 110 \rangle$  oxide axes and  $\langle 100 \rangle$  iron axes were parallel as were the (100) planes of the metal and oxide. Similar results were obtained for Fe-Co. The larger cobalt whiskers also had an oxide coating; CoO in this case. The relative orientations of metal and oxide were such that  $\langle 11.0 \rangle$  and  $\langle 110 \rangle$  were parallel and so were (00.1) and (111).

The measured values of coercivity, both of isolated whiskers and planar-random arrays, showed a marked dependence on particle diameter. Coercivities exceeding 2000 Oe. were found at a diameter  $\sim 0.05\ \mu$  while for whiskers with a diameter  $\sim 100\ \mu$ ,  $H_c \sim 0.5$  Oe. The dependence of coercivity, remanence and rotational hysteresis on particle diameter agreed very well with the incoherent curling mode of magnetization reversal for particles  $<1000\ \text{\AA}$ . This behavior of the smooth-sided whiskers is in contrast to that of the bumpy electrodeposited ESD particles in which the magnetization rotated by means of the fanning mode. Similar results were found for the Fe-Co whiskers, and since the only difference between the iron and iron-cobalt whiskers was the magnetocrystalline anisotropy, it was concluded that this anisotropy played a negligible role in these whiskers.

On the other hand in the cobalt whiskers where the crystalline anisotropy was not negligible, Luborsky and Morelock<sup>110</sup> found that in particles whose diameter was  $<250\ \text{\AA}$  the magnetization reversed coherently while in the larger particles an incoherent buckling mode occurred.

An alternative method of growing fine whiskers of the ferromagnetic elements was described by Brenner<sup>31</sup>. A boat filled with the metal chloride or bromide was heated to 650-750° C. in a tube furnace through which flowed hydrogen. When the reduction was complete, the boat was pulled into a cooling chamber by means of a tungsten wire. Finally the system was flushed with helium and the sample was removed. The method produced iron, cobalt and nickel whiskers of maximum lengths 200 mm, 3 mm and 2 mm respectively.

## Pyrophoricity of Metal Particles

One practical disadvantage which is common to all the small metal particles discussed above is that they are liable to burn spontaneously on exposure to the atmosphere unless measures are taken to protect them. The rate of oxidation increases with the surface area of the particles while the temperature increase which is associated with the heat of oxidation varies inversely as the particle volume. Thus it is expected (and found) that the pyrophoricity of the metal particles depends critically on their surface area-to-volume ratio. That is, acicular particles or, more especially, porous particles are more pyrophoric than, say, solid spherical particles. To a second order, we might expect that pyrophoricity also depends on the chemical activity of the element so that iron would be more pyrophoric than cobalt and cobalt more than nickel.

In general, all metal particles of diameter less than about  $0.5\mu$  must be treated with caution. There are two principal methods of overcoming the problem. The first of these has already been discussed above in other connections and consists of applying a suitable plastic overcoat to the particles so that the reactive surface of the metal is shielded from the air. The second method is to allow air to reach the particles slowly and controllably so that a thin protective film of oxide is formed on the particle surface. This may conveniently be achieved by keeping the particles under a liquid such as benzene or toluene so that the oxygen must diffuse through the liquid in order to reach the particles. When it is required to coat the particles onto a recording surface, the protective liquid is replaced by the solvent-binder mixture. However, even after the coating has dried, there is the possibility with some binder compositions that air may diffuse in and oxidize the particles. The published literature on this subject is extremely sparse.

## Metal Particles with Oxide Coating

A modification of the electrodeposition method which resulted in particles of very high coercivity ( $\sim 2000$  Oe.) was described by Falk<sup>52, 53</sup>. Particles of iron, cobalt or iron-cobalt were prepared as before by electrodeposition into a mercury cathode. The electrodeposited particles were then thermally removed from the mercury and oxidized in moist air at  $200^{\circ}$  C. for about 12 minutes to produce a shell of metal ferrite around a core of the metal (or alloy). The presence of the two phases was detected by electron-and x-ray-diffraction analysis. The oxygen content of the particles was usually in the range 10-13% by weight. It was found that the coercivity was relatively independent of the particle packing fraction when compared with the behavior of metal particles. On the other hand the temperature dependence of coercivity was relatively high. This suggests that magnetocrystalline anisotropy was probably more important than the shape of the particles in determining the coercivity. The value of  $I_r/I_s$

for an aligned assembly was  $\sim 0.85 - 0.90$ . The coercivity of these particles is, of course, much too high for present recording techniques, but it is conceivable that the method could be modified so as to give particles of lower coercivity.

In attempting to explain the high coercivity of the metal particles. With an oxide shell it should be remembered that composite particles of this type usually exhibit exchange anisotropy at low temperatures. That is, the rotational hysteresis approaches a finite value (rather than zero) at high fields and (in some cases) the hysteresis loop is displaced along the field axis if the sample is cooled in a magnetic field. These effects are attributable to the exchange coupling between the ferromagnetic core and the antiferromagnetic shell. Meiklejohn<sup>119</sup> discussed the occurrence of exchange anisotropy in ferrimagnet-ferromagnetic systems such as the present one. He concluded that if the ferrimagnetic material has a larger crystalline anisotropy than the ferromagnetic material, the net anisotropy of the particle will be that of the ferrimagnetic. If the preferred magnetization directions of crystalline anisotropy and shape anisotropy are the same then, clearly, an elongated particle with a ferrite shell will have a larger coercivity than the same particle without a shell. This was certainly true of the oxide coated iron-cobalt particles of Falk and Hooper<sup>53</sup> in which the effect of the ferrimagnetic coating was to increase the coercivity of the metal particles by  $\sim 500$  Oe.

#### Oxide Particles with Metal Coating

An interesting approach to the problem of preparing elongated single domain particles of iron was described by Schuele<sup>149</sup>. It consisted of depositing a layer of iron oxide onto small acicular particles of clay and then reducing the iron oxide to iron. Thus the final product consists of elongated particles in which the outer shell is iron and the inner core is a nonferromagnetic material.

The core material was Attapulugus clay; a hydrous magnesium aluminum silicate which consists of small needle-shaped crystals having average length  $0.2 - 1.5 \mu$  and axial ratio 20:1 to 30:1. To prevent the core particles from flocculating, it was necessary to give them a charge, generally negative, by adding a dispersing agent such as sodium pyrophosphate which contains the  $P_2O_7^{3-}$  radical. Iron oxide may then be precipitated and grown on the charged core particles by the method of Penniman, Zoph-Camras discussed on page 10. When the formation of the oxide film was completed, the coated particles were separated from the aqueous medium and dried. Finally the oxide was reduced to metallic iron in hydrogen at a pressure of  $\leq 50$  mm Hg. at temperatures between  $180^\circ C.$  and  $200^\circ C.$  for about 16 hours. Particles having coercivities between 950 and 1450 Oe. were made in this way. The ratio of  $I_r/I_s$  was low, however, and did not exceed 0.5. This was presumably attributable to relatively unsuccessful attempts to align the particles.

## OTHER PARTICLES

### Manganese-Bismuth

Extremely high values of coercivity in fine particles of this material were reported by Guillaud<sup>69</sup>. The particles may be prepared by the method described by Adams et al.<sup>1</sup>. Finely powdered manganese and bismuth in weight proportions 17:83 were placed in an alumina crucible inside a rotating stainless-steel furnace and heated to 700° C. under an atmosphere of helium for five hours. The material was then cooled to 440° C. for 16 hours, then to 320° C. for eight hours, and the furnace was tipped to allow the excess bismuth to run out. The MnBi was pulverized (under helium to prevent oxidation) and irregular particles of average diameter  $\sim 8\mu$  were obtained. The particles were extremely pyrophoric. Any remaining non-magnetic material was removed in a magnetic separator so that the final product was 90% pure MnBi.

Goldman and Post<sup>67</sup> prepared MnBi particles by reacting manganese and bismuth in heated mercury. The mercury was then vacuum distilled at a low temperature leaving a ferromagnetic powder residue of MnBi. On re-grinding the material and annealing at 400° C. a powder was obtained which has  $\sigma_s = 83.0$  emu/gm when measured at 79° K. The particles were covered with toluene to prevent spontaneous combustion on exposure to air.

Guillaud<sup>69</sup> found that the coercivity of MnBi particles was strongly size-dependent. For diameters  $< 80\mu$  the coercivity was  $\sim 700$  Oe. while for particle of  $3\mu$  diameter the coercivity was as high as 12,000 Oe. The high coercivity is a result of the very high values of magnetocrystalline anisotropy;  $K_1 = +8.9 \times 10^6$  erg/cc. and  $K_2 = +2.6 \times 10^6$  erg/cc at room temperature. The structure of MnBi is of the hexagonal nickel arsenide type.

Thin films of MnBi were made by Williams et al.<sup>187</sup>. First a layer of manganese then one of bismuth was vacuum deposited onto a glass substrate in a vessel which was evacuated and sealed off at  $1.5 \times 10^{-7}$  mm Hg. while being baked at 200°. The films were then baked at 225-350° C. for three days. However, the process did not result in uniform films although areas of about one square inch which were suitable for the subsequent experiments were found. Mayer<sup>115</sup> showed that this non-uniformity resulted from the growth of ferromagnetic MnBi from a few randomly distributed nucleation sites. Rather surprisingly the thin films did not deteriorate on exposure to the air.

Thin films of MnBi have their easy axis of magnetization (the hexagonal "c"-axis) normal to the plane of the film. Thus Williams et al.<sup>187</sup> were able to write on the films (thickness  $\sim 1000 \text{ \AA}$ ) with a magnetized wire and to read out the pattern by means of the Faraday effect. A large differential rotation of the polarization plane of  $\sim 10^\circ$  was found. The

pattern could be erased by applying a field of 3000 Oe. normally to the film plane whereupon a fine domain structure was observed. Since the finest detectable line was  $\sim 10^{-3}$  cm wide, he concluded that the method was potentially capable of storing information at a density of  $10^6$  bits/cm<sup>2</sup>.

### Manganese-Aluminum

In a search for materials with the magnetic properties of MnBi but without its disadvantages of low corrosion resistance and large temperature coefficient of anisotropy, Koch et al.<sup>92a</sup> found a metastable phase of manganese and aluminum. This phase had the approximate composition Mn<sub>1.11</sub>Al<sub>0.89</sub> and a tetragonal structure with  $a = 2.77 \text{ \AA}$  and  $c = 3.57 \text{ \AA}$ . To produce the desired specimens containing 72.3% Mn were homogenized at 1150° C. for an hour and then cooled at  $\sim 30^\circ \text{ C./sec}$  when, at about 700° C. transformation into the supercooled tetragonal phase occurred. The saturation magnetization ( $\sigma_s$ ) of the bulk material was found to be 96 emu/gm and  $I_s \sim 500$  emu/cc. The anisotropy constant was estimated to be  $\sim 10^7$  erg/cc and coercivities of  $\sim 3500$  Oe. were measured on pulverized samples whose average particle size was  $\sim 50 \mu$ . No clear correlation was established between coercivity and particles size, however. It was possible to make the material in the form of a fine powder ( $< 1 \mu$ ) by anodic corrosion of the bulk material. The powder had a coercivity of 500-1000 Oe. which was nearly equal to that of the bulk material. On deforming the powders  $H_c$  increased to about 3000 Oe.

An alloy of Mn-Ga (66 at. % and 34 at. %) having similar magnetic properties to Mn-Al, i.e.,  $H_c \sim 1800$  Oe.  $\sigma_s \sim 40$  emu/gm, was recently reported by Tsuboya and Sugihara<sup>175</sup>.

### Iron-Cobalt-Phosphides

The section Fe<sub>2</sub>P-Co<sub>2</sub>P in the system Fe-Co-P was investigated by de Vos et al.<sup>44</sup>. They found that all the (Fe, Co)<sub>2</sub>P alloys probably form a continuous range of solid solutions having the hexagonal Fe<sub>2</sub>P structure. The (Fe, Co)<sub>2</sub>P alloys prepared by lixiviation are in the form of fine particles immediately after leaching. The coercivity was found to be a function of composition (with a peak in the neighborhood of 85% Fe 15% Co) and also of cooling rate. The reported values were as high as 2000 Oe. at room temperature although variation in the method of preparation resulted in values of  $H_c \sim 500$  Oe. The saturation magnetization was  $\sim 65$  emu/gm at room temperature.

### Ternary Alloys

Henkel<sup>74</sup> reported on the anhysteretic susceptibility of magnetically-hard alloys of Fe-Ni=Cr, Fe-Co-V and Cu-Ni-Fe as a function of the degree of

TABLE IV

METAL PARTICLES	$\sigma_s$ emu/gm	$O_c$ in °C	$H_c$ * OERSTEDS	$I_r/I_s$ *	PARTICLE SHAPE AND SIZE	REFERENCE
Fe (FROM $Fe_2O_3$ ) (FROM WIRES) (FROM BOROHYDRIDE) (FROM CARBONYL) (BY ELECTRO- DEPOSITION) (WHISKERS)	218	770	560	0.51-0.77	$l = .024 \mu; \frac{l}{W} = 2$	36
	68-103					
			100-410	1.0	DIA. $\leq .03 \mu$	102, 103, 105
	159		515-645	0.57	$l \sim 1-2 \mu$ $W \sim 0.04-0.1 \mu$	133
	67		450		SPHERICAL, DIA. 0.01-1 $\mu$	159
	104		700-740	0.9	ACICULAR, $l/D = 10-20$ DIA. 0.015-0.02 $\mu$	105
			2000	0.7-0.8	DIA. .05 $\mu$	109
Fe-Co (ELECTRODEPOSITION) 38.5% Co (FROM CARBONYL) 27% Co	107		1000	0.9	ACICULAR, $l/D = 10-20$ DIA. .025 $\mu$	105
	$\sigma_r = 125$ $\sigma_r = 49$		560 1400		SPHERICAL DIA. 0.01-1 $\mu$	159
Fe-Co-Ni (FROM OXALATE) 40% Co 5% Ni,	$I_s \sim 800$ emu/cc		770-830	0.76	ACICULAR $\frac{l}{W} = 5$ $l \sim 0.1 \mu$	84, 116
Co (FROM CARBONYL) (WHISKERS)	$\sigma_r = 75$		350		SPHERICAL, DIA. 0.01-1 $\mu$ .	159
			2700-3300	0.5	DIA. 0.014-0.022 $\mu$ .	110
OTHER COMPOUNDS						
Mn Bi	83 (AT 79°K) $I_s = 620$ (AT 20°C)	330	$\sim 700$ 12000		DIA. 80 $\mu$ DIA. $\sim 3 \mu$	44, 67
	96 (BULK) 71 (POWDER)	380	$\sim 3500$ 500-1000		DIA. $\sim 50 \mu$ DIA. 1 $\mu$	92a
Mn Ga 66 AT % Mn	40	417	1800	$\sim 0.5$		175
(Fe, Co) <sub>2</sub> P Fe:Co = 85:15	69	120-140	200-2000			44

alignment, particle packing density and coercivity. As particles of these alloys have coercivities in the range 200-1000 Oe. and magnetization intensities comparable to those of Fe-Co particles, they appear to be quite suitable for magnetic recording purposes. The properties of other ternary alloys (e.g., Cu-Ni-Co, Fe-Co-W, Fe-Co-No, etc.) of high coercivity were reviewed by Wohlfarth<sup>189</sup>.

## THIN METAL FILMS

The thinness of a recording surface is a most important quality when well-resolved pulses are required at high recording densities. The problem is one of obtaining a thin surface without sacrificing other desirable attributes. For example, if the thickness of an oxide coating were reduced without a compensating increase in the particle packing fraction, then the magnetic moment of the surface would be reduced and also the level of the output signal, particularly at low densities. On the other hand, increasing the particle loading affects the mechanical properties of the surface adversely. With continuous metallic films, however, it is possible to have thin surfaces and still have moment comparable to those of the thicker oxide since the moment density of the ferromagnetic metals is so much higher than that of, say,  $\gamma$ -Fe<sub>2</sub>O<sub>3</sub>. Furthermore it is possible to obtain a wide range of coercivities (50-1500 Oe.) in metal films.

Three methods will be discussed whereby thin metallic recording surfaces may be made. They are electrochemical deposition, autocatalytic deposition and vacuum deposition. The properties of these films are summarized in Table V.

## ELECTROCHEMICAL DEPOSITION

Although this method was used by Pederson<sup>136</sup> as early as 1906 for speech recording, the modern history of electrodeposited recording surfaces begins in 1952. Zapponi<sup>195</sup> used a plating bath consisting of nickel and cobalt chlorides with boric acid as a buffer. The bath and deposition conditions are shown in Table VI. Since the standard potentials of nickel and cobalt are very similar (-0.25v. and -0.28v), as also are the hydrogen over-voltages (0.2lv. and 0.16v.), it is possible to codeposit the two metals<sup>66</sup>. The anode composition is usually 80 Co/20 Ni. It was later found to be necessary to add small amounts of certain sulfur containing compounds to the Zapponi bath in order to improve the values of Ir/Is of the platings. Sulfur may be conveniently added in the form of potassium thiocyanate and radiochemical studies have shown that sulfur is separated from the KCNS molecule and becomes incorporated in the plating. The role of the citrates as complexing agents will be discussed in the Section on autocatalytic plating.



TABLE V

METAL FILMS	$\sigma_s$ emu/gm	MAX $H_c$ * OESTEDS	$I_r/I_s$	FILM THICKNESS, STRUCTURE AND ORIENTATION	REFERENCE
<b>Fe</b> EVAPORATION AT ANGLES OF INCIDENCE $\theta = 0^\circ$ 65° 75°	218	50 270 > 800	1.0 0.85-0.90 0.90-0.95	$t = 0.1 - 0.2\mu$ NO CRYSTAL ORIENTATION	150, 160
<b>Ni</b> $\theta = 0^\circ$ 65° 75°	54.4	50 150 300	1.0 0.85-0.90 0.90-0.95	$t = 0.1 - 0.2\mu$ ; NO ORIENTATION	160
<b>Co</b> 0° 65° 75°	161	50 250 800	1.0 0.85-0.90 0.90-0.95	$t = 0.1 - 0.2\mu$ ; NO ORIENTATION	160
<b>Co-P</b> (ELECTRODEPOSITION) 2-3% P.	$I_s = 875$ emu/cc	400 1300	0.5 0.5	$t = 1 - 30\mu$ , PLATELETS $\sim 3\mu \times 0.5\mu$ (110) PARALLEL TO FILM PLANE (002) " " " "	144
(ELECTROLESS) 4% P	$I_s = 835-1110$ emu/cc.	> 650 500 360	0.9 0.74	HCP, CRYSTALLITE SIZE $0.3 - 1\mu$ (1010) PARALLEL TO FILM PLANE $t = 0.07\mu$ ; GRAIN SIZE = $0.1\mu$ = $0.23\mu$ = $0.45\mu$ = $1\mu$	57
(ELECTROLESS) 2.67 WT% P 4.52 WT% P	156 122.5	$t \rightarrow$ 1100-355 214-637	0.83 0.70	$t < .25\mu$ ; HCP CRYSTALLITE SIZE $0.02-0.1\mu$ C-AXES $\perp$ PLANE FOR $H_c < 300$ oe C-AXES $\perp$ PLANE FOR $H_c > 600$ oe	89b
<b>Co-Ni-P</b> (ELECTRODEPOSITION)		1000	0.48-0.54	$t = 30\mu$ ; NCP, C-AXIS RANDOM IN FILM PLANE LAMELLAE $\sim 3\mu \times (.05 - .1\mu)$ .	145, 144b,
		$\leq 1750$	$\geq 0.75$		28,
<b>85 WT% 0 WT% P 2.2 WT% P</b>	159 109	130 1050	0.7-0.9	$t = 0.1 - 1\mu$ , HCP AND FCC, CRYSTALLITE SIZE $100 \text{ \AA}$ NO ORIENTATION	JUDGE, MORRISON, SPELIDIS J. ELECTROCHEM SOC. TO BE PUBLISHED
<b>32% Co (</b> <b>76.2% Co</b> <b>(1-2 WT% P)</b>	LINEAR FUNCTION OF COMPOSITION	400 1300	$\rightarrow$ 0.6-0.8	$t = .025 - .25\mu$ , HCP AND FCC, [00.2] AND [111] $\perp$ FILM PLANE CRYSTALLITE SIZE $< 0.02\mu - 0.1\mu$	89e

TABLE VI

BATH COMPOSITIONS, PLATING CONDITIONS AND RESULTING MAGNETIC PROPERTIES OF ELECTRODEPOSITED FILMS PREPARED FROM TWO PLATING BATHS, WITH AND WITHOUT SUPERIMPOSED AC.

	ZAPPONI BATH		MODIFIED ZAPPONI BATH	
PLATING SOLUTION	Ni	1M	Ni	1M
	Co	1M	Co	1M
	H <sub>3</sub> BO <sub>3</sub>	0.4M	HOCH <sub>2</sub> COOH	0.4M
			KCNS	1.24 X 10 <sup>-4</sup> M
PLATING CONDITIONS	pH	3.4		3.4
	TEMPERATURE	50°C		50°C
	DIRECT-CURRENT	100 ASF		100 ASF
	DENSITY			
	AGITATION	300 RPM		300 RPM
PLATING COMPOSITION	81 Co / 19 Ni		82 Co / 18 Ni	
	$\frac{AC}{DC} = 0$	$\frac{AC}{DC} = 3$	$\frac{AC}{DC} = 0$	$\frac{AC}{DC} = 3$
MAGNETIC PROPERTIES	H <sub>c</sub>	100 Oe	240	120
	I <sub>r</sub>	873 emu/cc	318	873
	I <sub>r</sub> /I <sub>s</sub>	0.75	0.22	0.73
PLATING STRESS	+37 700 PSI	+10 300	+39 100	+9000

It is quite common in electroplating to find that the direct current which transports the metal ions to the cathode is supplemented by alternating current. Since the amplitude of the a.c. may be greater than the d.c., periodic deplating occurs which results in a brighter, smoother coating. The use of a.c. also has very marked effects on the magnetic properties of the plating as can be seen from Table VI, resulting in higher values of coercivity but in somewhat smaller value of  $I_r/I_s$ . On the other hand, the additional cost of the a.c. power and the added complexity of the power supplies make the use of super-imposed a.c. commercially less attractive. The maximum coercivity which is obtained reliably with this bath is  $\sim 280$  Oe. at  $\sim 2000 \text{ \AA}$  thickness. The coercivity decreases with increasing film thickness to  $\sim 200$  Oe. at  $6 \mu$ . The value of  $I_r/I_s$  of 0.75 is very similar to that obtainable with oriented  $\gamma\text{-Fe}_2\text{O}_3$  particles. However, the magnetization intensity (Table VI) is considerably higher than that of oxide coatings so that acceptable signal levels can be obtained from surfaces which are proportionately thinner.

Bonn and Wendell<sup>28</sup> showed that the addition of sodium hypophosphite to the Zapponi bath resulted in films having higher values of  $I_r/I_s$  ( $\geq 0.75$ ) and much higher values of coercivity ( $\leq 1750$  Oe.). Furthermore, these values could be obtained without the use of a.c. and at lower d.c. current levels (20 amps/sq. ft. versus 100 a.s.f. of the Zapponi bath). The dependence of coercivity on hypophosphite concentration in the bath is shown in Figure 15. Ammonium chloride ( $\geq 100$  gm/l.) was also added to the bath and apparently resulted in more uniform magnetic properties<sup>97</sup>. The pH of the plating solution was quite critical and was 4.0; the bath temperature was  $50^\circ \text{C}$ .

Tsu<sup>174</sup> reported that Co-Ni films of high coercivity (50-600 Oe.) could be obtained from a bath containing  $\text{Ni}^{2+}$  and  $\text{Co}^{2+}$  as cations and chloride and sulfamate ( $\text{NH}_2\text{SO}_3^-$ ) as anions. The additions of more sulfur in the form of hypophosphite and boric acid as a buffer were not needed with this bath; the pH was between 6.5 and 6.8. The bath was quite critical as regards current density which was  $\leq 5$  a.s.f. However, the cost savings resulting from the lower currents were offset to some extent by the higher cost of the sulfamates.

The alloy composition of the plated films can be varied by changing the Co/Ni ratio in the solution, and since the saturation magnetizations of cobalt (1450 emu/cc) and nickel (484 emu/cc) differ considerably the magnetization intensity of the alloys can be controlled within this range by changing the composition. It is possible that the ratio of Co/Ni in the films may also depend on the hypophosphite concentration of the bath by analogy with results obtained with electrodeposited Ni-Fe films<sup>63</sup>. At high temperatures the process of electrodeposition is supplemented by autocatalytic deposition (see page 73) which, in acid solutions, would preferentially deposit nickel. Thus with constant bath composition the Co/Ni ratio should decrease with increasing temperature. The coercivity of the electroplated

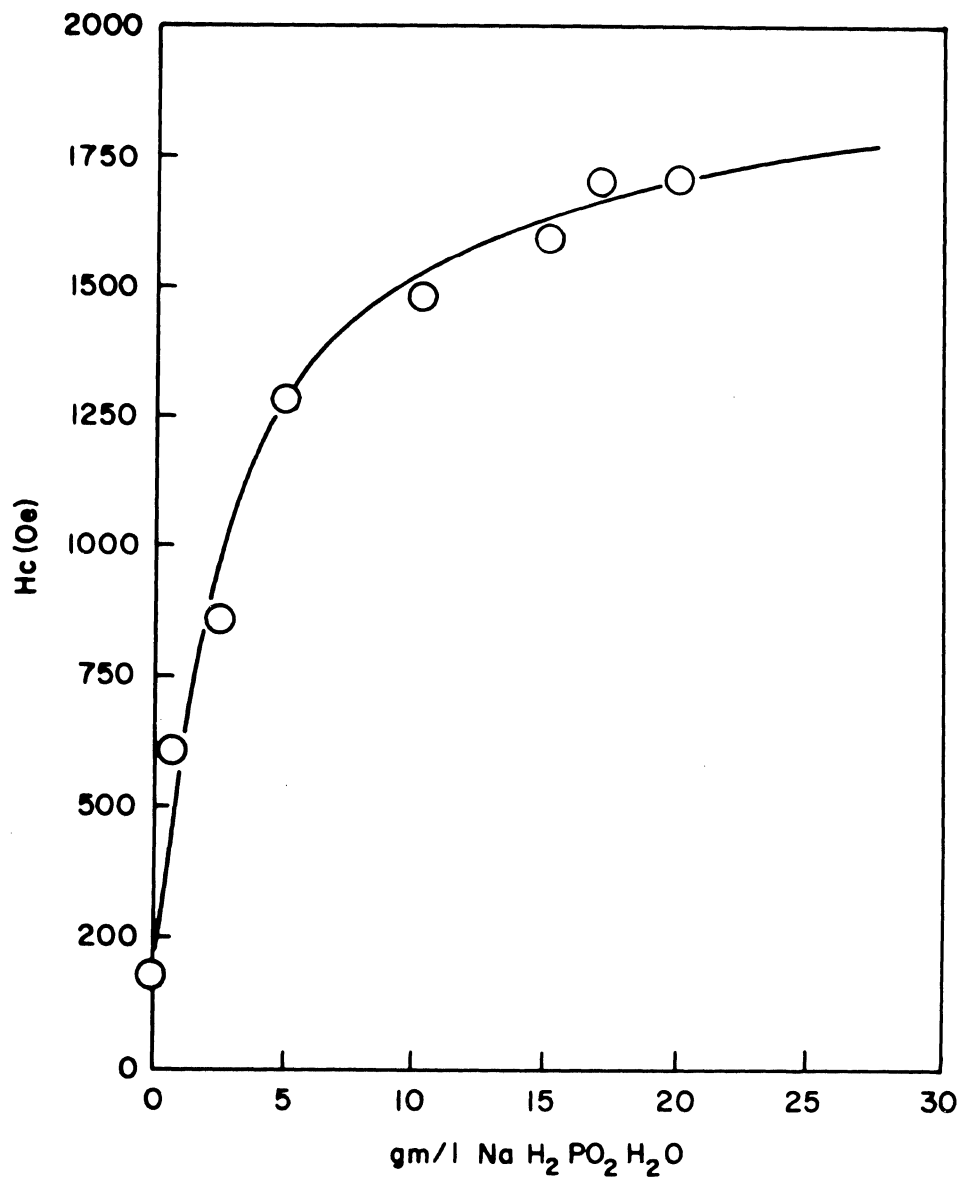


FIGURE 15

COERCIVITY OF ELECTRO DEPOSITED Co-Ni-P FILMS AS A FUNCTION OF THE HYPOPHOSPHITE CONCENTRATION IN THE BATH. (FROM KORETZKY, PROC. FIRST AUSTRALIAN CONFERENCE ON ELECTRO-CHEMISTRY, NEW YORK, PERGAMON 1964, p. 417.)

films is usually an increasing function of current density, pH, nickel content up to  $\sim 33.5\%$ , phosphorus content and sulfur content and a decreasing function of thickness.

Structure determination of films thinner than  $1\mu$  is very difficult since the diffraction lines are few, broad and ill-defined, implying a crystalline size  $< 100 \text{ \AA}$ . Stress in the plated films can also lead to diffraction line broadening but even when stress is relieved by annealing the lines obtained with the thin films are difficult to measure. With films thicker than  $1\mu$  the situation is rather better. Eight lines are observed whose positions correspond to a hexagonal close-packed (h.c.p) structure but whose intensities imply the existence of a face-centered cubic (f.c.c.) phase. No preferred orientation was found with these films but Sallo and Olsen<sup>145</sup>, working with thicker films ( $1-30\mu$ ) which had coercivities  $\sim 1000 \text{ Oe.}$ , found hexagonal crystallites whose c-axes were randomly arranged in the film plane. They also obtained evidence of a lamellar structure in which the lamellae ( $500-1000 \text{ \AA}$  wide) were arranged with their planes normal to the film plane.

Fisher<sup>56</sup> investigated the interrelation of stress, h.c.p./f.c.c. content and coercivity in Co-P films and concluded that the coercivity was controlled primarily by the crystalline anisotropy, with stress playing a secondary role. However, these films were of much lower coercivity ( $30-100 \text{ Oe.}$ ) than those of Co-Ni-P discussed above or films of Co-P prepared by Sallo and Carr<sup>144</sup>. In films of higher coercivity the effect of stress is expected to be still less important.

By varying the bath composition and the deposition parameters it is possible to control the coercivity of electroplated films within the range  $50-1500 \text{ Oe.}$  The ratio  $I_r/I_s$  is usually not independent of coercivity and, with the correct plating conditions may be in excess of  $0.9$ . The saturation magnetization per unit mass is usually  $5-20\%$  below the value which would be expected from the cobalt and nickel content (see Table V). In addition, to possessing high squareness ( $I_r/I_s$ ) the films have magnetic properties which are isotropic in the film plane. Not only is the hysteresis loop independent of the direction of measurement in the plane, but the graph of torque as a function of measurement angle is a straight line. The rotational hysteresis becomes zero at about  $6,500 \text{ Oe.}$  The integral has the value  $4.0$  for all but the thinnest films, indicating an incoherent mode of magnetization reversal. It appears that the explanation of the hysteretic properties is that the films behave like a random assembly of strongly-interacting single domain particles.

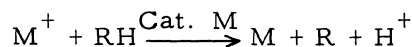
In order to electrodeposit films on plastics the substrate must first be made conducting. Wenner<sup>185</sup> described a method of accomplishing this which consisted of depositing autocatalytically a layer of Ni-P onto the polyethylene terephthalate substrate. The substrate was first cleaned with acetone and boiling water and then sensitized with acidic solutions of stannous chloride ( $30 \text{ gm/l.}$ ) at  $25^\circ \text{ C.}$  and palladium chloride ( $0.1 \text{ gm/l.}$ )

at 55-60° C. A film of nickel containing 7-10% phosphorus was then deposited autocatalytically from an aqueous solution of 30 gm/ℓ . nickel chloride (Ni<sup>2+</sup>) 10 gm/ℓ . sodium hypophosphite, 50 gm/ℓ . ammonium chloride, 100 gm/ℓ . sodium citrate, and 40 mℓ /ℓ ammonium hydroxide (28%). With the solution at a temperature of 90-95° C., a nickel layer of 6-8μ inches (1500-2000 Å) thick was produced in about 80 secs. This layer which usually was non-ferromagnetic could then be used as the cathode for the subsequent electrodeposition of a ferromagnetic film of Co-Ni-P.

## AUTOCATALYTIC DEPOSITION

This process is also called "Electroless Deposition." In 1946 Brenner and Ridell<sup>30</sup> described the deposition of nickel and cobalt films by immersing a catalytic substrate in an aqueous solution of the metal chlorides or sulfates. Plating began spontaneously with the metal being deposited only on the catalytic surface. The deposited metal then in turn catalyzes the reaction and causes it to continue depositing metal autocatalytically. The chemistry of the process was recently reviewed by Levy<sup>104</sup>.

The two essential ingredients are metal ions and reductant ions; their reaction equation is



This suggests that the reaction rate should increase with increasing temperature, pH, and reactant concentration. The hypophosphite ion and the borohydride ion are frequently used as reductants. Clearly the metal ions and the reductant ions must coexist at the catalytic surface for deposition to occur, but, if the concentration of the metal ions becomes too high, these ions inhibit the absorption of the reductant and the plating rate is decreased. Thus some method of controlling the concentration of M<sup>+</sup> must be used. This is usually done by arranging that the metal ion exists in solution as a complex ion which dissociates to form an equilibrium amount of the free metal ion. The nickel ion Ni<sup>++</sup>, for example, does not exist alone in water but is bonded by shared electrons, to eight molecules of water which are arranged with octahedral symmetry around the metal ion. The complex ion may be formed by substituting a ligand, e.g., an NH<sub>3</sub> group, for water and the concentration of the metal ion may then be controlled by choosing the proper ligand. Ammonia forms a relatively weak bond and therefore allows a considerable free metal ion concentration to be build up. Cobalt, nickel and iron are very suitable metals as catalysts since they possess incomplete 3d electron shells which readily accept electrons from molecules on the surface of the metal. The reactant molecules are thus chemisorbed on the catalyst and form more metal atoms which in turn catalyze the reaction. Limiting deposition rates are attained when the autocatalytic reaction, which at low rates has the lower activation energy, gives way at high rates to the homogeneous reaction throughout the

bath. When this occurs, the metal is deposited in fine particles which sink to the bottom of the bath. Typical<sup>90</sup> autocatalytic plating baths for cobalt films would be:

Co SO <sub>4</sub>	0.11 M	CoCl <sub>2</sub>	0.13 M
NaH <sub>2</sub> PO <sub>2</sub>	0.19 M		
(NH <sub>4</sub> ) <sub>2</sub> SO <sub>4</sub>	0.50 M	NH <sub>4</sub> H <sub>2</sub> PO <sub>2</sub>	0.18 M
Na <sub>3</sub> (citrate)	0.12 M	(NH <sub>4</sub> ) <sub>2</sub> H (Citrate)	0.155 M

Temperature = 80° C., pH = 8.7 at 50° C. (adjusted with NH<sub>4</sub>OH) no agitation. Here the complexing group is the citrate radical which is more strongly bonded to the metal than is the ammonia group. The complex ion dissociates at the same rate as plating occurs so that the free metal ion concentration remains constant. Since polynuclear complexes are not normally formed, at least one ligand for each reducible metal ion in solution is needed. Nickel chloride or sulfate could be substituted for cobalt in which case the films would not be ferromagnetic until the thickness exceeded 1000 Å.

The cobalt films would be immediately ferromagnetic and their coercivity depends on thickness as shown in Figure 16. The ratio of Ir/Is for films prepared in the sulfate bath and thicker than 1000 Å is ~ 0.8.

A wide range of magnetic properties may be obtained by using both cobalt and nickel chlorides (or sulfates) in the same bath. Judge<sup>89</sup> et al. found that the coercivity of electroless films increased rapidly with Co content up to about 70% Co and then decreased rapidly beyond about 90% Co. The detailed composition dependence varied somewhat with film thickness. At a composition of 76.2% Co a coercivity of ~ 1300 Oe. was found which was independent of film thickness in the range 500-2000 Å.

As in the case of electroplated films, the chemically deposited samples contain small amounts of phosphorus (0.5 - 6% by weight) which exerts a marked effect on the magnetic properties of the films. Increasing the phosphorus content from 0.5% to 3.0% by weight, in films of constant thickness, causes an increase in coercivity by a factor of 3-5 depending on thickness.

Structure analysis showed that the Co-P films discussed by Bate et al.<sup>17</sup> contained only the h.c.p. phase with a stacking fault frequency of ~ 0.13 and crystallite sizes from 200-700 Å. The lower coercivity films (< 300 Oe.) were found to be oriented so that the hexagonal c-axes were predominantly normal to the film plane. In the higher coercivity films (~ 1000 Oe.) the c-axes were randomly distributed in the film plane and these films looked much smoother under the electron microscope. Films of intermediate coercivity (300-700 Oe.) showed a random distribution of c-axes

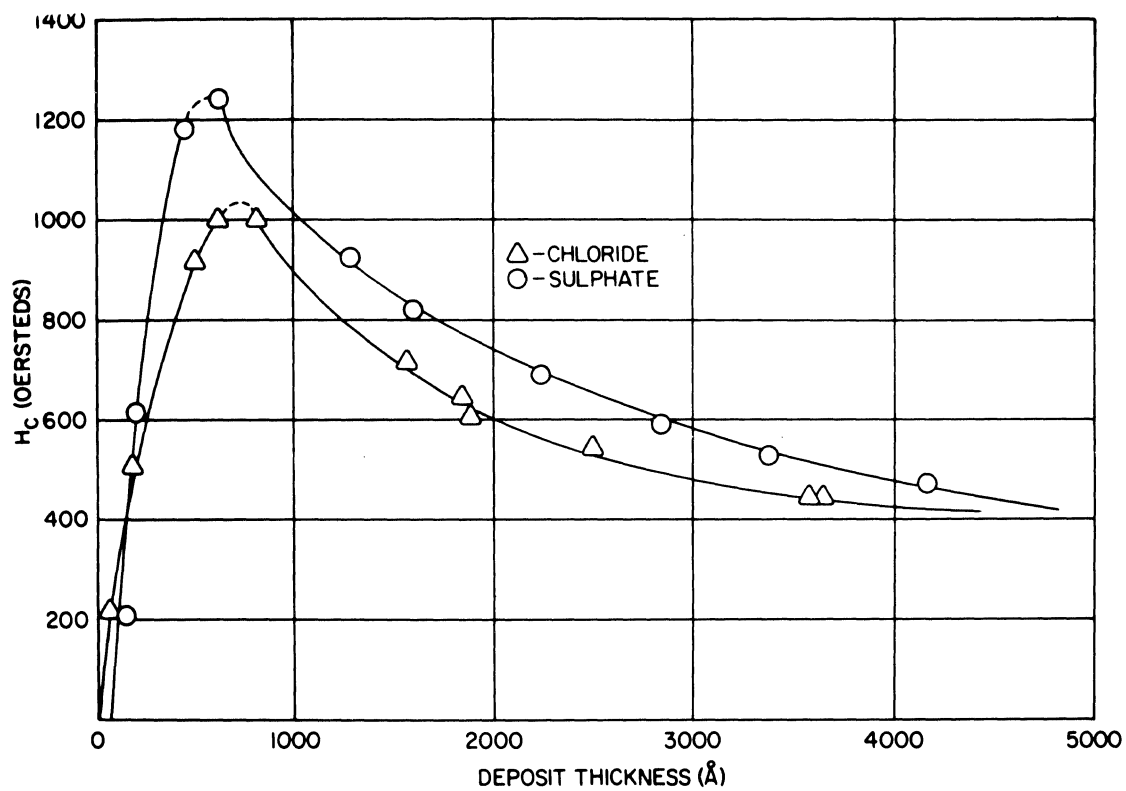


FIGURE 16

COERCIVITY OF ELECTROLESS Co-P FILMS AS A FUNCTION OF FILM THICKNESS. RESULTS ARE GIVEN FOR THE CHLORIDE AND THE SULPHATE BATHS. (FROM JUDGE, MORRISON, SPELIOTIS, BATE, J. ELECTROCHEM. SOC. 112, 681, (1965).



in and out of the film plane.

The saturation magnetization of Co-P films prepared from the chloride bath and containing a 5.0% phosphorus (by weight) was 116 emu/gm. Assuming that the phosphorus exists as non-ferromagnetic  $\text{Co}_2\text{P}$ , the saturation magnetization would be 125 emu/gm. The presence of  $\text{Co}_2\text{P}$  in the as-prepared films has not been conclusively demonstrated but on heating the films to 465° C., the  $\text{Co}_2\text{P}$  phase appeared<sup>17</sup>. Although phosphorus was quantitatively detected by x-ray fluorescence and chemical analysis, its location was revealed neither by lattice parameter measurements nor as a separate phase in the as-prepared cobalt films. The discrepancy in the saturation magnetization is perhaps the result of an amorphous (non-ferromagnetic) phase. Such a phase (together with the possible  $\text{Co}_2\text{P}$  phase) may be responsible for the hysteretic properties of the films, serving to isolate the single domain particles and to ensure a rotational mode of magnetization reversal. The isolation between domains is not complete, however, since a strong magnetostatic interaction is postulated to explain the isotropy and the high values of  $I_r/I_s$ . The crystallite size will also have an important bearing on the magnetic properties; too small a size resulting in super paramagnetism and too large a size in multidomain crystallites of lower coercivity and squareness. However, in view of the strong interactions it is to be expected that the critical limits of single domain behavior will be much less clearly defined than is the case with particles.

Films prepared by electrodeposition or electroless deposition as described above invariably show magnetic properties which are isotropic in the film plane. Indeed, attempts to induce anisotropy during deposition by the use of strong magnetic fields have so far been quite unsuccessful with films of high coercivity. However, electroless films of Co-P and Co-Ni-P with uniaxial anisotropy and low coercivity ( $< 15$  Oe.) which were prepared both with and without the application of a magnetic field have been reported by several workers<sup>12, 76, 140</sup>.

As with electroplated films, it is possible by varying the deposition parameters to select from a wide range of magnetic properties a combination which is likely to result in excellent recording performance. Thin films of Co-P and Co-Ni-P have been in use for several years as the recording surfaces of magnetic drums. However, in this application the head-to-drum separation is usually large and consequently the recording densities are low ( $\sim 100$ -200 b.p.i.). Recently accounts have been published<sup>4, 57, 90</sup> of a method whereby these films may be deposited on plastic substrates. In the case of polyethylene terephthalate, a common magnetic tape substrate, the first step is to make the substrate hydrophilic by dipping it into hot chromic-sulfuric acid solution and then into hot sodium hydroxide solution<sup>90</sup>. The substrate is then pre-sensitized in baths of stannous chloride solution and of palladium chloride solution<sup>57</sup> after which the autocatalytic process described above may be used to deposit the ferromagnetic film. In a variation on this method Fisher<sup>58</sup> applied a heat-curable adhesive to the substrate surface which had previously been cleaned in an alkaline solution

and rinsed with distilled water. The cured adhesive was then presensitized and coated with Co-Ni-P as described above.

## VACUUM DEPOSITION

Films of the common ferromagnetic elements and their alloys prepared by vacuum deposition have been discussed by several authors. Blois (Ni-Fe)<sup>27</sup>, van Itterbeek and Dupré (Ni)<sup>177</sup>, Hellenthal (Ni)<sup>73</sup>, Dupré (Fe, Co, Ni)<sup>48</sup>. However, the coercivities obtained with these films at room temperature were too low ( $\leq 100$  Oe.) for most recording applications. A possible method of increasing the coercivity might be to incorporate foreign atoms into the evaporated films since it is known that the coercivity of bulk materials can be considerably enhanced in this way, e. g., carbon in iron<sup>92, 127</sup>. The impurity can have the effect of impeding the motion of domain walls, or, if it is present in sufficient quantity, of causing the ferromagnetic material to behave like an assembly of single domain particles. In either case the result is to increase the coercivity. The films of Co-Ni-P and Co-P discussed above are examples of the second effect, the role of phosphorus being apparently to promote isolation of the metal crystallites. In practice the preparation of films predetermined magnetic properties by this method might be difficult in view of the different vapor pressures of the ferromagnetic metal and the impurity.

An alternative approach to the problem of increasing the coercivity of evaporated films has recently been reported<sup>17, 150</sup>. It consisted of evaporating onto a substrate at a high angle of incidence. The substrates, which were of glass, metal, or plastic, were usually subjected to glow discharge bombardment to remove surface impurities and were maintained at temperatures in the range 20-50° C. A variety of methods of heating is available; electron bombardment, focussed electron beams and r.f. induction have all been used successfully to provide evaporation rates of about 50 Å per second at pressures of  $10^{-4}$  to  $10^{-6}$  torr.

The crystallite size of the evaporated cobalt films (determined by diffraction line broadening) varied from 20-30 Å for those evaporated at normal incidence, to 80-100 Å for an angle of incidence of 65° and to  $\sim 1000$  Å at grazing incidence ( $> 75^\circ$ ). The cobalt films deposited at normal incidence showed a highly faulted, mixed h. c. p. and f. c. c. structure; the faulting was less at higher deposition angles. No preferred crystallographic orientation was found in these films, but there was evidence<sup>150, 160</sup>, of some degree of particle elongation in the electron micrographs taken of films evaporated at very high angles of incidence ( $> 75^\circ$ ).

The coercivity of the evaporated films was found to be a sharply increasing function of the angle of deposition when the angle was greater than  $\sim 60^\circ$ ; results for the three common ferromagnetic metals is shown in Figure 17. In contrast to the electrodeposited and electroless surfaces the evaporated films, not unexpectedly, showed anisotropic magnetic properties. The

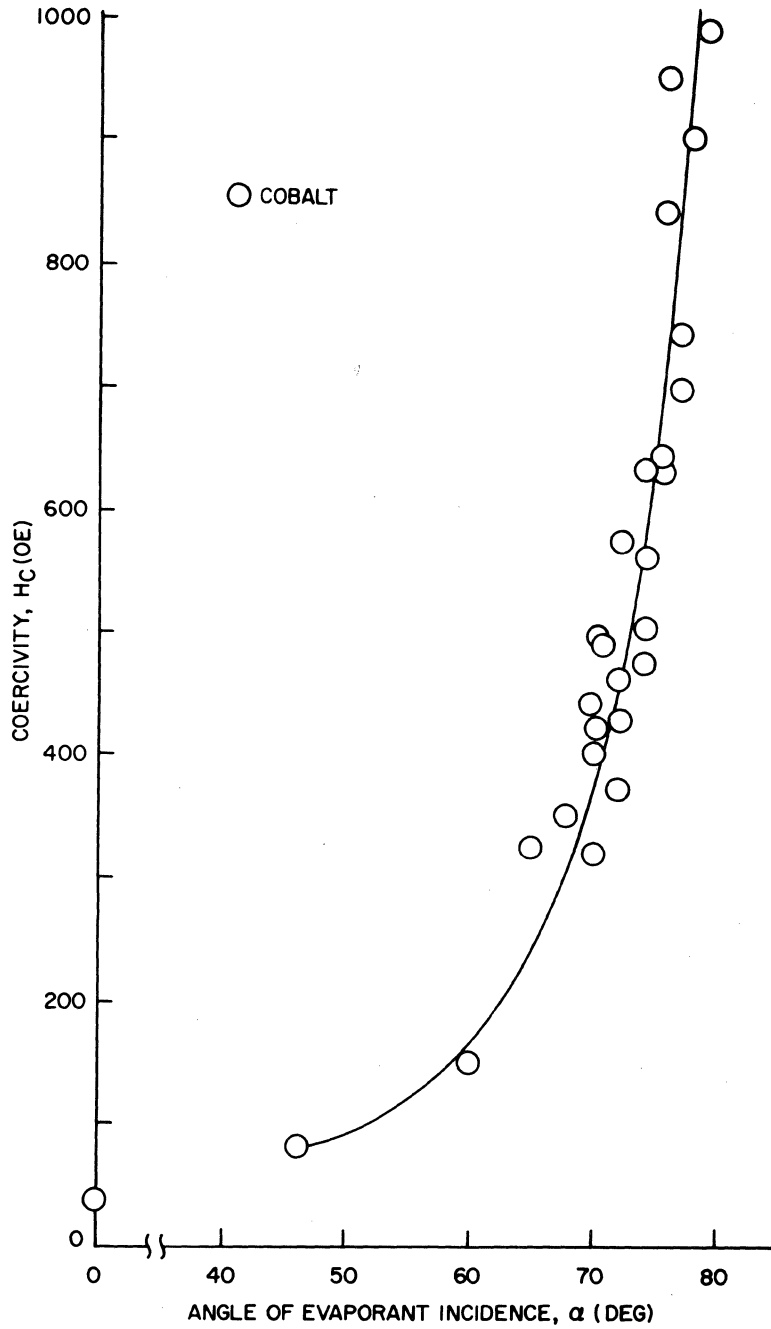


FIGURE 17a

COERCIVITY OF EVAPORATED FILMS OF Fe, Co, Ni, AS A FUNCTION OF THE ANGLE OF INCIDENCE DURING DEPOSITION. THE COERCIVITY WAS MEASURED PARALLEL TO THE PLANE OF INCIDENCE. (FROM SPELIOTIS, BATE, ALSTAD AND MORRISON, JOURNAL OF APPLIED PHYSICS, 36, 972 (1965)).

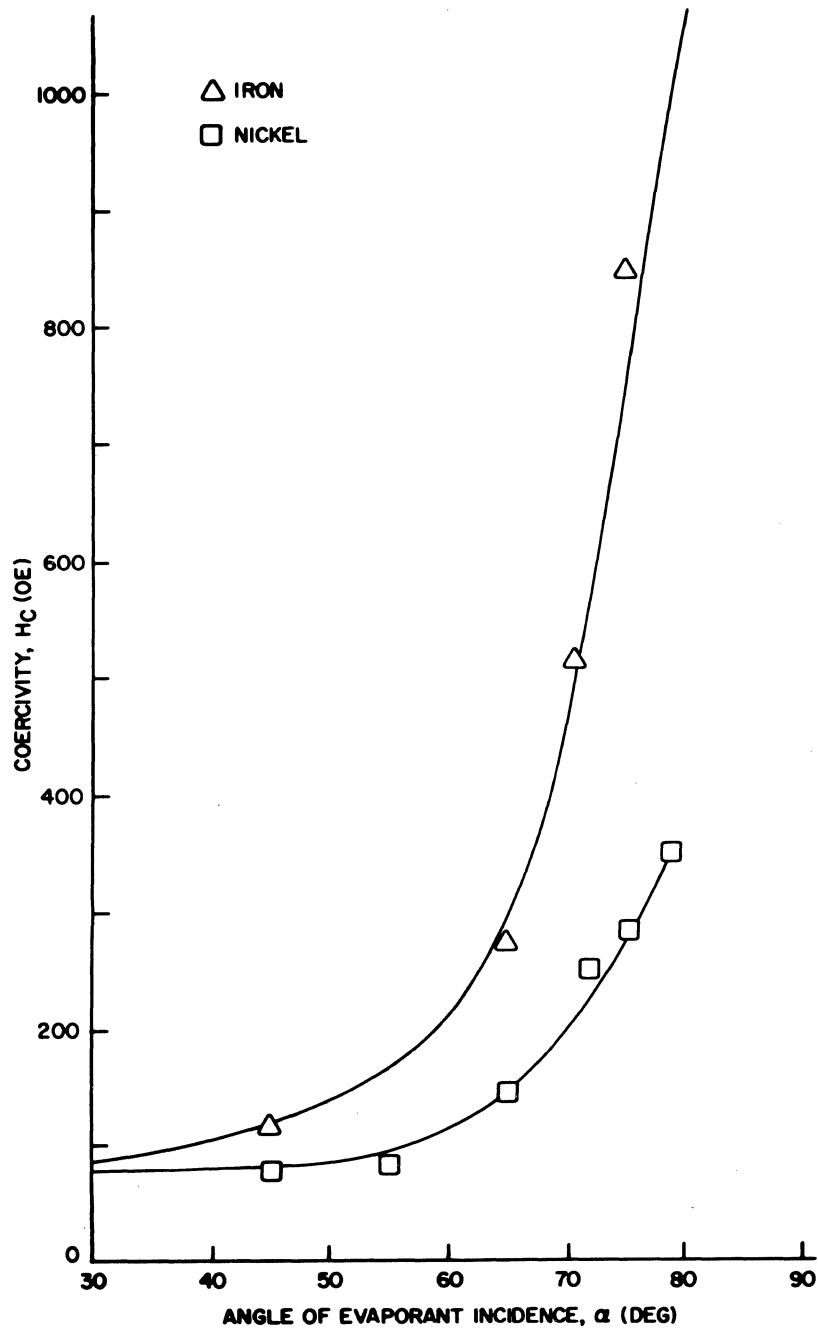


FIGURE 17b

COERCIVITY OF EVAPORATED FILMS OF Fe, Co, Ni, AS A FUNCTION OF THE ANGLE OF INCIDENCE DURING DEPOSITION. THE COERCIVITY WAS MEASURED PARALLEL TO THE PLANE OF INCIDENCE. (FROM SPELIOTIS, BATE, ALSTAD AND MORRISON, JOURNAL OF APPLIED PHYSICS, 36, 972 (1965).

easy axis of magnetization was found to lie in the plane of incidence and the anisotropy increased as a function deposition angle. The dependence of Ir/Is on deposition angle was much less pronounced. The squareness in the easy direction increased slightly and that in the hard direction decreased slightly, with increasing angles of incidence.

It appears possible that, as the crystallite size increased with increasing angle of incidence (and coercivity), a critical crystallite size is reached at which exchange and magnetostatic interactions are unable to cause the magnetization throughout each crystallite to deviate from its preferred direction. Thus the films having high coercivity consist of crystallites whose switching fields are largely determined by the local anisotropies (crystal-line and shape) while there still exists sufficient magnetostatic interaction to give the high values of Ir/Is ( $> 0.9$ ) which are found experimentally. This model is supported by the observation that samples which had been evaporated at high angles of incidence showed a fairly intense (111) line of CoO when examined by transmission electron diffraction. The oxide serves to isolate the crystallites from each other and so to ensure that magnetization reversal by wall motion does not occur. The saturation intensities of magnetization measured on these films were indistinguishable from the bulk values. Since high values of Ir/Is and coercivities in the range 100-1000 Oe. may be obtained in a highly controlled manner, evaporated films of iron or cobalt are likely to provide excellent recording surfaces, especially in high density digital applications.

## SPUTTERING

The apparatus used in sputtering consists essentially of a vacuum chamber inside which are an anode, a cathode and, between them, the substrate on which films are to be deposited. The chamber is first evacuated and then filled with a flowing inert gas (argon or krypton) to a pressure of  $10^{-1}$  -  $10^{-4}$  torr. A voltage of about 1000-5000 is applied across the anode and cathode by means of a d.c. power supply capable of delivering currents  $\sim 500$  ma. The electrodes which are usually water-cooled are often in the form of flat plates although other configurations have been used and found to influence the deposition process and the film properties<sup>60,80</sup>. The pressures used are much higher than those generally encountered in vacuum deposition, and a glow-discharge occurs in the inert gas atmosphere. Under bombardment by the (+) ionized gas molecules the cathode slowly disintegrates and material is ejected from it either as free atoms or as atoms combined with residual gas molecules. Until recently the mechanism by which atoms were removed from the cathode was not well understood. However, recent investigations by Wehner<sup>184</sup> in low-pressure glow-discharge systems, led to a momentum transfer model which suggested that atoms are ejected from the cathode with velocities at least two orders of magnitude higher than those found during evaporation. At pressures of  $\sim 10^{-1}$  mm. the transport mechanism is diffusion controlled while at pressures  $\sim 10^{-4}$  mm. the mechanism is one of molecular flow.

If the substrate-cathode distance is less than the mean free path, then particles arrive at the substrate with high energies (10-30 eV)<sup>184</sup>. The substrate is also subjected to electron bombardment since the electrons in the glow discharge are accelerated to the anode. This serves to clean the freshly-deposited surface by removing molecules of adsorbed gases. Maissel and Schaible<sup>112</sup> recently showed that this effect could be enhanced by applying a negative bias ( ~ 100 v. relative to the anode) to the film during deposition.

The properties of the sputtered films depend on the gas used in the discharge. While argon is often used in the deposition of pure metals and alloy, Kay<sup>91</sup> reported that by mixing argon and oxygen and controlling the partial pressure of the latter, different oxidation states and allotropic forms could be obtained selectively, e.g.,  $\gamma$ -Fe<sub>2</sub>O<sub>3</sub> rather than  $\alpha$ -Fe<sub>2</sub>O<sub>3</sub>. The deposition rates and the film characteristics are found to depend markedly on the currents, voltages and pressures used and also on the geometry of the substrate, the electrodes and the glow discharge zones. Kay obtained films of pure  $\alpha$ -iron with no apparent crystallite or magnetic orientation. The films had coercivities ~ 250 Oe. with  $I_r/I_s \geq 0.95$ . Films of f.c.c. nickel were also obtained which showed magnetic properties similar to those of films evaporated at normal incidence.

The principal advantages of the sputtering technique are 1) simplicity of operation (although the mechanism of the deposition process is not nearly so well understood as that of vacuum deposition), 2) uniform films on large-area substrates are possible by using cathodes, 3) the composition of the deposited films is the same as that of the cathode. The last advantage means that it is possible to deposit alloy and compound films of precise compositions even though the vapor pressures of the constituents may be very different (e.g. InSb, GaAs). The only requirement is that cathodes can be prepared of the composition required in the films. For example, Francombe, et al.<sup>60, 61</sup> prepared optically transparent films several thousand Angstroms in thickness of cobalt ferrite (CoFe<sub>2</sub>O<sub>4</sub>) and nickel ferrite (NiFe<sub>2</sub>O<sub>4</sub>) and nickel ferrite (NiFe<sub>2</sub>O<sub>4</sub>) by sputtering single-phase alloy films of CoFe<sub>2</sub> and NiFe<sub>2</sub> and subsequently oxidizing them.

## METAL FILMS VERSUS PARTICULATE COATINGS

The question of which method of preparing thin metal films is to be preferred depends to a large extent on the format of the recording surface. For example, electroplating would be most appropriate when used with metal substrates and vacuum deposition when coating long lengths (particularly since the technique of vacuum metallizing of flexible plastic substrates is commercially well-established). It is not at all clear that the magnetic anisotropy of evaporated films offers any advantages (or disadvantages) for recording purposes when compared with the isotropic films prepared by electrodeposition or electroless deposition. In fact there appear to be no reason, concerning their magnetic properties, why any one

method of preparation should be preferred as a general rule. All are capable of producing magnetic films with properties which imply excellent high density recording characteristics. But, since the vacuum deposition process involves fewer variables than the chemical methods, it is rather easier to control. Thin metal films are unsuitable for analog recording at very low frequencies (long wavelengths) since the combination of signal recording field and bias field can more easily extend completely through the thinner surface and thus produce harmonic distortion.<sup>117</sup>

One disadvantage which the metal films have in common when compared with particle coatings is that one is never completely sure, until after the surfaces have been deposited, what magnetic and physical properties will result even though characterization of the deposition process has previously been carried out. With particles, on the other hand, one has a detailed knowledge of the magnetic properties in powder form. There is, of course, some modification of these properties on coating but this is usually a relatively slight (and known) perturbation. With particulate coatings also it is possible to a large extent to exercise independent control of the magnetic and physical properties of the coating. In the case of metal films, however, it often happens that magnetic hardness is associated with mechanical hardness, and thus the choice of the former for recording considerations unavoidably dictates the latter.

Metal films also have common advantages some of which, in the field of high-density recording, have already been discussed. Three additional advantages may be mentioned. First, since the metal films possess a high degree of magnetic (and electrical) continuity, there is less likelihood of useful flux being lost through local flux closure around the individual particles or clusters. Second, because of the combined effects of the uniaxial particles and the shape of the trailing edge of the recording head, it is possible for some of the particles close to the surface to become magnetized in a direction opposite to that of the applied field in the center of the head gap. This results in an intensity of magnetization which at first, increases with depth below the surface<sup>172</sup>. Consequently the layers nearer to the head, which contribute the sharpest output pulses from a recorded transition, are less effective. This effect is not likely to occur in metallic films because of the closer magnetic coupling between the individual crystallites. The third additional advantage of thin metal films as a class over particulate coatings is that there exists the possibility of reading the information by the Kerr magneto-optic effect since the films are highly (and specularly) reflecting.

Finally it must be added that it is possible to deposit continuous ferrite films on smooth substrates such as glass, quartz, polyethylene terephthalate, etc. Lemaire and Croft<sup>101</sup> described a method in which an aqueous solution of ferrous chloride ( $\text{FeCl}_2 \cdot 4\text{H}_2\text{O}$ ) was added to sodium hydroxide in molar proportions 1:2.

The mixture was circulated in the presence of oxygen around the substrate which was held at a temperature a few degrees higher than liquid. Continuous films of  $\text{Fe}_3\text{O}_4$  having coercivities in the range 170-300 Oe. and thicknesses between 200 and 1000 Å were prepared in this way. By using mixtures of other metal salts with ferrous chloride it was found possible to grow films of nickel-, cobalt- and zinc ferrites having coercivities as high as 600 Oe.

## STAINLESS STEEL RECORDING WIRES

Magnetic recording was invented in 1898 by Valdemar Poulsen who used steel wires as the recording medium. Wires made of stainless steel with the composition 12% Ni, 12% Cr,  $\sim 0.1\%$  C and the remainder iron, were used as recording surfaces until the late 1940s when they were replaced by iron oxide tapes. The wire usually had a diameter of 0.004" or  $10^{-2}$  cm. A study of the magnetic properties of these wires as a function of drawing and annealing treatments was reported by Hobson et al.<sup>78,79</sup> It was suggested that the annealed and cold-worked material consisted of small ferritic particles dispersed in a non-ferromagnetic matrix of austenite and that the ferrite particles were produced along the slip planes of the f.c.c. austenite by cold working. They investigated the variation of remanence with heat-treatment and found by magnetic measurement and x-ray diffraction that the hard-drawn wires contained 50% ferrite while those which had been annealed to produce the optimum condition contained only 10%. It appears probable that the particles were elongated in the direction of drawing and thus high coercivities and high values of  $I_r/I_s$  are expected and found. Hobson and Osmond<sup>79</sup> reported coercivities as high as 500 Oe. and Bate<sup>13</sup> found that the optimum heat treatment produced samples of wire with  $I_r/I_s > 94\%$  at  $H_c = 340$  Oe. The objections to wire as a recording medium are a) its tendency to twist and thus increase the separation between the recorded pattern and the reading head, b) the impossibility of making an inaudible splice, c) its tendency to tangle after breaking. On the other hand, since the mass per unit length is less than that of plastic tapes, one expects that shorter start-stop times could be achieved with wire.

All-metal tapes have sometimes been used in recording. These may be divided into two classes; those in which a ferromagnetic coating of, say, Co-Ni-P, is applied to a phosphor-bronze tape and those in which the magnetic alloy itself is sufficiently ductile to be prepared in tape in tape form. Examples of the latter class are alloys of Fe-Co, Ni-Fe, and Ni-Co with copper or vanadium. The all-metal tapes have characteristic disadvantages; they are much less compliant than plastic tapes and thus suffer from separation losses; they have very high mass per unit length and they are difficult to splice.



## THERMAL RECORDING

The phenomenon of thermoremanent magnetization (TRM) has been studied mainly as a branch of rock magnetism. Frequently rock formations are found to be magnetized in the opposite direction to that of the earth's field. Two possible explanations of this result have been discussed,<sup>163</sup> they are 1) that at some time (or times) in the past the direction of the earth's field was opposite to its present direction and 2) that some rocks on being cooled in a field may acquire a magnetization in the opposite direction to that of the applied field. It now seems clear that self-exciting dynamos of the earth's type can have the property of self-reversal and so the first explanation is favored. However, it has also been shown that rocks can exhibit a reversed TRM which opposes the applied field.

Néel<sup>130</sup> reviewed the current theory of normal TRM. At sufficiently a high temperature, which is less than the Curie temperature, all single domain particles become super paramagnetic by virtue of the increased effect of thermal forces and the reduction of magnetocrystalline energy barriers opposing rotation. On cooling, each particle reaches what Stacey<sup>163</sup> calls a "blocking temperature" at which it ceases to be superparamagnetic and becomes a stable single domain. Néel showed that the transition is very sharp since the average time to between spontaneous reversals is proportional to  $\exp(\frac{vK}{kT})$ ; where  $v$  is the particle volume,  $K$  is the anisotropy constant,  $k$  is Boltzmann's constant and  $T$  is the absolute temperature. Each particle then assumes the direction of magnetization which it had while passing through the blocking temperature and the TRM of the assembly is determined by the superparamagnetic susceptibility at that temperature.

Studies of TRM have been principally concerned with the behavior of  $\text{Fe}_3\text{O}_4$  particles since magnetite is the most important constituent of magnetic rocks. Particles of natural magnetite have been used in recording surfaces and they are also used in the United States Senate as ink-blotting sand (which is, in a sense, a recording application!) Rimbart<sup>141</sup> showed that if a small field is applied to dilute assembled of particles of  $\gamma\text{Fe}_2\text{O}_3$  or  $\text{Fe}_3\text{O}_4$  while they are being cooled below the Curie temperature, a TRM is induced which is very large compared to that induced by the same field (applied normally or anhysteretically) at room temperature. The fields applied were small compared with the room temperature coercivity. Thus it should be possible to record on particulate coatings by the simultaneous application of heat and small magnetic fields; the fields being continuously applied while the coating is cooled to room temperature. Not only would large values of TRM be obtained but also magnetization acquired in this way is particularly stable at room temperature.

The difficulty presented by the high Curie temperature of many recording materials would be not nearly so serious if, for example, particles of  $\text{CrO}_2$  were used. With suitable additives, e. g., fluorine, Curie temperatures as low as  $80^\circ \text{C}$ . can be obtained in the material. It is possible that the effect of thermoremanent magnetization will play an important part in the future development of magnetic recording.

#### COST OF RECORDING MATERIALS

In a field where the use of one material is so predominant (the other possible materials being at the laboratory stage of development), it is only meaningful to give cost figures for that one material. Particles of  $\gamma\text{-Fe}_2\text{O}_3$  suitable for use in magnetic recording surfaces may be bought for about 50 cents/lb. from such suppliers as Charles Pfizer and Co., Inc. (Minerals, Pigments and Metals Division), Easton, Pa., Hercules Powder Co. (Imperial Color and Chemical Dept.) Glen Falls, N. Y.; Wright Industries, Brooklyn, N. Y.

A 2400' reel of 1/2" computer tape costing \$25.00 - \$40.00 contains about 1/3 lb. (i. e. about 16 cents worth) of  $\gamma\text{-Fe}_2\text{O}_3$ . The other material costs are considerably greater than this and arise, in decreasing amounts, from the tape reel and case, the tape base and the binder materials (including solvents).

## REFERENCES

- 1) E. Adams, W. M. Hubbard, A. M. Syeles, J. Appl. Phys. 23, 1207 (1952).
- 2) P. Adams, L. E. Knees, U.S. Patent 3,042,639 (7/3/62).
- 3) A. Aharoni, E. H. Frei, M. Schieber, J. Phys. Chem. Solids. 23, 545 (1962).
- 4) H. R. Allen, M. G. Petersen, J. M. Carr and J. S. Sallo, Proc. 1964 Intermag Conf. p. 641.
- 5) H. Amar, J. Appl. Phys. 30, 139S, (1959).
- 6) Ampex, Netherlands Patent 6,400,382 (7/22/64).
- 7) C. H. Arrington, U. S. Patent 3,080,319 (3/5/63).
- 8) I. Arshinkov, P. Peshier, O. Tsumnorechki, Izr. Nauchnoizsled. Inst. Kinematogr. Radio (Sofia) 3, 31, (1961 - 2).
- 9) P. Arthur and J. N. Ingraham, U.S. Patent, 3,117,093 (1/7/64).
- 10) J. W. Ayers and R. A. Stephens, U.S. Patent 3,015,627 (1/2/62).
- 11) J. W. Ayers and R. A. Stephens, U.S. Patent 3,015,627 (1/2/62).
- 12) J. Bagrowski and M. Lauriente, J. Electrochem. Soc. 109, 987 (1962).
- 13) G. Bate, Ph.D Thesis University of Sheffield, Sheffield, England (1952).
- 14) G. Bate, J. Appl. Phys. 32, 239S, (1961).
- 15) G. Bate, J. Appl. Phys. 33, 2263 (1952).
- 16) G. Bate, J. R. Morrison, D. E. Speliotis, Proc. Int. Conf. Mag. Recording (London) p.7 (1964).
- 17) G. Bate, D. E. Speliotis, J. K. Alstad, J. R. Morrison, Proc. Int. Conf. Magnetism Nottingham (England) p.816 (1965).
- 18) G. Bate, H. S. Templeton, J. W. Wenner, IBM J. Res. 6, 348 (1962).
- 19) O. Baudisch, U. S. Patent 1,894,749 (1/2/33).
- 20) O. Baudisch, U. S. Patent 1,894,750 (1/17/33).
- 21) C. P. Bean and J. D. Livingston, J. Appl. Phys. 30, 120S, (1959).
- 22) H. B. Beer and G. V. Planer, Brit, Comm. Electron. 5, 939 (1958).
- 23) A. E. Berkowitz and W. J. Schuele, J. Appl. Phys. 30, 134S (1959).
- 24) L. R. Bickford, Phys, Rev. 78, 449 (1950).

- 25) L. R. Bickford, J. M. Brownlow, R. F. Penoyer, Proc. Instn. Electr. Engrs. 104B, Suppl. no. 5, 238 (1957).
- 26) J. B. Birks, Proc. Phys. Soc. 63, 65 (1950)
- 27) M. S. Blois, J. Appl. Phys. 20, 975 (1955).
- 28) T. H. Bonn and D. C. Wendell, Jr., U.S. Patent 2,644,787 (7/7/53).
- 29) P. B. Braun, Nature 170, 1123 (1952).
- 30) A. Brenner and G. Riddell, J. Res. Nat. Bur. Stds. 37, 1 (1946).
- 31) S. S. Brenner, Acta Met. 4, 62 (1956).
- 32) W. F. Brown, Jr., J. Appl Phys, 30, 62S (1959).
- 33) W. F. Brown, Jr. and C. E. Johnson, Jr., J. Appl. Phys. 33, 2572 (1962).
- 33a) B. B. Bycer "Digital Magnetic Tape Recording" Hayden Book Co. (New York) (1965)
- 34) R. B. Campbell, J. Appl Phys. 28, 381 (1957)
- 35) M. Camras, U.S. Patent 2,694,656 (11/16/54).
- 36) E. H. Carman, Brit. J. Appl. Phys. 6, 426 (1955).
- 37) U. Colombo, G. Fagherazzi, F. Gazzarini, G. Lanzavecchia, G. Sironi, Nature, 202, 176 (1964).
- 38) U. Colombo, G. Fagherazzi, F. Gazzarini, G. Lanzavecchia, G. Sironi, Chim. Ind. (Milan) 46, 357 (1964).
- 39) D. J. Craik and P. M. Griffiths, Brit. J. Appl Phys. 9, 280 (1958).
- 40) E. D. Daniel and I. Levine, J. Acoust. Soc. Amer. 32, 258 (1960).
- 41) F. J. Darnell, J. Appl. Phys, 32, 1269 (1961).
- 42) I. David and A. J. E. Welch, Trans. Farad, Soc. 52, 1642 (1956).
- 43) K. J. de Vos, W. A. J. J. Velge, M. G. van der Steeg and H. Zijlstra, J. Appl. Phys. 33, 1320 (1962).
- 44) K. J. de Vos, W. A. J. J. Velge, M. G. van der Steeg, Z. angew Physik 15, 256 (1963).
- 45) D. J. Doan, U.S. Bur. Mines Bulletin No. 425 "Magnetic Separation of Ores" ed. R. S. Dean and C. W. Davis, p. 113 (1941).
- 46) C. D. Downs, U.S. Patent 2,524,433 (10/3/50).
- 47) S. Duinker, A. L. Stuijts, H. P. J. Wijn, and W. K. Westmijze, U.S. Patent 3,023,166 (2/27/62).
- 48) A. Dupré, Verhandl. K. Vlaamse Acad. Wetensch. Transaction

No. 59, 62pp (1959)

- 49) T. Elder, J. Appl. Phys. 36, 1012 (1965).
- 50) D. F. Eldridge, I.E.E.E. Trans. Comm. and Electronics, 83, 585 (1964).
- 51) R. W. Fabian and J. L. Sienczck, U.S. Patent 2,884, 319 (4/28/59).
- 52) R. B. Falk, U.S. Patent 3,156, 650 (11/10/64).
- 53) R. B. Falk and G. D. Hooper, J. Appl. Phys. 32, 190S (1961).
- 54) G. A. Ferguson and M. Hass, Phys. Rev. 112, 1130 (1958).
- 55) FIAT Final Report No. 923, Her Majesty's Stationary Office, London (1947).
- 56) R. D. Fisher, J. Electronchem. Soc. 109, 479 (1962).
- 57) R. D. Fisher and W. H. Chilton, J. Electrochem. Soc. 109, 485 (1962).
- 58) R. D. Fisher, R. P. Williams, F. J. Harsacky, U.S. Patent 3, 116, 159 (12/31/63).
- 59) P. J. Flanders and S. Shtrikman, J. Appl. Phys. 33, 216 (1962).
- 60) M. H. Francombe, Trans. 10th Nat. Vac. Symp., Macmillan Co. N. Y., p. 316 (1963).
- 61) M. H. Francombe, J. E. Rudisill, R. L. Coren, J. Appl. Phys. 34, 1215 (1963).
- 62) E. H. Frei, M. Schieber, S. Shtrikman, U.S. Patent 3, 093, 453 (6/11/63).
- 63) W. O. Freitag and J. S. Matthias, Electroplating and Metal Finishing 17, 42 (1964).
- 64) S. Fukuda, T. Miyake, G. Akashi, M. Seto, U.S. Patent 3, 026, 215 (3/20/62).
- 65) S. Fukuda, H. Goto, G. Akashi, T. Miyake, U.S. Patent 3, 046, 158 (7/24/62).
- 66) S. Glasstone, "The Fundamentals of Electrochemistry and Electrodeposition" Franklin, N.J., 2nd Edn. (1960).
- 67) A. Goldman and G. I. Post, J. Appl. Phys. 30, 204S (1959).
- 68) H. Goto and G. Akashi, U.S. Patent 3, 047, 428 (7/31/62).
- 69) C. Guillaud, J. Rech. CNRS 2, 267 (1949).
- 70) O. L. Harte and J. R. Thomas, French Patent 1, 357, 214 (4/3/64).
- 71) F. H. Healey, J. J. Chessick, A. V. Fraioli, J. Phys. Chem. 60, 1001 (1956).

- 72) G. Heimke, Zeits. angew Physik 15, 271 (1963).
- 73) W. Hellenthal, Z. Naturforschg. 14a, 1077 (1959).
- 74) O. Henkel, Phys. Stat. Sol. 2, 1393 (1962).
- 75) W. E. Henry and M. J. Boehm, Phys. Rev. 101, 1253 (1956).
- 76) R. J. Heritage and M. T. Walker, J. Electronics and Control 7, 542 (1959).
- 77) A. S. Hoagland, "Digital Magnetic Recording" Wiley, N. Y. pl10, 1963.
- 78) P. T. Hobson, E. S. Chatt, W. P. Osmond, J. Iron & Steel Inst. 159, 145 (1948).
- 79) P. T. Hobson, W. P. Osmond, Nature, 161, 562 (1948).
- 80) L. Holland "Vacuum deposition of thin films" Chapman and Hall (London) p 401 (1956)
- 81) A. Z. Hryniewicz and D. S. Kulgachuk, Acta. Phys. Polonica 24, 689 (1963)
- 82) J. N. Ingraham and T. J. Swoboda, U.S. Patent 2, 923, 683 (2/2/60).
- 83) J. N. Ingraham and T. J. Swoboda U.S. Patent 3,068,176 (12/11/62).
- 84) S. Iwasaki and K. Nagai, Rep. Res. Inst. Elect. Commun. Tohoku Univ. B15, 85, (1963).
- 85) I. S. Jacobs and C. P. Bean, Phys. Rev. 100, 1060 (1955).
- 86) I. S. Jacobs and F. E. Luborsky, J. Appl. Phys. 28, 467 (1957).
- 87) C. E. Johnson and W. F. Brown, J. Appl. Phys. 29, 1699 (1958).
- 88) G. H. Jonker. H.P.J. Wijn, P. B. Braun, Philips Tech. Rev. 18, 145 (1956/7).
- 89) J. S. Judge, J. R. Morrison and D. E. Speliotis, J. Appl. Phys. 36, 948 (1965).
- 90) J. S. Judge, J. R. Morrison, D. E. Speliotis and G. Bate, J. Electrochem. Soc. 112, 681 (1965).
- 91) E. Kay, J. Appl. Phys. 32, 99S (1961).
- 92) M. Kersten, Phys. Zeits. 44, 63 (1943).
- 92a) A. J. J. Koch, P. Hokkeling, M. G. van der Steeg, K. J. deVos Jour. Appl. Phys. 31, 75S, (1960)
- 93) H. Kojima, Sci. Rep. Res. Inst. Tohoku Univ. 6, 178, (1954).
- 94) H. Kojima, Sci. Rep. Res. Inst. Tohoku Univ. A8, 540 (1956).
- 95) H. Kojima, Sci. Rep. Res. Inst. Tohoku Univ. A10, 175 (1958).

- 96) E. Kondorskii, *Izvest. Akad. Nauk. SSSR, Ser. Fiz.* 16, 398 (1952).
- 97) H. Koretzky, *Proc. 1st Austral. Conf. on Electrochemistry*, Pergamon, N. Y. p. 417 (1964).
- 98) F. Kroner, *Mitt. Forschungslab. Agfa.* 1, 289 (1955).
- 99) F. Kroner, "Technik der Magnetspeicher" (Berlin; Springer-Verlag) p. 479 (1960).
- 100) P. Langevin, *J. de Physique* 4, 678 (1905).
- 101) H. P. Lemaire and W. J. Croft, U.S. Patent 3, 100,158 (8/6/63).
- 102) F. P. Levi, *Nature* 183, 1251 (1959).
- 103) F. P. Levi, *J. Appl. Phys.* 31, 1469, (1960).
- 104) D. J. Levy, *Proc. Am. Electrol. Soc* 50, 29 (1963).
- 105) F. E. Luborsky, *J. Appl. Phys.* 32, 171S (1961) .
- 106) F. E. Luborsky, *J. Appl. Phys.* 34, 1706 (1963).
- 107) F. E. Luborsky, E. F. Fullam, D. S. Hallgren, *J. Appl. Phys.* 29, 989 (1958).
- 108) F. E. Luborsky, E. F. Koch and C. R. Morelock, *J. Appl. Phys.* 34, 2905, (1963).
- 109) F. E. Luborsky, C. R. Morelock, *J. Appl. Phys.* 35, 2055 (1964).
- 110) F. E. Luborsky, C. R. Morelock, *Proc, Int. Conf. Magnetism, Nottingham (England)* 763, (1965).
- 111) F. E. Luborsky and J. D. Opie, *J. Appl. Phys* 34, 1317 (1963).
- 112) L. I. Maissel and P. M. Schaible, *J. Appl. Phys.* 36, 237 (1965).
- 113) G. C. Marcot, W. J. Cauwenberg, S. A. Lamanna, U.S. Patent 2, 558, 302 (6/26/51).
- 114) G. C. Marcot, W. J. Cauwenberg. S. A. Lamanna, U.S. Patent 2, 558, 303 (6/26/51).
- 115) L. Mayer, *J. Appl. Phys.* 31, 384S (1960).
- 116) C. D. Mee "The Physics of Magnetic Recording" North-Holland, Amsterdam p. 191 (1964).
- 117) C. D. Mee, loc. cit. p. 15.
- 118) C. D. Mee and J. C. Jeschke, *J. Appl. Phys.* 34, 1271 (1963).
- 119) W. H. Meiklejohn, *J. Appl. Phys.* 33, 1328 (1962).
- 120) A. Michel and J. Bernard, *J. Bull Soc. Chim.* 10, 315 (1943).
- 121) A. Michel, G. Chandron, J. Bernard, *J. Phys. Radium* 12, 189 (1952).
- 122) A. H. Mones and E. Banks, *J. Phys. Chem. Solids* 4, 217 (1958).

- 123) C. R. Morelock, *Acta Met.* 10, 161 (1962).
- 124) A. H. Morrish and L. A. K. Watt, *Phys. Rev.* 105, 1476 (1957).
- 125) A. H. Morrish and S. P. Yu, *J. Appl. Phys.* 26, 1049 (1955).
- 126) J. R. Morrison and D. E. Speliotis, to be published.
- 127) L. Néel, *Comptes Rendus*, 223, 198 (1946).
- 128) L. Néel, *Comptes Rendus Acad. Sci.* 224, 1550 (1947).
- 129) L. Néel, *Ann Geophys.* 5, 99 (1949).
- 130) L. Néel, *Advanc. Phys.* 4, 191 (1955).
- 131) S. Nobuoka, T. Ando, F. Hayama, U. S. Patent 3,081,264 (3/12/63).
- 132) A. L. Oppegard, U. S. Patent 2,885,365 (59).
- 133) A. L. Oppegard, F. J. Darnell and H. C. Miller, *J. Appl. Phys.* 32, 184S (1961).
- 134) W. P. Osmond, *Proc. Phys. Soc.* 66B, 265 (1953).
- 135) W. P. Osmond, *Proc. Phys. Soc.* 67B, 875 (1954).
- 136) P. O. Pedersen, U. S. Patent 836,339 (11/20/06).
- 137) R. S. Penniman, Jr. and N. M. Zoph, U. S. Patent 1,368,748 (2/15/21).
- 138) A. G. Pickett and M. M. Lemcoe "Preservation and storage of sound recordings," *Library of Congress, Washington*, p.58 (1959).
- 139) F. Preisach, *Z. Physik* 94, 277 (1935).
- 140) L. D. Ransom and V. Zentner, *J. Electrochem. Soc.* 111, 1423 (1964).
- 141) F. Rimbert, *C. R. Acad. Sci. (Paris)* 245, 406 (1957).
- 142) T. V. Rode and V. E. Rode, *Zhur. Physcheskoi Chem.* 35, 2475 (1961).
- 143) S. Ruben, U. S. Patent 1,889,380 (11/29/32).
- 144) J. M. Sallo and J. M. Carr, *J. Electrochem. Soc.* 109, 1040 (1962).
- 145) J. S. Sallo and K. H. Olsen, *J. Appl. Phys.* 32, 203S (1961).
- 146) M. Sato, S. Yokoyama, Y. Hoshino, *Kogyo Kagaku Zasshi* 65, 1336 (1962) (in Japanese).
- 147) R. Schrader and G. Büttner, *Zeits. für Anorg. u. Allgem. Chemie* 320, 205 (1963).
- 148) W. J. Schuele, *J. Phys. Chem.* 63, 83 (1959).
- 149) W. J. Schuele, U. S. Patent 3,042,543 (7/2/62).
- 150) W. J. Schuele, *J. Appl. Phys.* 35, 2558 (1964).



- 151) W. J. Scheule and V. D. Deetscreek, J. Appl. Phys. 32, 235S (1961).
- 152) W. J. Schuele and V. D. Deetscreek "Ultrafine Particles" Ed. Kuhn, Lamprey and Sheer, John Wiley, New York, p. 218, 1963.
- 153) P. W. Selwood, "Magnetochemistry," Interscience Pub. Inc. 2nd Edn. p.308 (1956).
- 154) E. V. Shtol'ts, Bull Acad. Sci. U.S.S.R. (Phys. Ser.) 26, 318 (1962).
- 155) S. Shtrikman and D. Treves, J. Phys. Radium 20, 286 (1959).
- 156) J. C. Slonczewski, Phys. Rev. 110, 1341 (1960).
- 157) J. Smit and H. P. J. Wijn, "Ferrites," p. 157, Wiley (1959).
- 158) D. O. Smith, Phys. Rev. 102, 959 (1956).
- 159) Societé d UGINE, U. K. Patent 590, 392 (7/16/47).
- 160) D. E. Speliotis, G. Bate, J. K. Alstad, J. R. Morrison, J. Appl. Phys. 36, 972 (1965)
- 161) D. E. Speliotis, G. Bate, J. R. Morrison and R. E. Braun, IEEE Trans. Magnetics MAG-1, 101 (1965).
- 162) D. E. Speliotis, J. R. Morrison, G. Bate, Proc. Int. Conf. Magnetism, Nottingham, England, p. 623 (1965).
- 163) F. D. Stacey, Advanc. Physics. 12, 45 (1963).
- 164) A. I. Stoller, U.S. Patent 3,001,891 (9/26/61).
- 165) E. C. Stoner and E. P. Wohlfarth, Phil Trans. Roy. Soc. A240 , 599 (1948).
- 166) A. L. Stuijts and H. P. J. Wijn, Philips Tech.Rev. 19, 209 (1957/8).
- 167) Y. Sugiura, J. Phys. Soc. Japan 15, 1461 (1960).
- 168) T. J. Swoboda, P. Arthur, N. L. Cox, J. N. Ingraham, A. L. Oppegard, M. S. Sadler, J. Appl. Phys. 32, 374S (1961).
- 169) H. S. Templeton and G. Bate, IEEE Trans. Comm and Electronics, 83, 429 (1964).
- 170) R. K. Tenzer, J. Appl. Phys. 34, 1267 (1963).
- 171) R. K. Tenzer, J. Appl. Phys. 36, 1180 (1965).
- 172) D. L. A. Tjaden, Proc. Int. Conf. Magnetic Recording (London) p. 135 (1964).
- 173) K. Torkar and O. Fredriksen, Powder Metall, Bull. 4, 105 (1959).
- 174) I. Tsu, Plating, 48, 379 (1961).
- 175) I. Tsuboya and M. Sugihara, J. Phys. Soc. Japan 20, 170 (1965).

- 176) E. P. Valstyn, J. P. Hanton, A. H. Morrish, *Phys. Rev.* 128, 2078 (1962).
- 177) A. van Itterbeek and A. Dupré, *J. dePhys. et Radium* 19, 113 (1958).
- 178) G. W. van Oosterhout, *Acta Cryst.* 13, 932 (1960).
- 179) G. W. van Oosterhout, *Proc. Int. Conf. Magnetism, Nottingham*, 529 (1965).
- 180) F. von Kobell, "Grundzuge der Mineralogie" p. 304, Nurnberg (1838).
- 181) G. W. van Oosterhout and C. J. Klomp. *Appl. Sci. Res.* B9, 288 (1962).
- 182) G. W. van Oosterhout and C. J. M. Rooijmans, *Nature*, 181, 44 (1958).
- 183) L. A. K. Watt and A. H. Morrish, *J. Appl. Phys.* 31, 71S (1960).
- 184) G. K. Wehner, *Phys. Rev.* 114, 1270 (1959).
- 185) J. W. Wenner, U.S. Patent 3,150,939 (9/29/64).
- 186) W. K. Westmijze, *Philips Res. Rep.* 8, 245, (1953).
- 187) H. J. Williams, R. G. Sherwood, F. G. Foster, E. M. Kelley, *J. Appl. Phys.* 28, 1181 (1957).
- 188) F. Wohler, *Ann. Chem. Liebigs.* 111, 117 (1859).
- 189) E. P. Wohlfarth, *Advances in Physics*, 8, 87, (1959).
- 189a) E. P. Wohlfarth, Chpt 7, "Magnetism Vol. III, Ed. Rado and Suhl, Academic Press, N. Y. (1963).
- 190) E. P. Wohlfarth, *J. Appl. Phys.* 35, 783 (1964).
- 191) E. P. Wohlfarth, *J. Appl. Phys.* 29, 595 (1958)
- 192) E. P. Wohlfarth, *J. Appl. Phys.* 30, 1465 (1959)
- 193) E. P. Wohlfarth and D. G. Tonge, *Phil. Mag.* 2, 1333 (1957).
- 194) E. J. Yamartino and R. B. Falk, U.S. Patent 2,999,777 (9/12/61).
- 195) P. P. Zapponi, U.S. Patent 2,619,454 (11/25/52).